INTERNATIONAL ATOMIC ENERGY AGENCY
UNITED NATIONS EDUCATIONAL, SCIENTIFIC AND CULTURAL ORGANIZATION

INTERNATIONAL CENTRE FOR THEORETICAL PHYSICS
34100 TRIESTE (ITALY) - P.O.B. 586 - MIRAMARE - STRADA COSTIERA 11 - TELEPHONE: 2240-1
CABLE: CENTRATOM - TELEX 460392-1

SMR/208 - 23

SPRING COLLEGE IN MATERIALS SCIENCE

ON

"METALLIC MATERIALS"

(11 May - 19 June 1987)

BACKGROUND MATERIAL FOR LECTURES ON "RADIATION DAMAGE"

by

R. BULLOUGH
Materials Development Division
B552 Harwell Laboratory
Oxfordshire OX11 ORA
U.K.

Dislocations and Radiation Damage

R. Bullough

ABSTRACT

The influence of dislocations on the response of crystalline materials to irradiation is reviewed. Those dislocation properties that are essential to our understanding of the evolution of the microstructure during irradiation are identified and it is shown how the rate theory model can thereby describe the collective behaviour of the microstructure.

Theoretical Physics Division
AERE Harwell

October 1984

HL84/4500

1. INTRODUCTION

Dislocations have a profound influence on the various effects of irradiation in crystalline materials. The clustering of intrinsic point-defects (interstitials and vacancies) produced by irradiation can lead to the formation of dislocations; these new dislocations and the pre-existing dislocations can act as sinks for such point-defects and climb; alternatively the clusters can impede the glissile motion of the dislocations. Irradiation can thus create dislocations and have a gross effect on their individual and collective behaviour. Such technologically important phenomena as void swelling, irradiation creep and growth all occur because dislocations are present in the microstructure of materials and may be quantitatively modelled and understood by exploiting our knowledge of the fundamental properties of the dislocations. The aim of the present review is thus to identify those dislocation properties that are essential to our understanding of the evolution of the microstructure and to show how we may thereby construct appropriate models to represent the collective behaviour of the microstructure. The emphasis of our discussion will relate to the relatively high temperature behaviour of irradiated materials when the intrinsic point-defects are mobile. To avoid duplication with the associated reviews of dispersion hardening etc. we shall deliberately exclude detailed consideration of irradiation hardening and high stress mechanical properties of irradiated materials.

When a metal is bombarded with particles (by particles we mean charged particles such as high energy electrons, protons or heavy ions or neutral particles such as fast neutrons) whose energy is sufficiently high to displace host atoms from their equilibrium

lattice sites, these atoms come to rest some distance away as interstitials leaving vacancies behind at the respective lattice sites. If the temperature of the material is appropriate, these interstitials and vacancies (henceforth referred to as point-defects unless we wish to distinguish them) can migrate through the host matrix. In general the interstitials are much more mobile than the vacancies with typically respective migration energies of ~0.2 eV and ~1 eV for common structural metals. The fate of these point-defects depends very much on the microstructural state in which they are generated.

If few dislocations are already present, as in a well annealed material, the point-defects can either be lost by recombination with each other in the bulk material or they can nucleate and grow interstitial and vacancy aggregates. When these aggregates are planar their perimeter defines a dislocation loop. Some of the conditions for such loop formation and relevant properties of such loops, together with some of the direct consequences of such aggregate formation to the overall radiation damage response of materials are described in section 2.

If the dislocation density is high then many of the point-defects will survive for sufficient time to arrive at the dislocations rather than be lost by bulk recombination or form dislocation loop nuclei. The details of this loss of point-defects to dislocations are very important for a quantitative understanding of irradiation damage and depend on both the long-range interactions between the dislocations and point-defects and on the behaviour of the point-defects when they arrive at the cores of the dislocations; some details of these interactions are presented in section 3.

In section 4 we describe the concept of an effective medium and show how the above specific dislocation properties are used to deduce effective dislocation sink strengths for use in such a medium. Such a procedure enables many of the other sink types present in the microstructure to be consistently included in a rate theory description of the evolution of the microstructure during irradiation. The power of this approach is illustrated in section 5 where we give several examples of predictions of swelling, irradiation creep and growth together with several appropriate examples of successful correlations with experiment. Finally in section 6, we present a number of concluding remarks that are intended to identify some of the outstanding omissions in our understanding of radiation damage that could be rectified by further research into dislocation properties.

2. DISLOCATION FORMATION BY POINT-DEFECT AGGREGATION

The three point-defect aggregates whose formation constitute the production of extra dislocations in irradiated materials are the platelet of interstitials - the interstitial dislocation loop, the collapsed platelet of vacancies - the vacancy dislocation loop and the vacancy tetrahedron. It is clearly not appropriate to present a comprehensive survey of all the material, temperature and irradiation conditions upon which the formation of such aggregates depends. The properties and behaviour of these aggregates has been largely studied using transmission electron microscopy and the extensive literature has been reviewed in several excellent articles [1,2,3,4,5]. In the present section it will suffice to identify only some of the general features of such aggregate formation that particularly owe their existence to the dislocation

properties of the aggregates. In addition since the vacancy tetrahedron is a special dislocation configuration that has evolved from a planar vacancy dislocation loop we will mainly restrict the discussion to the two kinds of planar dislocation loops.

2.1 Introductory considerations

The notion that point-defects should cluster to form dislocation loops was first proposed by Frank [6] in 1949 who suggested that vacancies in quenched face-centred cubic (f.c.c.) metals should tend to arrange themselves in discs in the (111) planes and then collapse to form a vacancy dislocation loop, (henceforth, for reasons of brevity, the word 'dislocation' will be omitted when referring to interstitial or vacancy dislocation loops), in order to minimize the energy of the aggregate. Such a vacancy loop with a Burgers vector $\underline{b} = \frac{a}{3}\langle 111\rangle$, has an intrinsic stacking fault and is frequently referred to as a Frank faulted loop. It can unfault by the nucleation and propagation of a Shockley partial across it to produce a perfect loop by a reaction such as:

$$\frac{a}{3}\{111\} + \frac{a}{6}\{11\bar{2}\} + \frac{a}{2}\{110\} \quad . \qquad (1)$$

Alternatively the $\frac{a}{3}\langle 111\rangle$ dislocation segments surrounding the fault can dissociate into a so-called stair-rod pure edge dislocation and a Shockley partial on an intersecting (111) slip plane according to reactions such as:

$$\frac{a}{3}\{111\} + \frac{a}{6}\{110\} + \frac{a}{6}\{112\} \quad ; \qquad (2)$$

the Shockley partials then glide across the intersecting slip planes, meet and react to form a tetrahedron whose edges are all stair-rod dislocations with each face containing an intrinsic stacking-fault. Direct mechanisms for the formation of such tetrahedra from three dimensional vacancy clusters have also been identified [7]. In body-centred cubic (b.c.c.) metals vacancy loops form by the collapse of a disc of vacancies in a (110) plane [1]. In this case, however, such a vacancy loop, with a Burgers vector $\underline{b} = \frac{a}{2}\langle 110\rangle$ can remove its stacking fault by two possible unfaulting shears described by the dislocation reactions [8]:

$$\frac{a}{2}\{110\} + \frac{a}{2}\{00\bar{1}\} + \frac{a}{2}\{1\bar{1}1\} \qquad (3)$$

or

$$\frac{a}{2}\{110\} + \frac{a}{2}\{\bar{1}10\} + a\{010\} \quad . \qquad (4)$$

In either case a perfect loop is formed, although the first reaction (3) should be usually energetically more favourable than the second (4) and the product of the first reaction is a glissile loop in contrast to the sessile loop produced by the second reaction. Such vacancy loops have never been observed after quenching b.c.c. metals - presumably the relatively low degree of vacancy supersaturation achievable by quenching b.c.c. metals together with the usually very high stacking fault energies in such metals preclude their successful nucleation. On the other hand they can, under certain circumstances, be formed in both irradiated f.c.c. and b.c.c.

metals [1]. The reasons and conditions for such vacancy loop formation in irradiated materials will be elucidated below.

Interstitial loops are defined by the interstitials arranging themselves as a disc of extra lattice. The initial crystallographic orientations of these loops are identical to the corresponding vacancy loops for the f.c.c. and b.c.c. lattices and the unfaulting reactions (1), (3) and (4) also apply; the only significant difference is that in the f.c.c. lattice the extrinsic nature of the stacking fault precludes the possible transition to a tetrahedron configuration. Interstitial loops are not observed after quenching; the equilibrium concentration of interstitials is usually quite negligible up to the melting point. They do form under appropriate circumstances in irradiated metals as will be discussed below.

Before concluding this introductory section it is appropriate to make several elementary remarks concerning the physical properties of the intrinsic point-defects whose aggregation we are considering. The interstitial is in general much more mobile than the vacancy, for typical structural metals the migration energy of the interstitial is ~0.2 eV compared with ~1.0 eV for the vacancy [9]. In f.c.c. and b.c.c. metals the interstitial has a split - dumbell configuration in which the extra atom shares a normal lattice site with another atom; there is both theoretical (atomic simulation) and experimental (internal friction) evidence that in f.c.c. metals the interstitial has its dumbell axis parallel to a <100> direction whereas in b.c.c. metals the axis is parallel to a <110> direction [10]. As we shall discuss in section 2.3 these geometrical features of the interstitials are very important in relation to the nucleation of interstitial loops. In contrast to the interstitial, the vacancy does not adopt a split configuration and retains the point symmetry

of the host lattice. Modulus defect measurements [11] and lattice dynamic studies [12] of these point-defects indicate that the interstitial may be regarded elastically as a small inclusion 'soft in shear' compared with the matrix and with a rather large positive relaxation volume ~1 Ω (where Ω is the atomic volume). The vacancy may be regarded as an effective elastic inclusion somewhat softer in compression than the matrix but with a relatively small negative relaxation volume ~ -0.4 Ω; these effective inclusion considerations will be important when we discuss the effects of interactions between dislocations and point-defects.

2.2 Some relevant properties of loops

The elementary crystallography of the loops in f.c.c. and b.c.c. metals has been outlined in the previous section. In this section we present some of the physical properties of loops that will provide further useful background to subsequent sections when specific effects of irradiation are discussed. In particular we present results for the elastic fields of such loops, their energies and their interactions with point-defects and other loops.

2.2.1 The elastic field of a dislocation loop

The displacement field $\underline{u}(\underline{x})$ produced by an arbitrary dislocation loop of Burgers vector $\underline{b}$ in an anisotropic medium is given by the well known Volterra result [13]:

$$u_i(\underline{x}) = \int_S b_j \, c_{jkrs} \, G_{ir,s} \, (\underline{x}' - \underline{x}) dS_k \, (\underline{x}') \, , \qquad (5)$$

where S is a surface bounded by the dislocation line and the subscripts refer to the Cartesian components of the various quantities; c_{ijkl} are the elastic moduli, $G_{ij}(\underline{x}' - \underline{x})$ are the components of the elastic Green's

function and the comma notation means partial differentiation. The elastic distortion

$$\beta_{ij}(\underline{x}) = u_{i,j}(\underline{x}) \qquad (6)$$

then follows by differentiating (5) and Hookes Law yields the stress $p_{ij}(\underline{x})$:

$$p_{ij}(\underline{x}) = \int_S c_{ijkl}\, b_q\, c_{qprs}\, G_{kr,sl}\,(\underline{x}' - \underline{x})dS_p(\underline{x}') \ . \qquad (7)$$

A simple application of Stokes' theorem [14] shows this stress field can be expressed as

$$p_{ij}(\underline{x}) = -\oint_\Gamma \epsilon_{lmp}\, c_{ijkl}\, b_q\, c_{qprs}\, G_{kr,s}(\underline{x} - \underline{x}')dx'_m \qquad (8)$$

where the line integral is taken over the dislocation loop Γ coincident with the boundary of the surface S, $\underline{x}'$ is a point on the loop and ϵ_{ijk} is the Cartesian permutation tensor. The total strain energy associated with such a loop is

$$E = \frac{1}{2}\int_V p_{ij}(\underline{x})\beta_{ij}(\underline{x})dV \qquad (9)$$

where V is the volume of the complete body excluding the cylindrical core region of radius δ surrounding the dislocation; at closer distances than δ to the dislocation line the distortions exceed the range of validity inherent in linear elasticity theory. For a planar loop a simple application of Gauss's theorem and using the fact that the elastic field of a dislocation is body-force free, transforms (9) into the sum of two

surface integrals [15]:

$$E = \frac{1}{2}\int_S p_{ij}(\underline{x})\, b_i n_j dS + \frac{1}{2}\int_{S_\delta} p_{ij}(\underline{x})u_i(\underline{x})dS_j \qquad (10)$$

$$= E_S + E_{S_\delta} \ ,$$

where S is the plane surface (unit normal $\underline{n}$) enclosed by the loop, but terminating a distance δ from the dislocation, S_δ is the curved surface of the core region surrounding the dislocation. The result (10) is valid for either a finite body with zero surface tractions or for an infinite body [15,16].

If the point-defect is represented by an elastic inclusion and has an associated relaxation volume δV, then the size effect interaction energy between the loop and the point defect is [17,18]

$$E_I = -\frac{1}{3}\delta V\, p_{ii}(\underline{x}) \qquad (11)$$

where $\underline{x}$ defines the location of the point-defect; to obtain this simple expression we have assumed that the inclusion is spherical and so small that stress variations over its volume can be neglected. We note also that when expressed in terms of the actual relaxation volume expression (11) for the size-effect interaction energy is also correct when the elastic properties of the inclusion differ from those of the host. Of course in this situation a second order inhomogeneity interaction will also be present and will be described below when we present results for the isotropic medium.

In obvious notation the interaction energy between the loops labelled A and B is

$$E_{AB} = \int_{S_B} P^A_{ij}(\underline{x}') \, b^B_i n^B_j dS(\underline{x}') \qquad (12)$$

where the integration is taken over the plane surface, with normal n^B_j, surrounded by loop B.

When the long range fields or interactions are required it is convenient to use the so-called infinitesimal loop approximation. The stress expression (7) for a plane loop of area A becomes

$$P_{ij}(\underline{x}) = A c_{ijkl} \, b_q \, c_{qprs} \, G_{kr,sl}(\underline{x}) \, n_p \qquad (13)$$

and the long-range interaction between two such loops is then, from (12),

$$E_{AB} = A_B \, P^A_{ij} \, b^B_i \, n^B_j$$

$$= A_A A_B \, c_{ijkl} \, b^A_q \, c_{qprs} \, G_{kr,sl}(\underline{x}) n_p \, b^B_i \, n^B_j \qquad (14)$$

and the corresponding long-range interaction between a loop and point-defect is again given by (11) but with $P_{ij}(\underline{x})$ given by the infinitesimal loop stresses (13).

Several explicit and detailed calculations of loop stresses and the interactions that loops have with point-defects and with other loops been made using these general anisotropic elasticity results. These applications will be referred to below when we discuss the importance of these loops in the irradiation environment but for the theoretical and numerical details required for the evaluation the integrals of the Greens tensor we can usefully refer to the works of Willis [19], Barnett [20],

Meissner [17] and a recent extensive review of the theory of dislocations in anisotropic elastic media by Bacon et al. [21].

The isotropic forms of these various fields and energies associated with loops have been particularly useful for the understanding of radiation damage phenomena and it is therefore appropriate to give some explicit results in this section for later reference. In an elastically isotropic medium the elastic constants may all be expressed in terms of the shear modulus μ and Poisson's Ratio ν:

$$c_{ijkl} = \frac{\mu}{1-2\nu} \left[2\nu \, \delta_{ij} \, \delta_{kl} + (1-2\nu)[\delta_{ik}\delta_{jl} + \delta_{il}\delta_{jk}]\right] \qquad (15)$$

and the Greens' tensor has the analytic form

$$G_{kr}(\underline{x}) = \frac{1}{16\pi\mu(1-\nu)} \left[2(1-\nu)\delta_{kr}|\underline{x}|_{,pp} - |\underline{x}|_{,kr}\right] . \qquad (16)$$

The stress field of a loop is thus given by a single line integral around the loop as in (8); this is essentially the well known Peach-Koehler[22] result. Explicit results for circular loops have been derived by Kroupa [23] and by Bullough and Newman [24] and in this case the stresses can be expressed in terms of elliptic functions [25]. The self-energies of both polygon and circular loops, derivable from (10), for an isotropic medium have been calculated by Bacon [26] and the importance of the core surface traction correction to ensure the energy is unique was first pointed out by Bullough and Foreman [6] in their analysis of the rhombus loop configuration observed in some quenched f.c.c. metals. The elastic energy of a circular loop of radius a and arbitrary Burgers vector $\underline{b}$ as derived by Bacon [26] is

$$E = \frac{\mu a}{2(1-\nu)} \{[b_3^2 + \frac{(2-\nu)}{2}(b_1^2 + b_2^2)][\ln(\frac{8a}{\delta}) - 2]$$

$$+ [2(3-2\nu)b_3^2 - (1-2\nu)(b_1^2+b_2^2)]/8(1-\nu)\} , \qquad (17)$$

where the loop is orientated with its normal parallel to the x_3 direction and thus (17) with $b_1 = b_2 = 0$ represents the energy of a pure edge or Frank loop; when $b_3 = 0$ it represents the energy of a slip or shear loop. The only approximation inherent in (17) is the assumption that the radius of the loop is much greater than the core radius δ; such a restriction must be reasonable since if it were not so any even more accurate loop energy derived using an elastic linear continuum would have little physical significance.

In an isotropic medium Bullough and Willis [27] have derived a general expression for the interaction energy between any applied strain field e_{ij}^A and a small elastic inclusion when the latter is both misfitting and has elastic constants that differ from the host material. When the inclusion represents an interstitial point-defect it is appropriate to set the value of its elastic shear modulus to zero and then the interaction energy takes the simple form [25]

$$E_I = -V\mu\{\frac{15}{8} {}'e_{ij}^A {}'e_{ij}^A + \frac{8}{3} e^A \frac{\delta V}{V}\} \qquad (18)$$

where V is the atomic volume and for simplicity Poisson's Ratio has been set equal to 1/3. The second term in (18) is the size effect interaction and is identical to (11) when the applied dislocation strain e^A arises only from the loop field. The hydrostatic stress is $p_{ii}/3$ which is related to the associated dilatation e_{ii} by $p_{ii}/3 = \frac{2\mu(1+\nu)}{3(1-2\nu)} e_{ii} = \frac{8\mu}{3} e^A$ (when $\nu = 1/3$).

The first term in (18) is the inhomogeneity interaction and has arisen because of the modulus difference between the point-defect and the host. Bullough et al. [25] have obtained analytic expressions for both these interactions for a circular (pure edge) loop when e_{ij}^A arises from both an internal loop field and an external applied stress. This latter consideration is of considerable importance when we discuss irradiation creep and the effects of externally applied stress during irradiation. In view of the relatively small relaxation volume of the vacancy compared to the interstitial, the long-range interaction between a loop and vacancy can be safely neglected. The inhomogeneity expressions for a loop subjected to external stress are very complex [25] and will not be presented here; it will suffice to give only the relatively simple results pertaining to straight dislocations when these sinks are discussed in section 3. However the size-effect interaction energy, corresponding to the second term in (18), or to (11) with $\nu = 1/3$, has the simple form [25]

$$E_I = \frac{2\mu b\delta V}{3\pi} \{K(k) + \left(\frac{a^2-r^2-z^2}{(r-a)^2+z^2}\right)E(k)\}/[(r+a)^2+z^2]^{\frac{1}{2}} \qquad (19)$$

where E(k), K(k) are complete elliptic integrals with arguments defined by

$$k^2 = 4ar/[(r+a)^2 + z^2] \quad , \qquad (20)$$

and (r,z) are the cylindrical coordinates defining the position of the interstitial, with the coordinate origin located at the centre of the circular loop of radius a and the z-axis is normal to the loop plane.

When the long-range interactions between two loops or between a loop and a point-defect are required, then the infinitesimal loop approximation is valid and in an isotropic medium the stress field (13) becomes, for a pure edge infinitesimal interstitial loop (using (15) and (16))

$$P_{ij}(\underline{x}) = \frac{Ab\mu}{4\pi(1-\nu)} \frac{1}{\underline{x}^3}\left[(1-4\nu)\,\delta_{ij} - 2(1-2\nu)\delta_{i3}\delta_{j3}\right]$$

$$- \frac{3}{\underline{x}^5}\left[(1-2\nu)\delta_{ij}x_3^2 + 2\nu(\delta_{3i}x_3x_j + \delta_{3j}x_3x_i)\right. \qquad (21)$$

$$\left. + (1-2\nu)x_ix_j\right] + \frac{15}{\underline{x}^7}\, x_ix_j\, x_3^2 \quad ,$$

where A is the loop area, $\underline{b}=(o,o,b)$ and $\underline{n}=(o,o,1)$. The interaction energy between this loop and another infinitesimal loop with arbitrary Burger's vector and orientation is given directly by (14) with p^A_{ij} replaced by (21). Similarly the long-range interaction between the pure edge loop with the stress field (21) and a point-defect with a relaxation volume δV is given by (11) with $P_{ii}(\underline{x})$ derived from (21) or directly from the limiting form of the finite loop result (19), as $a/r \to 0$ and $A = \pi a^2$. By either procedure we obtain the simple result for the size-effect interaction energy between an infinitesimal loop and a point-defect [25]:

$$E_I = -\frac{\mu b}{3\pi} A\, \delta V(1 - 3\cos^2\theta)/r^3 \quad , \qquad (22)$$

when $\nu = 1/3$ and (r,θ) are the spherical polar coordinates centred at the loop with θ measured from the z-axis that define the location of the point-defect.

2.3 Loop formation and growth

Interstitial loop formation usually occurs from two dimensional interstitial aggregates on the close-packed planes. In f.c.c. metals the planar aggregation is on {111} planes and the loop is faulted with a Burger's vector $\underline{b} = \frac{1}{3}\langle 111\rangle$; such loops can unfault to form a perfect loop by the passage of a Shockley partial dislocation according to the reaction (1). In b.c.c. metals the initial planar aggregation occurs on {110} planes and the relatively high stacking fault energy in such metals leads to unfaulting, probably by homogeneous shear, following either of the reactions (3) and (4) to form loops with $\frac{1}{2}\langle 111\rangle$ or $\langle 100\rangle$ Burger's vector respectively.

Such interstitial loop formation will occur in any high energy irradiation environment when the point-defect generation is uniform, as in the case of electron irradiation, or very inhomogeneous, as in the case of heavy-ion or fast-neutron irradiation, when the point-defects are produced in localized regions or cascades. In contrast, vacancy loops, which again form from two dimensional (vacancy) aggregates on the close-packed planes with similar associated unfaulting reactions as for the interstitial aggregates, are not, in general, observed in electron irradiated materials[5]. Exceptionally they have been observed in thin foils of zirconium irradiated with 1 MeV electrons but the reasons are probably due to the generation of high vacancy supersaturations by oxidation reactions rather than from the homogeneous irradiation. Their formation requires the very high

supersaturation prevailing in the central or denuded regions of the cascades produced by ions or fast neutrons.

The nucleation of loops is influenced by the presence of other loops in the material and these aspects together with the effects of external stresses on loop nucleation will be discussed in this section. The growth aspects to be discussed in this section are largely those pertaining to the behaviour of a single loop; the collective behaviour of loops is deferred to section 4 when we describe the factors influencing the overall evolution of the microstructure. For a detailed review of the experimental observations of loop formation and growth in f.c.c., b.c.c and h.c.p. metals the reader is referred to comprehensive reviews by Eyre [1,5,28].

2.3.1 Interstitial loop nucleation

The temperature dependence and impurity sensitivity of the observed interstitial loop concentrations have been measured in a wide range of f.c.c., b.c.c. and h.c.p. metals and it appears that, except for extremely pure metals, the minimum stable loop nucleus is a di-interstitial and the nucleation is heterogeneous in nature. Figure 1 shows such interstitial loops [29], faulted and perfect, formed in copper after irradiation with 57 KeV protons at 200°C. The details of the initial stages of such loop formation have been studied using atomic simulation techniques. Bullough and Perrin [30] thus confirmed the earlier suggestion by Eyre and Bullough [8] that the interstitials in α-iron would prefer to aggregate as a platelet in a {110} plane with all their split-dumbell axes parallel to a common <110> direction; they demonstrated with the atomic simulation model that such a planar aggregate of interstitials can make the transition to an unfaulted

dislocation loop, with either of the final Burger's vectors, $\frac{1}{2}$ <111> or <100>, when the number of interstitials in the aggregate is sixteen. The former glissile loop was then observed to rotate on its glide prism towards the lower energy pure edge configuration. Ingle et al. [31] have used similar atomic simulation methods to examine the stability and morphology of such interstitial clusters in a range of metals. In f.c.c. and h.c.p. metals the initial nucleation stage consists of a small planar aggregate on a close-packed and prismatic plane respectively which then usually unfaults to form a perfect interstitial loop. It is only in the b.c.c. lattice that there exists the possibility of unfaulting by two different reactions with the possible formation of dislocation loops with different Burger's vector. We shall see later in section 4 that the creation of two different dislocation sinks can have a great influence on the overall response of b.c.c. metals to radiation damage [32]. To actually calculate the evolution during irradiation of the interstitial loop number density-size distribution function it has been found necessary to adopt rather sophisticated numerical schemes [33,34]. A comparison of calculated results with those from an experiment at a single temperature has shown encouraging agreement for the loop number density in nickel and for their subsequent growth [34]. It is relevant to remark here that under irradiation conditions pertinent to such phenomena as void swelling, when the vacancies are also mobile, the irradiation time for completion of the interstitial loop nucleation is usually very short and studies of collective radiation damage processes such as void swelling need only include the growth of such loops and not their nucleation.

The presence of stress arising from either external or internal sources can influence the nucleation of loops. In b.c.c. metals the

stress field of an existing interstitial loop is believed to be responsible for stimulating the nucleation of additional loops in its vicinity; similarly interstitial loop nucleation is observed in the vicinity of existing straight dislocations. Examples of clusters of loops [35] are shown in figure 2 which are dark-field micrographs of neutron irradiated molybdenum at 600°C imaged at a foil normal $\underline{z} = [001]$ with $s = o$. In (a) $\underline{g} = [2\bar{1}\bar{1}]$ and in (b) $\underline{g} = [2\bar{1}1]$. The change in image type of the groups of loops arrowed indicates that all the loops in each group have the same Burgers vector. In the same material and conditions the loop distribution near an edge dislocation [36] is shown in figure 3a. In 3b we show a schematic diagram to indicate that the loops are found predominantly in a wedge shaped volume on the dilatational side of the dislocation. Calculations of the normal stresses on the six possible {110} planes around a loop, using expression (13) for the stress field of a loop, indicate that preferred nucleation does indeed occur on those {110} planes across which the normal stress is tensile and of maximum magnitude; the unfaulting shear stress distribution also plays a role in determining the final Burger's vectors of the new loops. The same conclusion probably applies to the loop distributions observed near the straight-dislocations. Of course in an irradiation situation such an argument is only valid if one assumes that the existing dislocation (straight or loop) has ceased to be a sink for interstitials, presumably because of early unfaulting of the loop or contamination of the straight dislocations. The early unfaulting of the loops in b.c.c. metals probably also assists the loop colony formation because a small perfect loop is usually very glissile. The Peierls stress to move a glissile loop should decrease with decreasing loop radius and

thus loops formed in high stacking fault energy metals (such as the refractory b.c.c. metals) should unfault when small and glide easily when subjected to a suitable stress field. The small perfect loop thus can respond by glide to the loop-loop interactions (14) to further 'concentrate' the colony. Such loop-loop interactions coupled with glide and climb processes are also involved in the formation of rafts of loops so important in the collective microstructural response of b.c.c. metals [32,37,38]. In a similar fashion to these internal stress effects an external tensile stress can enhance the probability of interstitial loops nucleating on the appropriate crystallographic planes that are orientated in sympathy (i.e. orthogonal to the tensile stress axis) with the external stress. Such a preferred nucleation of interstitial loops will cause the body to increase in length in the direction of the applied tension and is the basis of the so-called 'Stress Induced Preferred Nucleation' (S.I.P.N.) mechanism of irradiation creep [39]. There is evidence for this process in some cubic metals at relatively low irradiation doses and further details will be given in section 5 when we discuss irradiation creep.

If n interstitials are required before the interstitial aggregate can form an interstitial loop (n was sixteen in the loop simulation study of Bullough and Perrin [30] for α-iron) then the probability σ^i of a co-operative fluctuation of such an aggregate in response to a normal stress p^i, where i indicates the i^{th} orientation of n_o possible orientations is

$$\sigma^i = e^{p^i n\Omega/k_B T} \Big/ \sum_{j=1}^{n_o} e^{p_j n\Omega/k_B T} \qquad (23)$$

and the number of loops in the i^{th} orientation will be

$$N_L^i = \sigma^i N_L \quad , \tag{24}$$

where N_L is the total number of interstitial loops nucleated. Finally if f^i is the excess fraction of interstitial loops in the i^{th} orientation then

$$\frac{1}{n_o}\left(1 - \sum_{j=1}^{n_o} f^j\right) N_L + f^i N_L = \sigma^i N_L, \quad i=1 \ldots n_o, \tag{25}$$

and thus

$$f^i = \left[e^{p_i n\Omega/k_B T} - 1\right] / \sum_{j=1}^{n_o} e^{p_j n\Omega/k_B T} \quad . \tag{26}$$

If the applied stress is tensile, uniaxial and orthogonal to the i=1 orientation and the other two orientation (i=2,3) are orthogonal ($p^2=p^3=0$) then

$$f^1 = \left[e^{p_1 n\Omega/k_B T} - 1\right] / \left[e^{p_1 n\Omega/k_B T} + 2\right] \quad , \tag{27}$$

and $f^2=f^3=0$; this simple orthogonal scheme was used by Brailsford and Bullough [39] as their basis of the S.I.P.N. model of irradiation creep. In the real b.c.c. situation there are 6 possible [110] orientations corresponding to i=1 ... 6 in (26) and the resolved stress p^i normal to

each must be calculated to obtain the values of σ^i or f^i. Again the specific relevance of these nucleation considerations to irradiation creep is deferred to section 5.

Finally double or higher layer interstitial loops have been observed in f.c.c. metals such as copper and an example can be clearly seen in figure 1c. A mechanism for the nucleation of a second loop just above the first was proposed by Bacon and Bullough [42] for quenched-in vacancy loops; it involved the notion that an appropriate aggregate could form above the fault of the first loop which could then nucleate the loop when the first loop climbed away. Such a mechanism should be even more appropriate for interstitial loop nucleation since the interstitial supersaturation should locally be much higher than that for the vacancies.

2.3.2 Vacancy loop nucleation

The presence of mobile interstitials precludes the formation of vacancy loops in homogeneously irradiated cubic metals. They form only in the high vacancy supersaturation prevailing in the denuded zones of displacement cascades [5]. In figure 4 we show micrographs [43] of ordered Cu_3Au foils that have been irradiated to a dose of 5.3×10^{21} n/m^2 (E > 1 MeV) at 80°C with fission neutrons. In (a) the area is imaged in the dark-field superlattice reflection $\underline{g} = (0\bar{1}\bar{1})$ when the disordered zones formed within cascades are visible by structure factor contrast. (The large black areas are anti-phase boundaries). In (b) the area is imaged under bright-field kinematic conditions using $\underline{g} = (02\bar{2})$, when dislocation loops are visible. The arrowed disordered zones contain loops while the circled disordered zones do not. The precise mechanism of the vacancy aggregation and collapse to form the small vacancy loops from the high vacancy concentrations present in such denuded zones is not fully understood. The size of the vacancy loops upon formation is such that only about one-third

of the available vacancies in the zone are involved in their formation and of the cascades that could collapse to form such loops only about one-third do so. Such loops form at temperatures below that when isolated vacancies are mobile and therefore if the loop formation is thermally activated the effective vacancy mobility when their concentration is as high as 10% must be considered. At such concentrations presumably one can consider the divacancy as the mobile entity, in which case a much higher mobility than the single vacancy is to be expected. With such a model it is easy to show[44] that a three dimensional cavity could not grow - too many divacancies would diffuse out of the zone rather than inwards towards the growing cavity. On the other hand, if a very small vacancy loop ever forms in the central region of the zone the inwards motion of divacancies would be enhanced by the drift flow to the loop arising from the elastic interaction between such a loop and a divacancy (equation 19). Thus we can see that vacancy loop growth to an observable size could occur at temperatures well below those required for vacancy migration and also understand why cavities do not form in such denduded zones. However, plausible as this seems, there is now some growing evidence that vacancy loop formation in such zones may not be thermally activated; they apparently form at liquid helium temperatures[45]. Further study is needed to clarify this situation since if these last observations are confirmed we are forced to consider a shock wave or thermal spike model for such loop formation.

In an irradiation environment vacancy loops produced from the collapse of denuded zones will usually have only a finite lifetime; the high line tension and the fact that they are a preferential sink for interstitials

both conspire to remove them. However since they are being continuously produced their presence can have a significant effect on the evolution of microstructure; the global effects of such loops will be discussed in section 4. In some materials vacancy loops can grow under irradiation. In neutron irradiated zirconium vacancy and interstitial loops of equal size are observed [46]. We believe this growth occurs because the small vacancy loops are a weaker sink for interstitials than are the larger interstitial loops; they therefore must receive a net vacancy flux [47]. Again further discussion of this collective behaviour of loops will be deferred to section 4, since considerations of net point-defect fluxes to sink types involve considerations of the total population of sink types, including voids, etc., that make up the total microstructure. Suffice it to remark that vacancy loops will only grow in irradiated materials if relatively neutral sinks such as voids are not present and such is generally the case in zirconium.

2.3.1 Annealing of isolated loops

Although we have deferred the discussion of the collective behaviour of loops in irradiated materials to a later section it is appropriate to explain how such loops should respond to annealing conditions. Such a discussion enables us to introduce many of the physical quantities involved in the behaviour of point-defects near dislocations that will be needed for the sink strength derivations required for later discussions of the collective behaviour of dislocation loops.

We thus consider a circular faulted loop of radius a that can be of either interstitial or vacancy character and seek to determine its rate of shrinkage when subjected to a high temperature anneal. At some distance R

>> a from the loop we therefore set the vacancy concentration to its equilibrium value C_v^e for the annealing temperature. When the collective influence of other microstructure upon the growth behaviour of a particular loop is required this vacancy concentration would have to be the self-consistent average concentration as used for sink strength calculations (section 4). We should also emphasise that no interstitials are involved in this discussion; we are concerned only with annealing considerations. To calculate the net vacancy flux to such a loop we replace it by an effective spherical sink [48,47], also of radius a and ensure that the vacancy flux into the sphere is precisely equal to the actual vacancy flux into the loop core; the loop, with a square x-section core of side b where b is the Burgers vector of the loop, and its affective sphere are depicted in figure 5. If the loop is of vacancy type then in detail we have:

Vacancy loop

Number of vacancies entering the loop/second is

$$\underset{(1)}{\left[2\pi a b^2 \frac{c_v}{b^3}\right]} \times \underset{(2)}{[\nu]} \times \underset{(3)}{[\alpha_v]} \times \underset{(4)}{[nb]} \times \underset{(5)}{\left[\exp\left(-\frac{\bar{E}_m^v}{k_B T}\right)\right]} \quad , \qquad (28)$$

where each term may be identified as follows:

(1) The number of vacancies available to jump into the loop; c_v is the fractional vacancy concentration just outside the loop and for simplicity the atomic volume is taken as b^3.

(2) Frequency of atomic vibration plus the entropy factor.

(3) A geometrical factor defining the probability of a vacancy jumping in the direction of the loop.

(4) Probability of a suitable site being present on the loop to accept the vacancy; n is concentration of jogs/unit length.

(5) Probability of overcoming the activation energy at the matrix-core interface; the activation energy surfaces adjacent to the loop-core are depicted in figure 6. Equation (28) may be written

$$\frac{2\pi a}{b^2} n \eta_v D_v c_v \qquad (29)$$

where

$$D_v = b^2 \alpha_v \nu \exp(-E_m^v/k_B T) \qquad (30)$$

is the usual vacancy diffusion coefficient and

$$\eta_v = \exp\left[(E_m^v - \bar{E}_m^v)/k_B T\right] \quad . \qquad (31)$$

Number of vacancies leaving the loop/second is

$$\underset{(1)}{[2\pi a n]} \times \underset{(2)}{[\nu]} \times \underset{(3)}{[\alpha_v]} \times \underset{(4)}{[\exp -(E_f^v + \bar{E}_m^v)/k_B T]} \times \underset{(5)}{[\exp(\gamma_I + F_{el}) b^2/k_B T]} \qquad (32)$$

where again each term may be identified:

(1) The number of sites (jogs) from which vacancy emission is possible.

(2) Frequency of atomic vibration plus entropy factor.

(3) An appropriate geometrical factor.

(2) and (3) are taken equal to the corresponding values in (28).

(4) Probability of emitting the vacancy into the matrix according to the activation energies in figure 6.

(5) The energy change of the loop when the vacancy is emitted. γ_I is the intrinsic stacking-fault energy and $F_{el} = (1/2\pi a)(dE/da)$ is the line tension force/unit length of dislocation tending to shrink the loop, where E is the elastic energy of the loop; for the present pure edge loop (17) yields

$$F_{el} = \frac{\mu b^2}{4\pi(1-\nu)a}\left[\ln\frac{8a}{b} - \frac{(1-2\nu)}{4(1-\nu)}\right] \quad . \tag{33}$$

$\gamma_I b^2$ is thus the fault energy lost when the vacancy is emitted and $F_{el}b^2$ is the elastic energy lost when the vacancy is emitted. Equation (32) may be written

$$\frac{2\pi a}{b^2}\, n\, \eta_v\, D_v\, \bar{c}_{VL} \quad , \tag{34}$$

where

$$\bar{c}_{VL} = c_v^e \exp[(\gamma_I + F_{el})b^2/k_B T] \quad , \tag{35}$$

and the subscript VL indicates 'Vacancy Loop'. The net vacancy flux into the vacancy loop is thus, from (29) and (34)

$$\frac{2\pi a}{b^2}\, n\eta_v\, D_v(c_v - \bar{c}_{VL}) \tag{36}$$

which equals

$$\frac{d}{dt}\left[\frac{\pi a^2 b}{b^3}\right] = \frac{2\pi a}{b^2}\frac{da}{dt} \quad . \tag{37}$$

The concentration c_v adjacent to the loop in (36) is then deduced by forcing the net vacancy flux (36) into the loop to be identical to the net vacancy flux

$$\frac{4\pi a^2}{b^3} D_v \frac{dc_v}{dr}\Big]_a \quad , \tag{38}$$

into the effective sphere, as shown in figure 5. The boundary condition on the sphere then follows by equation (37) and (38):

$$\frac{dc_v}{dr} = \frac{b}{2a}\, n\, \eta_v\, (c_v - \bar{c}_{VL}) \text{ at } r = a \quad . \tag{39}$$

With this boundary condition and the condition

$$c_v \to c_v^e \text{ as } r \to \infty \quad , \tag{40}$$

the quasi steady state vacancy concentration around the sphere is

$$c_v = c_v^e - \frac{abn\,\eta_v}{r(2 + bn\,\eta_v)}\,(c_v^e - \bar{c}_{VL}) \quad . \qquad (41)$$

Hence the concentration at r = a required in (36) then yields, from (36) and (37), for the rate of change of loop radius:

$$\frac{da}{dt} = \left[\frac{2nb\,\eta_v}{2 + nb\,\eta_v}\right] \frac{D_{vs}}{b}\left[1 - \exp\left[(\gamma_I + F_{el})b^2/k_BT\right]\right] , \qquad (42)$$

where

$$D_{vs} = D_v c_v^e \quad , \qquad (43)$$

is the self-diffusion coefficient.

Interstitial loop

By following exactly the same effective sphere procedure for the interstitial loop, recognizing the fact that such a loop shrinks by absorbing vacancies rather than by emitting them as in the vacancy loop situation, we obtain for the annealing rate of change of the interstitial loop radius

$$\frac{da}{dt} = \left[\frac{2nb\eta_v}{2 + nb\,\eta_v}\right] \frac{D_{vs}}{b}\left[\exp\left[-\,(\gamma_E + F_{el})b^2/k_BT\right] - 1\right] \qquad (44)$$

where γ_E is the extrinsic stacking fault energy.

Results analogous to (42) and (44) for the behaviour of a loop under annealing conditions have been given previously by Eyre and Maher [38] and indicate quite different shrinkage behaviour of the two kinds of loop; thus we may summarize: both kinds of loop if unfaulted and large, should

shrink very slowly at about equal rates since the magnitude of F_{el} will then be small. Large faulted loops will shrink faster at the constant rate

$$\frac{da}{dt} = -\left(\frac{2nb\,\eta_v}{2 + nb\,\eta_v}\right) \frac{D_{vs}}{b}\left[\frac{\gamma b^2}{k_BT}\right] \qquad (45)$$

where γ is either γ_I or γ_E; since $\gamma_E > \gamma_I$, the faulted interstitial loop should shrink faster in this size regime. As the loop radius decreases a transition in shrinkage rate should occur when $F_{el} \gtrsim \gamma$. After this transition the two kinds of loops behave quite differently; the rate of shrinkage of the vacancy loop will increase exponentially whereas the rate of shrinkage of the interstitial loop increases to and then remains at the constant value

$$\frac{da}{dt} \to -\left(\frac{2nb\,\eta_v}{2 + nb\,\eta_v}\right) \frac{D_{vs}}{b} \quad . \qquad (46)$$

The two kinds of perfect loop also ultimately behave in a similar fashion when the magnitude of F_{el} becomes significant. This predicted behaviour is shown schematically in figure 7 and is qualitatively consistent with experimental observations of loop annealing kinetics [29,38,49].

3. NETWORK DISLOCATIONS

The dislocation (loop or straight segment) has a long-range interaction[50,18] with both interstitials and vacancies. However the larger relaxation volume associated with the interstitial compared to that of the vacancy ensures that there is potentially a greater flux of interstitials than

vacancies to the dislocations. It follows that under irradiation, when equal numbers of interstitials and vacancies are being continuously created, any interstitial loops that have nucleated should grow and any vacancy loops should shrink. Such interstitial loops will continue to grow until they evolve into a radiation produced dislocation network. At this stage the total dislocation network consists of the initial 'deformation produced' dislocations plus this radiation produced component. Of course, if the material was severely cold-worked prior to irradiation it is likely that all the radiation produced point-defects will be lost at the existing network and no new interstitial loop nucleation and growth will occur. Details of these microstructural evolution questions are deferred to later sections. It will suffice to comment here that such continual loop growth under irradiation together with network generation and evolution can only continue if a suitable relatively neutral sink type exists to recieve a net vacancy flux. Such a sink-type would be voids or grain-boundaries etc. If only dislocations (of one type) are present and no other sink type is present then all the irradiation produced point defects would be lost by mutual recombination at the dislocations or in the bulk and radiation would cease to affect the microstructure.

To set the scene for the discussion of these evolutionary processes we present in this section some details of the long and short-range interactions between 'straight' dislocations and point-defects.

3.1 The long-range interaction between a dislocation and point-defects

The long-range interaction energy between a dislocation and a nearby point-defect can be estimated by representing the point-defect as a misfitting inhomogeneity [51] of small volume V with a bulk and

shear modulus $\bar{\kappa}$ and $\bar{\mu}$ respectively, that may differ from the corresponding host moduli κ and μ; the misfit is defined by the uniform misfit strain, which is the strain required to deform the inclusion back to the size and shape of the hole in the host into which it was forced. Since the inclusion is of atomic dimensions the spatial variations of stress and strain within it may be ignored and for this situation the interaction energy between such an inclusion and a general applied strain field e^A_{ij} has the form: [27,52,53]

$$E_I = -V\{\mu A' e^A_{ij} {}' e^A_{ij} + \frac{\kappa}{2} C(e^A)^2 + 2\mu B' e^A_{ij} {}' \bar{e}_{ij} + \kappa D e^A \bar{e}\} \qquad (47)$$

where $e = e_{kk}$ and $'e_{ij} = e_{ij} - \frac{1}{3}e\delta_{ij}$ is the deviatoric part of e_{ij}. In equation (47) we have:

$$A = (\mu - \bar{\mu})/[\mu - \beta(\mu - \bar{\mu})] \quad , \qquad (48)$$

$$B = \bar{\mu}/[\mu - \beta(\mu - \bar{\mu})] \quad , \qquad (49)$$

$$C = (\kappa - \bar{\kappa})/[\kappa - \alpha(\kappa - \bar{\kappa})] \quad , \qquad (50)$$

$$D = \bar{\kappa}/[\kappa - \alpha(\kappa - \bar{\kappa})] \quad , \qquad (51)$$

where,

$$\alpha = (1 + \nu)/3(1 - \nu) \quad , \qquad (52)$$

$$\beta = 2(4 - 5\nu)/15(1 - \nu) \quad , \tag{53}$$

and ν is Poisson's ratio for the host medium. If the applied strain field e^A_{ij} arises from a dislocation strain field e^D_{ij} and a strain field e^E_{ij} due to an external applied stress, such that

$$e^A_{ij} = e^D_{ij} + e^E_{ij} \tag{54}$$

then the interaction energy between a dislocation and the inclusion, in the presence of an external stress follows from equations (47) and (54):

$$E^D_I = -V\{\mu A[{}'e^D_{ij}\ {}'e^D_{ij} + 2{}'e^E_{ij}\ {}'e^D_{ij}] \tag{55}$$

$$+ \tfrac{\kappa}{2} C[(e^D)^2 + 2e^E e^D] + 2\mu B{}'e^D_{ij}\ {}'\bar{e}_{ij} + \kappa D\, e^D \bar{e}\}.$$

This expression may be further simplified by dropping the terms second-order in the dislocation strain field and by assuming the misfit strain is the pure dilatation strain $\bar{e}$, so that

$${}'\bar{e}_{ij} = 0 \quad , \tag{56}$$

when equation (55) becomes[27]

$$E^D_I = -V\{2\mu A\ {}'e^E_{ij}\ {}'e^D_{ij} + \kappa C e^E e^D + \kappa D e^D \bar{e}\} \quad . \tag{57}$$

If the dislocation lies along the x_3 axis of a Cartesian coordinate

system (x_1,x_2,x_3) with Burgers vector $\underline{b} = (b,o,o)$, then its strain field e^D_{ij} has the deviatoric components

$$\begin{aligned}
{}'e^D_{11} &= -L\frac{\sin\theta}{r}[1-2\nu + 6\cos^2\theta] \quad , \\
{}'e^D_{22} &= -L\frac{\sin\theta}{r}[1 - 2\nu - 6\cos^2\theta] \quad , \\
{}'e^D_{33} &= 2L\frac{\sin\theta}{r}(1-2\nu) \quad , \\
{}'e^D_{12} &= 3L\frac{\cos\theta}{r}(2\cos^2\theta - 1) \quad ,
\end{aligned} \tag{58}$$

and dilatation

$$e^D = -6L(1 - 2\nu)\frac{\sin\theta}{r} \quad , \tag{59}$$

where $L = b/12\pi(1 - \nu)$. Similarly if the e^E_{ij} strain field is due to the application of a uniaxial tensile stress τ parallel to the Burgers vector of this edge dislocation (i.e. parallel to the x_1-axis) then

$$\begin{aligned}
{}'e^E_{11} &= \tau/3\mu \quad , \\
{}'e^E_{22} &= {}'e^E_{33} = -\tau/6\mu \quad ,
\end{aligned} \tag{60}$$

and

$$e^{E} = \tau(1 - 2\nu)/2\mu(1 + \nu) \quad , \qquad (61)$$

with obvious permutations when the applied tensile stress is rotated parallel to either of the other two axes. When the external stress is removed the interaction energy, equation (57), becomes the well known size effect interaction E_I^0 and for this dislocation has the explicit form [50]:

$$E_I^0 = \frac{\alpha\, b\, \mu}{\pi} \Delta V \frac{\sin\theta}{r} \quad , \qquad (62)$$

where ΔV is the relaxation volume suffered by the arbitrarily large but finite host when the point defect is introduced into it. We note that ΔV is related, for this general misfitting inhomogeneity, to the misfit strain $\bar{e}$ of the inclusion by

$$\Delta V = D\, V\, \bar{e} \quad ,$$

and to the 'hole strain' (i.e. the strain defined by the displacement of the surface of the hole into which the inclusion is forced) $\bar{e}_o$ by

$$\Delta V = V\bar{e}_o/\alpha \quad .$$

The 'hole strain' $\bar{e}_o$ may be formally identified with the relaxation volume change ΔV_∞ when the point defect is introduced into an <u>infinite</u> body:

$$\bar{e}_o = \Delta V_\infty / V \quad .$$

However ΔV and not ΔV_∞ is the observable quantity usually referred to as the relaxation volume of the point defect. Finally, for completeness, the actual strain within the inclusion, when embedded in the host is

$$e_I = \bar{e} - \bar{e}_o = \frac{\Delta V}{V} \cdot \frac{\kappa}{\bar{\kappa}} (1 - \alpha) \quad .$$

It follows, from equation (57) and the above explicit formulae, that the long range interaction between the point-defect and the dislocation depends critically on the magnitude of ΔV and will be sensitive to both the magnitude and direction of any external applied stress. For the stress free situation, defined by equation (62), it is immediately clear that as the interaction energy for the interstitial, $\Delta V_i \sim 1.2\Omega$, is greater than that for the vacancy, $\Delta V_v \sim -0.5\Omega$, a bias exists for the capture of an interstitial by a dislocation. The same basic conclusion holds equally for edge dislocation loops of vacancy and interstitial type.

In the presence of an external tensile stress, the interaction energy follows from (57) with (58) and the varients of (60). For the three orthogonal orientations of external stress shown in figure 8 we may write the total interaction energy between the dislocations and the point-defect:

$$E_I^D = E_I^0 + \left(\frac{\tau}{\mu}\right) E_I^{11} \quad , \qquad (63)$$

where E_I^0 is the interaction energy (62) in the absence of the external stress τ and E_I^{11} is the coefficient of (τ/μ) in the total interaction energy, when the uniaxial tension is parallel to the x_1 axis. We find

$$E_I^{11} = \frac{\mu Vb}{12\pi(1-\nu)} \frac{\sin\theta}{r} \left\{A\left[(1-2\nu)+6\cos^2\theta\right] + 2C(1-2\nu)\right\}$$

$$E_I^{22} = \frac{\mu Vb}{12\pi(1-\nu)} \frac{\sin\theta}{r} \left\{A\left[(1-2\nu)-6\cos^2\theta\right] + 2C(1-2\nu)\right\} \qquad (64)$$

$$E_I^{33} = \frac{\mu Vb}{6\pi(1-\nu)} (1-2\nu) \frac{\sin\theta}{r} \{-A + C\} \quad .$$

The sensitivity of the interaction energy to the magnitude and direction of the external applied stress has important consequences in theories of irradiation creep [27,54,55]. To demonstrate that this is so we consider the inclusion representation of the dumbell interstitial [27]. It is known from measurements of the defect modulus in irradiated materials [11,12,27] that such interstials have a characteristic soft shear mode and therefore it is appropriate to represent the dumbell interstitial by a small inclusion that is soft in shear ($\bar{\mu} \to 0$) but highly incompressible ($\bar{\kappa} \to \infty$) with a positive relaxation volume strain $\Delta V/V \gtrsim 1$. With this, albeit rather extreme representation,

$$A \to \frac{15(1-\nu)}{7-5\nu} \quad ,$$

$$B \to 0 \quad , \qquad (65)$$

$$C \to -\frac{3(1-\nu)}{1+\nu} \quad ,$$

and (64) becomes

$$E_I^{11} = \frac{3\mu\, Vb}{2\pi} \frac{\sin\theta}{r} \frac{(1 + 8\nu - 5\nu^2)}{(7-5\nu)(1+\nu)} \quad ,$$

$$E_I^{22} = -\frac{3\mu\, Vb}{2\pi} \frac{\sin\theta}{r} \frac{(4-3\nu + 5\nu^2)}{(7-5\nu)(1+\nu)} \quad , \qquad (66)$$

$$E_I^{33} = -\frac{6\mu\, Vb}{\pi} \frac{\sin\theta}{r} \frac{(1-2\nu)}{(7-5\nu()1+\nu)} \quad ,$$

where, for simplicity, we have replaced $\cos^2\theta$ and $\sin^2\theta$ in equation (64) by their mean value of $\frac{1}{2}$.

In this continuum model all these energies must be terminated at some core 'cut-off' radius, say $r = b$. From equation (66) we see that only E_I^{11} is positive and thus only when the uniaxial tension τ is parallel to the Burgers vector of the edge dislocation (Fig. 8(b)) does the presence of such an external stress increase the total interaction energy. It follows that more interstitials will migrate to dislocations disposed relative to τ as in Fig. 8(b) than to dislocations disposed as in Figs. 8(a) or 8(c). An excess flux of interstitials to such oriented edge dislocations will cause the body to extend preferentially in the direction of the external tension; this is the fundamental source of the so called Stress Induced Preferred Absorption (S.I.P.A.) mechanism of irradiation creep [27,54,25].

In contrast to the dumbell interstitial a vacancy is probably best represented in the continuum model by a small inclusion that is soft in compression ($\bar{\kappa} \to 0$), with only a small defect modulus in shear ($\bar{\mu} \simeq \mu$) and with a negative relaxation volume strain that is

smaller in magnitude than that of the interstitial ($\Delta V/V \sim -0.5$). With this representation

$$A \to 0$$

$$B \to 1 ,$$

$$C \to \frac{3(1-\nu)}{2(1-2\nu)} ,$$

and equation (64) then yields for the vacancy

$$g_I^{11} = g_I^{22} = g_I^{33} = \frac{\mu V b}{4\pi} \frac{\sin\theta}{r} . \qquad (67)$$

For the vacancy it is clear from equation (67) that the external stress yields a contribution that is independent of the orientation of the edge dislocation and therefore we expect little contribution to a S.I.P.A. mechanism of irradiation creep from asymmetries in the vacancy fluxes to the dislocations present in the medium.

3.2 The short-range interaction between a dislocation and a point-defect

In section 2.3.3 we discussed the factors controlling the emission or absorption of a vacancy at a dislocation loop and hence determined the shrinkage rate of such a loop under annealing conditions. In this section we wish to supplement that discussion to include the expected behaviour of an interstitial as well as a vacancy in the vicinity of the dislocation core; we shall then be able to define the appropriate boundary conditions needed for the subsequent dislocation sink-strength calculations outlined

in section 4. Since we are now dealing with network dislocations the stacking fault energy and line tension, so important in the analysis of loop annealing, will be relatively unimportant and we may consider the network dislocations to be long, straight, cylindrical sinks with the long-ranged interaction fields described in section 3.1; the presence of these long-range fields was neglected for the vacancy-dislocation loop discussion in section 2.3.3.

As we discussed in section 2.3.3, when a point-defect arrives at one of the sites adjacent to the dislocation core its probability of jumping into the core will depend on whether its entry into the core requires the presence of a jog. There is considerable evidence [56] that a vacancy can formally enter a dislocation core and then rapidly 'pipe-diffuse' to the nearest jog. On the other hand it has been suggested [56] that if a dumbell-interstitial enters a dislocation core its subsequent motion in the core may be slower than it was in the matrix. Such a distinction, in which the vacancies are preferentially absorbed into the core, can be considered a short-ranged bias and has been used [57] to partially mitigate the strong interstitial bias that would follow from considerations of the long-range interaction alone with the dislocation an ideal sink for both interstitials and vacancies. Even if this relative pipe diffusion mobility is not acceptable, similar short-range mitigation can follow by recalling that there is considerable atomic simulation evidence [58,59] that the attractive inhomogeneity interaction between a vacancy and a dislocation becomes dominant over the strongly angular size-effect interaction at sites adjacent to the dislocation core whereas for the interstitial the size-effect interaction always dominates. This means that the vacancy can probably enter the core from any site adjacent to the core whereas the

interstitial will be repelled from certain sites [57,60]; interstitials would not be expected to enter the core from sites on the compressed side of the edge dislocation core. Both or either of these processes can be modelled by the construction of a suitable rate limitation boundary condition for interstitial or vacancy capture at the dislocation core [57,60] and some details will be given in section 4.

4. MICROSTRUCTURAL EVOLUTION AND THE DISLOCATION SINK-STRENGTH

To obtain a quantitative understanding of the evolution of any sink-type, such as the growth of voids (the swelling rate) or the climb-rate of particularly oriented dislocations (to yield the irradiation creep rate) during irradiation, it is necessary to treat simultaneously the various point-defect loss processes to all the sinks and by bulk recombination. A complete description of the evolving microstructure under irradiation is thus required. In figure 9 we show a typical microstructure of irradiated steel containing voids, loops and network all of which are clearly visible. The micrograph, provided by D. Mazey, is of a PE16 alloy after irradiation by 46 MeV Ni^+ ions at 525°C to a total dose of 60 dpa. Such a description of the microstructure can be provided by replacing the crystalline material, with its spatially varying intrinsic local point-defect concentrations associated with the various geometrically defined atomic or extended defects, with their associated internal stress fields, by an effective homogeneous continuum [48,61-63]. In this effective or lossy continuum the intrinsic point-defect concentrations are homogeneous and the actual sinks are replaced by effective sinks. The values of these sink strengths for each of the real sink types that make up the total

microstructure are obtained by an embedding procedure which is basically analogous to that first used by Maxwell [64] in his analysis of electrical conduction through heterogeneous media. The general form of the rate theory model of the total evolving microstructure is outlined in section 4.1 and the method for obtaining the various required sink strengths is illustrated particularly for the straight dislocation sink in section 4.2. Finally in section 4.3, some problems specific to the other sink types will be briefly mentioned.

4.1 The rate theory model

The theoretical description of irradiation damage by chemical rate theory has about a 10 year history [48,65], and has reached the stage where general purpose codes for calculating void swelling and irradiation creep are being made available to an audience wider than just those workers involved deeply in the theoretical development [66].

In the following, the rate equations are presented for a system under irradiation and containing voids, interstitial loops, dislocation network and grain boundaries as sinks [62,66]. The equations are:

$$\frac{dc_v}{dt} = K_v - k_v^2 D_v c_v - \alpha c_i c_v \quad , \tag{68}$$

$$\frac{dc_i}{dt} = K_i - k_i^2 D_i c_i - \alpha c_i c_v \quad , \tag{69}$$

$$\frac{dq_{vC}}{dt} = k_{vC}^2 D_v c_v - k_{iC}^2 D_i c_i - K_{vC}^e \quad , \tag{70}$$

$$\frac{dq_{iN}}{dt} = k_{iN}^2 D_i c_i - K_{vN}^2 D_v c_v + K_{vN}^e \quad , \tag{71}$$

$$\frac{dq_{iIL}}{dt} = k^2_{iIL} D_i c_i - k^2_{vIL} D_v c_v + K^e_{vIL} \quad , \qquad (72)$$

and

$$\frac{dq_{vGB}}{dt} = k^2_{vGB} D_v c_v - k^2_{iGB} D_i c_i - K^e_{vGB} \quad . \qquad (73)$$

Here, α is the rate constant for the bulk recombination of interstitials and vacancies, c_v and c_i are the fractional concentrations of vacancies and interstitials in the medium respectively; q_{vC}, q_{iN}, q_{iIL} and q_{vGB} are the fractional number of vacancies in cavities, interstitials in network and interstitial loops and vacancies in grain boundaries respectively; D_v and D_i are the vacancy and interstitial diffusion coefficients (as above); and, K_v and K_i their production rates, both through the irradiation and by thermal emission from the sinks. Hence, if K is the defect production rate through irradiation;

$$K_i = K \quad , \qquad (74)$$

and

$$K_v = K + K^e_{vC} + K^e_{vN} + K^e_{vIL} + K^e_{vGB} \quad , \qquad (75)$$

where K^e_{vC}, K^e_{vN}, K^e_{vIL} and K^e_{vGB} are the vacancy emission rates from cavities, network, interstitial loops and grain boundaries respectively; the exact form of these is not presented herein, but can be obtained from Windsor et al. [66]. The terms such as $k^2_{vC} D_v c_v$ describe the loss rates of point defects to the various point defect sinks, in this case vacancies to cavities. The quantities such as k^2_{vC} are called <u>sink strengths</u>, in this case the sink strength of cavities for diffusing vacancies. The total sink strengths for

vacancies, k^2_v, and interstitials, k^2_i, are written;

$$k^2_v = k^2_{vC} + k^2_{vN} + k^2_{vIL} + k^2_{vGB} \quad , \qquad (76)$$

and

$$k^2_i = k^2_{iC} + k^2_{iN} + k^2_{iIL} + k^2_{iGB} \quad , \qquad (77)$$

and the quantities $(k_i)^{-1}$ and $(k_v)^{-1}$ are the mean distances a free interstitial or vacancy moves in the medium before becoming trapped. The central problem in the rate theory of microstructural evolution is the determination of the various sink strengths for migrating point-defects.

The rate theory equations (68-73) above do not deal with the effects of the damage produced by cascade collapse to form vacancy loops. The modifications required to include this phenomenon involve [67] two additional rate equations for the number of vacancy loops per unit volume, N_{VL}, and the fractional number of vacancies in loops, q_{vVL}. Thus;

$$\frac{dN_{VL}}{dt} = \frac{n_{VL}}{\Omega} - \frac{N_{VL}}{\tau} \quad , \qquad (78)$$

and

$$\frac{dq_{vVL}}{dt} = \epsilon K - k^2_{iVL} D_i c_i + k^2_{vVL} D_v c_v - K^e_{vVL} . \qquad (79)$$

In these equations, n_{VL} is the fractional concentration of vacancy loops created per second;

$$n_{VL} = \frac{\varepsilon K b^2}{\pi r_{VL}^2(0)} \quad , \qquad (80)$$

where b is the magnitude of the Burgers vector (as above) and Ω, the atomic volume, has been set equal to b^3, εK is the fractional rate at which vacancies are removed from solution to form vacancy loops, and $r_{VL}(0)$ is the initial radius of newly formed vacancy loops. τ is the lifetime of the vacancy loops and is given, from a Taylor series expansion of $r_{VL}(t)$, by,

$$\tau = - \frac{r_{VL}(0)}{dr_{VL}/dt}\Big|_{r_{VL}(0)} \quad . \qquad (81)$$

The loop shrinkage rate, dr_{VL}/dt, can be expressed in terms of the vacancy loop sink strengths for interstitials, k^2_{iVL}, and vacancies, k^2_{vVL}, and the vacancy emission rate from vacancy loops, K^e_{vVL}. To complete the modifications, equations (75) to (77) become, respectively;

$$K_v = (1-\varepsilon)K + K^e_{vC} + K^e_{vN} + K^e_{vIL} + K^e_{vGB} + K^e_{vVL}, \qquad (82)$$

$$k^2_v = k^2_{vC} + k^2_{vN} + k^2_{vIL} + k^2_{vGB} + k^2_{vVL} \quad , \qquad (83)$$

and

$$k^2_i = k^2_{iC} + k^2_{iN} + k^2_{iIL} + k^2_{iGB} + k^2_{iVL} \quad . \qquad (84)$$

This formulism to include the formation of vacancy loops from displacement cascades therefore introduces two new parameters into the rate theory model: (i) $r_{VL}(0)$, the radius of the vacancy loops immediately following their formation, which can be estimated directly from experiment; and (ii) ε, where εK is the fractional rate at which vacancies are removed from solution to form vacancy loops. In practice ε is the adjustable parameter which distinguishes between electron (ε = 0) and cascade damage (0<ε<1), and may be derived in the manner outlined by Bullough and Quigley [68] and Bullough et al.[67]. Alternatively, it may be possible to gain more direct information on ε from detailed experimental observations of displacement cascades. It is the values of $r_{VL}(0)$ and ε in the theory which chiefly serve to distinguish fusion and fast fission neutron damage.

4.2 The dislocation sink-strength

Two approaches have been proven for deriving sink strengths for use in the rate theory of microstructural evolution. One of these is concerned with spatially periodic sink arrays, and the other with completely random sink distributions. The fundamental validity of these two approaches has been discussed at length by Brailsford and Bullough [63]. In the present short summary, only the effective medium model for a random distribution of sinks is discussed, since long range order is only rarely observed.

In this section we illustrate the calculational procedure by summarizing a recent analysis for the dislocation sink strength by Bullough and Quigley [57,69] that leads to an analytical result and incorporates aspects of both the long and short-ranged interactions described in section 3.

The edge dislocation is a line sink with a cylindrical domain of influence within which it interacts with the intrinsic point-defects as described in section 3. The dominant long-ranged interaction energy stems

from the interaction between the hydrostatic stress field of the dislocation and the distortion field of the point-defect and is given by the expression (62). The long-ranged and angular form of this interaction energy makes the averaging process required for the derivation of an equivalent sink strength for the net-work dislocations in the lossy continuum rather complex. By embedding the dislocation with a surrounding associated sink-free region within which the interaction is present, into the lossy continuum with no spatially varying interactions, Brailsford and Bullough [60,63] have previously given an approximate prescription for the derivation of a dislocation sink strength; unfortunately it was not possible to justify fully the choice of the radius of the sink-free region, since the exact embedding problem could not be easily solved. The essential mathematical difficulty arises from the presence of the angular term in the interaction energy and we have thus performed a sequence of calculations to justify the dropping of this term which then permits an embedding procedure which yields analytic sink strengths for the dislocations whose accuracy is known. A cellular model, with an implied periodic distribution of dislocations, has been used to justify replacing the angular interaction potential with a purely radial one. In the cellular calculations the presence of a second sink type within each cell is allowed for and furthermore, the direct effects of bulk recombination on the resulting sink strengths is also included. It is found, as might be expected [63], that such a cellular model can lead to appreciable error in the sink strengths and in the consequent swelling when the second sink types are omitted from within each cell. However, with the second sink types present (i.e. the actual voids for example), we conclude that both the angular variation of the interaction and direct effects of bulk

recombination can be safely neglected. Having established that the angular form of the interaction energy between the edge dislocation and a nearby point-defect can be safely dropped we can use this purely radial interaction in the embedding approach to derive a rigorous dislocation sink strength.

We consider a long straight edge dislocation lying along the z axis of the cylindrical coordinate system (r,z). If E(r) is the purely radial interaction energy between this dislocation and a point-defect at r, given by (62) with the angular term $\sin\theta$ replaced by unity, then in order to derive an analytical sink strength for such dislocations we follow the embedding procedure developed by Brailsford and Bullough [48,63] and define a sink free region $r < R$ surrounding the dislocation within which E(r) is present but outside of which the interaction vanishes and other sinks are present. The dislocation surrounded by the sink free region embedded in the lossy continuum is depicted in figure 10.

The field equations for the steady state point-defect concentration c(r) are

$$\frac{d^2c}{dr^2} + \left(\frac{1}{r} + \frac{d\phi}{dr}\right)\frac{dc}{dr} + \left(\frac{d^2\phi}{dr^2} + \frac{1}{r}\frac{d\phi}{dr}\right)c + \frac{K}{D} = 0 \qquad (85)$$

for $r_c < r < R$ and

$$\frac{d^2c}{dr^2} + \frac{1}{r}\frac{dc}{dr} - k^2c + \frac{K}{D} = 0 \qquad (86)$$

for $r > R$

where

$$\phi(r) = E(r)/k_BT \qquad (87)$$

and k_B is Boltzmann's constant, T is the absolute temperature, r_c is the dislocation core radius, K is the point-defect production rate (dpa/sec), k^2 is the total sink strength of all the defect types present in the effective medium. These equations have been solved with continuity of concentration and point-defect flow at r = R and with the simple radial interaction defined, from (62), by

$$\phi(r) = -L/r \qquad (88)$$

where

$$L = \frac{(1+\nu)\mu b\ \Delta V}{3\pi(1-\nu)k_B T} \quad ; \qquad (89)$$

μ is the shear modulus, ν is Poisson's Ratio, b is the magnitude of the Burgers vector of the dislocation and ΔV is the relaxation volume of the point-defect.

The form and approximate magnitude of the radius R of the sink free zone may be obtained, following the procedure adopted by Brailsford and Bullough [63] when the angular form of E was retained, by equating the coefficients of c in (85) and (86) to yield

$$\frac{d^2\phi}{dr} + \frac{1}{r}\frac{d\phi}{dr} = -k^2; \qquad (90)$$

that is, from (88),

$$R = (L/k^2)^{1/3} \quad . \qquad (91)$$

The accuracy of this estimate for R has been checked by detailed numerical solutions of the single field equation with E(r) and k^2 present

simultaneously; in this case we were not able to obtain an analytic solution of the differential equation and hence the resort to separation of E(r) and k^2 embodied in equations (85) and (86) with a sink free region. The results of this numerical study will be commented upon shortly. Before doing so some remarks concerning the necessary boundary conditions at the dislocation core are appropriate.

The most general core boundary conditions has the rate limitation form [18,62] at $r = r_c$

$$\frac{dc}{dr} + \frac{d\phi}{dr}c = (n_j b)f\frac{\bar{K}}{D}c \qquad (92)$$

where

$$\bar{K} = \frac{D}{b}\exp\left[(E_m - E_m')/k_B T\right] \qquad (93)$$

is the transfer velocity into the core itself, E_m is the normal perfect crystal defect migration energy and E_m' allows for the possibility of a modified final jump barrier, as discussed in section 2.3.3 for the dislocation loop; for simplicity we will neglect this barrier modification and set $E_m = E_m'$.

Recalling the discussion on the possible short-range interactions in section 3.2, $n_j b$ in (92) is the jog concentration per atom plane along the dislocation and the quantity f, given by

$$f = \alpha b/2\pi r_c \qquad (94)$$

defines the fraction of such adjacent sites from whence such a jump into the core is possible (α is the actual number of available sites from which capture is possible). In (94) $\alpha = 2\pi r_c/b$ ($f = 1$) thus means that capture is possible from all such sites. Again from the discussion in section 3.2 the dominance of the inhomogeneity interaction over the size effect interaction for vacancies near the core suggests $f^v = 1$, whereas for interstitials the size-effect interaction remains always dominant and $f^i < 1$. The precise values of f and $n_j b$ are difficult to estimate and we shall see in section 5 that the values of these parameters must be fitted when we correlate the predictions of the rate theory to swelling in actual materials.

Finally to ensure the validity of the field equations (85) and (86) the core radii must be chosen to exclude interaction energy gradients that are too large; in fact we require that

$$b\frac{d\phi}{dr} < 1 \qquad (95)$$

which, with the equality, yields the lower bound core radius value

$$r_c = (Lb)^{\frac{1}{2}} \quad . \qquad (96)$$

We note from (89) since $L^i > L^v$ that $r_c^i > r_c^v$.

Subject to the various boundary conditions an analytic solution of (85) and (86) has been obtained and used to calculate the loss rate of point-defects to unit length of the dislocation:

$$2\pi r_c D\left(\frac{dc}{dr} + \frac{d\phi}{dr}c\right)_{r_c} \quad . \qquad (97)$$

This flow is then equated to the corresponding loss rate to a dislocation in the effective medium (i.e. a large distance from the identified dislocation) [63]:

$$ZK/k^2 \quad . \qquad (98)$$

The final result for the bias parameter Z for the dislocation is then

$$Z = \frac{\pi\{[2+k^2 e^{L/R}(Q-Pr_c^2)]kRK_1(kR)+k^2(R^2-r_c^2)K_o(kR)\}}{K_o(kR) + Pe^{L/R}kRK_1(kR)} \qquad (99)$$

where

$$P = E_1(L/R)-E_1(L/r_c) + \frac{b}{(n_j b)f}\frac{e^{-L/r_c}}{r_c} \qquad (100)$$

$$Q = \frac{L^2}{2}\left(E_1(L/R) - E_1(L/r_c)\right)$$

$$+ \tfrac{1}{2}\left[R(R-L)e^{-L/R} + r_c(L-r_c)e^{-L/r_c}\right] + \frac{b}{(n_j b)f} r_c\, e^{-L/r_c}, \qquad (101)$$

K_o, K_1 are modified Bessel functions of the second kind and E_1 is the exponential integral. The bias parameter when the dislocation core is assumed to provide an ideal sink for the point-defect ($c = 0$ at $r = r_c$) follows from (99) with the final terms in P and Q omitted ($f \to \infty$ say).

The accuracy of this bias parameter using the sink free region concept and a truncated interaction energy has been checked against a purely numerical solution of the single field equation with no truncation of the interaction energy and the second sink present everywhere. The agreement is

excellent for a wide range of values of L and k^2 when R is assumed to have precisely the value given by the deduced relation (91).

4.3 Summary of present sink strength situation

To use the rate theory, as described in section 4.1, to analyse the swelling or irradiation creep in irradiated materials we require reliable and easily computable sink strengths for each of the various sink-types that together define the total microstructure. The dislocation sink strength described in some detail in section 4.2 is an example of such a sink strength and is currently used in rate theory analyses of steels. For completeness, in this section, we merely identify the various sink-types that have been studied, together with a brief commentary on each corresponding sink strength that is currently available for inclusion in the rate theory. The stage is then set for the next section where we present some of the results that have been obtained using rate theory together with an indication of the degree of successful correlation between the predictions and experimental observations in real irradiated materials.

4.3.1 The interstitial loop [48,60]

In general this is a growing toroidal sink and to avoid the obvious geometrical complexity of such a diffusion field an equivalent spherical sink, as described in section 2.3.3 is used. The sphere has the same radius as the loop and the rate limitation on the spherical sink is adjusted to ensure that the flux of point-defects to the sphere is equal to the flux into the torus. The sphere is then embedded in the lossy continuum as described below in section 4.3.3. When the loop is an ideal sink and relatively isolated its sink strength can be deduced using a

simple capacitance analogy [63] to a charged metal torus to scale the far diffusion field.

4.3.2 The vacancy loop [47]

In general this is a small shrinking toroidal sink and again an equivalent spherical sink has been used to obtain its strength. Because of stress field cancellation effects the sink strength of loops should decrease with loop size. This is why, when voids are not present, vacancy loops, in the presence of large interstitial loops and network dislocations can actually grow by absorbing vacancies since they are the "most neutral" sinks present. Such effects are observed in zirconium [46] where swelling is not, in general, observed.

4.3.3 The spherical void or cavity [48,61]

The spherical void is usually considered to be a relatively neutral sink and its sink strength has been obtained using the fully consistent embedding procedure. Its growth can be rate controlled with a low point-defect transfer velocity at its interface or diffusion controlled as an ideal sink. The long-ranged induced interactions between the void and a nearby point-defect are small but some authors [70] consider these interactions have an important influence on the growth of the voids, particularly if segregation of a 'hardening' element around the voids occur during irradiation.

4.3.4 The grain boundary [63,72,73]

These sinks are usually assumed to have spherical form, although for strong texture a suitable ellipsoidal form can be adopted. The spherical shell representing the grain boundary can be a rate limited or ideal sink. The essential feature of such sinks is that their strength is dominated by the point-defect losses to sinks within the grains as they migrate to the

grain boundaries; that means that they are an example of a sink whose strength is 'to first order' dominated by loss to other sinks and not to themselves. The empty grain limit is not a useful extreme in practice. We refer to such sinks as strongly interactive.

4.3.5 The foil surface [74]

This is a one dimensional limit of the above grain boundary sink and is important for the interpretation of radiation damage data from thin foil experiments such as in the 1 MeV High Voltage Electron Microscope (HVEM). It is also strongly interactive since the point-defect loss at the foil surface depends to first order on the total sink content of the foil interior.

4.3.6 Atom and precipitate traps [73]

These are traps that are saturable and do not nucleate growing voids; if they did they would be virtually indistinguishable from the void sinks. The sink strength of the single atom traps are obtained by defining a point-defect occupation probability at such traps. Thus a vacancy trap will either be unoccupied when it can then accept a vacancy or it will be occupied by a vacancy when it can accept an interstitial. Recombination will then occur and the trap will become unoccupied. Finally an occupied vacancy trap can release its vacancy by overcoming a specified binding energy. By time averaging this trapping and release situation over all such traps we can define the required occupation probability and hence the sink strength. Similarly an interstitial trap will only accept an interstitial when unocupied etc. The saturable precipitate trap is simply a recombination site and the prohibition of vacancy accumulation there is achieved by it automatically adopting an appropriate interstitial bias.

Such behaviour might be expected at the surface of coherent precipitates where micro-void nucleation should be difficult.

4.3.7 Other Sinks

Several calculations have been made to emphasize special features of the above sink types. These include sink strength changes when the sinks are spatially ordered, as for the voids that make up a void lattice [75] and the modifications needed to include transient changes in the position or morphology of the sinks. Thus the net flux of interstitials to the dislocations cause them to climb. This finite climb rate can be self-consistently incorporated into the sink strength [76] estimate and does yield modifications that can be important in certain radiation damage regimes. Similarly, the actual transient motion of the void surface can be self-consistently incorporated into the void sink strength [77] and again yields modifications with possible regimes of significance. Some of these aspects will be raised again in the final section where we discuss some outstanding problems and prospects for future research.

5. SWELLING, CREEP AND GROWTH OF REACTOR MATERIALS

In this section we present some results of actual attempts to model, with the rate theory, the radiation damage response of some real reactor materials. We begin in section 5.1 with the swelling of M316 stainless steel under heavy-ion and neutron irradiation, then in section 5.2 we decribe the low temperature irradiation creep correlation in the same steel. Finally in section 5.3 we present some results of a study of irradiation growth in zirconium and the direct measurements of dislocation climb in HVEM irradiation experiments in that material.

5.1 The swelling in M316 steel

In this attempt by Bullough and Quigley [68] to understand the observed swelling behaviour of M316 steel the microstructure was assumed to consist primarily of network dislocations and voids and the various physical parameters required to define the sink strengths of these two sink-types were determined by fitting the theoretically predicted swelling under electron irradiation to relevant HVEM data [78]. This calibrated rate theory was then used, without further modification, to predict the swelling behaviour of the steel under 46.5 MeV Ni^{6+} and fast neutron irradiation; the only further 'parameter' required is the cascade collapse efficiency ε (described in equation 80) to account for the very different recoil spectra of heavy ions and fast neutrons compared with the electrons.

Two theoretical curves for the Ni^{6+} irradiations are shown in figure 11 together with the experimental results of Hudson [79] at 40 dpa. The calculations were started with the experimental swellings at 16 dpa, so that only the transition from the swelling at 16 dpa to the swelling at 40 dpa was predicted. The dashed curve in figure 11 was obtained without vacancy loops (ε=0) and the very good correlation at 40 dpa (the solid curve) was obtained with ε=1.2%. The results clearly demonstrate the importance of cascade collapse processes for the heavy ion irradiation of this steel.

With no further adjustment of <u>any</u> parameters, including ε, the dose rate was reduced to that appropriate for the fast reactor and the predictions given in figure 12 for the swelling transition from 39 dpa to 62.5 dpa were obtained. The relevant data [80] at these two doses is also shown in the figure. We now see a much reduced sensitivity to ε and a prediction of the swelling at 62.5 dpa (the solid line) that is quite close to the observed values over the entire temperature range. The lack of

sensitivity to the recoil spectrum under fast neutron irradiation occurs in this steel because the total sink densities are rather high at the lower temperatures and thus the presence of vacancy loop sinks do not make a significant increase to the total sink strength of the microstructure. It follows that, for this steel, recoil effects are not qualitatively significant and the high energy electron simulation can itself enable a reasonable prediction of the swelling under fast neutron irradiations to be made.

5.2 Irradiation creep in M316 steel

Irradiation creep occurs because the intrinsic point-defects can be selectively absorbed by the evolving microstructure in such a fashion that the body extends in sympathy with an applied stress. This process of selective or preferred absorption can yield either creep strain due to the net climb of dislocations alone or can lead to the de-stabilization of segments of dislocation which can then glide under the applied stress and so yield creep strain due to slip. In general it is not yet clear whether climb or slip is the dominant source of the irradiation creep strain. However, various possible mechanisms have been identified and it is clear that a judgment concerning the source of the creep strain can only be made when a rigorous mathematical framework is used to interpret and analyse the available experimental data. In this section we identify only two of these mechanisms: The Stress Induced Preferred Nucleation (S.I.P.N.) [81,39,40] and the Stress Induced Preferred Absorption (S.I.P.A.) [54,27,82] mechanisms. Brief comments concerning each of these will be made and the latter S.I.P.A. will be shown to provide a good explanation of the irradiation creep of M316.

5.2.1 S.I.P.N. - stress induced preferred nucleation [81,39,40]

The stress can enhance the probability of the planar interstitial aggregates nucleating on crystallographic planes that are oriented in sympathy (i.e. orthogonal to the stress axis) with the external stress. The excess numbers of such interstitial loops in the "aligned" orientation thus means that more extra lattice planes have been put down in this orientation (orthogonal to the stress axis). The body has thus increased its length in the direction of the stress and irradiation creep has occurred. Alternatively, the vacancies may also aggregate to form vacancy loops but in this case the stress can enhance the probability of the loops lying on suitable planes parallel to the stress. Again such a process will enhance the length increase of the body in the direction of the tensile stress. This is the basis of the S.I.P.N. mechanism of irradiation creep. As discussed in section 2.3.1 if f is the excess fraction of aligned interstitial loops then the concentration of such aligned loops, N_{AL}, is[39]

$$N_{AL} = \frac{1}{3}(1-f)N_L + fN_L \quad , \qquad (102)$$

and the concentration of non-aligned loops, N_{NL} is

$$N_{NL} = \frac{2}{3}(1-f)N_L \quad , \qquad (103)$$

where N_L is the total loop concentration and f has the 'Boltzmann' form [31]

$$f = \exp[\tau\Omega n/k_B T) - 1]/[\exp(\tau\Omega n/k_B T) + 2] \; . \qquad (104)$$

In equation (104), τ is the applied tensile stress, Ω is the atomic volume, n is the number of interstitials in the critical nuclei of the loop, k_B is Boltzmann's constant and T is the absolute temperature. The resulting creep strain arising from this asymmetry in the loop population is

$$\varepsilon = \frac{2}{3}\left[\pi r_L^2 b\, N_{AL} - \frac{1}{2}\pi r_L^2 b\, N_{AL}\right] \qquad (105)$$

$$= \frac{2}{3}\pi b\, f\, N_L r_L^2 \quad , \qquad (106)$$

where b is the lattice spacing (or magnitude of the Burger's vector of the interstitial loops) and r_L is the average radius of the loops. If $\rho_L = 2\pi r_L N_L$ is the density of dislocations associated with the loop population then, by differentiating (106), the strain rate may be written

$$\dot{\varepsilon} = \frac{2}{9}\frac{b\tau n}{k_B T}\rho_L \dot{r}_L \quad . \qquad (107)$$

Finally, if the microstructure consists of a total dislocation density ρ (network plus loops) and voids then this creep rate $\dot{\varepsilon}$ is related to the swelling rate $\dot{S}$ by

$$\dot{\varepsilon} = \frac{2f}{3}\frac{\rho_L}{\rho}\dot{S} \quad . \qquad (108)$$

The relation (108) is only valid at temperatures well below the peak swelling temperature for the material and, of course, when no other creep mechanisms are active.

Several aspects of this mechanism and its consequences are worthy of comment:

a) The magnitude of this creep rate can be in reasonable agreement with observations in solution treated steel at low temperature; however this agreement involves choosing a rather large value of n for the initial interstitial aggregate. It is also a linear function of the stress τ, again in agreement with observation; however the inexorable increase in ρ_L, implied by (107), is unreasonable at high doses and some recovery processes should eventually occur after loop-loop interference effects take place. Such limitations on the dislocation density will inevitably lead to a non-linear stress dependence [83].

b) This mechanism is really a kind of stress induced growth and once the loop nucleation regime is over the 'creep rate' ought to be independent of any subsequent stress change; there is evidence that such independence of creep rate on stress does not occur. We must therefore conclude that this mechanism cannot be appropriate at high doses.

c) The creep rate should be directly proportional to the swelling rate; there is some evidence for such a correlation [84].

d) There is also some direct T.E.M. evidence for asymmetries in the loop population that could be qualitatively consistent with this mechanism.

However, such asymmetries can also arise from the S.I.P.A. mechanism to be discussed below.

5.2.2 S.I.P.A. - stress induced preferred absorption [54,27,82]

It was shown in section 3.1 (equation 66) that the presence of an external tensile stress τ can lead to a small perturbation in the amplitude of the usual first-order interaction between a dislocation and a nearby interstitial. This perturbation is sensitive to the orientation of the dislocation relative to the external stress and leads to an enhanced flux of interstitials to those dislocations orientated with their extra planes orthogonal to the direction of the external stress axis. In addition, since the effect is a simple modification of the amplitude of the long range interaction between dislocations and point-defects, it can easily be incorporated into the rate theory formalism. This means that questions regarding the effects of other damage processes, such as swelling, can also be studied. Thus for example, the creep strain rate in the presence of a volume concentration C_c of growing voids of average radius r_c can be shown to have the relatively simple form [85,86]

$$\dot{\varepsilon} = \frac{75}{384\pi} K \tau \left[\frac{\rho Z_{oi}^2}{(4\pi r_c C_c + Z_{oi}\rho)\, \mu e_i^o}\right] \quad . \qquad (109)$$

In this equation, K is the damage rate, τ is the applied tensile stress, μ is the shear modulus, e_i^o is the relaxation volume strain associated with an isolated dumbell interstitial which is modelled by an effective inclusion with zero shear modulus and $Z_{oi}\rho$ is the sink strength of the dislocation

network, where ρ is the total dislocation density. Z_{oi} is the stress-free bias parameter defining the first-order preference that dislocations have as sinks for interstitials compared to vacancies.

The simple relation (109) suggests the following:

a) The creep rate is proportional to damage rate K and to the stress τ, as observed [84].

b) The magnitude of the predicted creep rate [85] is in quite good agreement with experimental data; particularly at low temperatures, as shown in figure 13. At high temperatures, thermal emission processes will become important and expression (109) is not applicable.

c) If the dislocation network is the dominant sink, equation (109) becomes

$$\dot{\varepsilon} = \frac{75\ K\ \tau\ Z_{oi}}{384\pi\ \mu\ e_i^o} \quad . \qquad (110)$$

This is consistent with the observed independence of creep rate on the degree of cold work.

d) The direct dependence of the creep rate on the swelling is evident through the term $4\pi r_c C_c$ in the denominator of (109). In general, therefore, the S.I.P.A. mechanism leads to an inverse coupling between swelling and creep rate such that the onset of void swelling should lead to a reduction in creep rate. There is, unfortunately, little direct evidence for such a dependence. However, the simplistic nature of (109) should be emphasized and a study of the coupling using the more sophisticated temperature and dose dependent bias parameter [68] could well yield the kind of direct coupling that is usually observed (or inferred). Further study

of this question is in progress.

5.3 The irradiation growth in zirconium

The nature of irradiation damage in zirconium and its alloys has been investigated in detail for some time [46,87,88] due to their important role as core component materials in several designs of thermal reactor systems. It has been established that under neutron irradiation such hexagonal materials undergo irradiation growth and that the microstructure evolves into a complicated combination of both vacancy and interstitial loops and other less well defined microstructural features. It is clear however that the dominant reason for such growth stems from the preferrential nucleation and growth of interstitial loops on the prismatic planes; the vacancies are then lost at such sinks as grain boundaries, existing network dislocations or aggregate to form vacancy loops on the basal planes. In alloys the vacancies are also trapped at impurity atom traps (e.g. tin atoms in Zircaloy are apparently efficient vacancy traps [89,90]).

To circumvent the obvious complexity of the damage in bulk material under neutron irradiation, experiments have made in the HVEM in which the actual climb rate of the interstitial loops have been measured [90]. Such accurate and relatively direct measurements provide a stringent test of the rate theory. In this section we therefore outline the interpretive study of such climb in pure zirconium foils. In this work the only sinks present are the climbing interstitial dislocation loops, all located on the six prismatic planes, and the two foil surfaces. Only very occasionally were voids observed to form and their presence had little effect on the average growth kinetics. In pure zirconium the growth strain was observed to increase linearly with dose as indicated in figure 14 with no sign of any

saturation process. In contrast the alloy materials were all observed to saturate but all showed the same growth rates at low doses. The reasons for such saturation effects are now reasonably well understood [89,90] and we believe they occur because of vacancy trapping on appropriate solute atoms. These features are however rather detailed and will not be discussed further; the interested reader is referred to reference (89) for a reasonably complete interpretative account of growth in zirconium and its alloys. In figure 14 we show also the theoretical growth rate curve for pure zirconium; the excellent agreement between theory and the experimental points was only achieved by adopting a vacancy migration energy of 0.65 eV. At the time of publication of the interpretation this predicted low migration energy was severely criticised and cast some doubt upon the overall validity of the interpretation. However, subsequent diffusion studies [91] have now completely substantiated the predicted 'low' value. The rate theory approach must therefore be regarded as further vindicated.

6. CONCLUDING REMARKS

In this brief review of the significance of dislocations to radiation damage processes we have restricted the discussion to those dislocation properties that seem to us to dominate the situation. Much of our understanding is as yet very imprecise and great reliance has to be put on calibration procedures when we attempt to predict the behaviour of real materials. The calibration of the rate theory parameters for a given material is usually made using simulation data and we have had some success in then using such calibrated models to predict the material response under neutron irradiation. However, because of the large number of material variables that are involved in such representations of real alloys it is

obvious that our parameterization cannot be regarded as unique. For this reason it is essential to reduce the number of such unknown parameters by appropriate theoretical or experimental effort. Of particular relevance to the dislocation components of the microstructure we may identify the following, where more information or understanding would be valuable.

(i) The dislocation sink strength contains several physical parameters which, for a given material, should be known. Thus, the long-range interaction between the dislocation and a point-defect requires a knowledge of the relaxation volumes of the point-defects; the short-range behaviour of the point-defects near and within the dislocation core could be carefully studied using atomic simulation methods and with the recent construction of more physically based interatomic potentials for the transition metals [92] such a study would be particularly timely.

(ii) The self-consistent influence of the dislocation climb and the motion of the void surface during swelling needs to be fully understood. Such 'dynamic' effects may well be important during pulse irradiation [93] conditions such as may be expected in a fusion reactor environment.

(iii) The mechanism of helium trapping on dislocations and any resolution processes need further study, possibly using atomic simulation procedures as for the intrinsic point-defect interactions in (i) above. In addition, other impurity elements may be expected to segregate at the dislocations and other sinks during irradiation. We need to know whether such segregation would be expected to radically change the strength of such sinks for subsequent intrinisic point-defect absorption or emission.

(iv) The effect of external stress on the long-range interaction between a dislocation and a point-defect should be calculated with a better model than the elastic inclusion representation of the point-defect. The significance of the interactions at the point-defect saddle-point also needs clarification when estimating the overall S.I.P.A. mechanism of irradiation creep.

(v) The mechanism of dislocation loop ordering or void lattice formation needs to be understood. One of the most beautiful examples of such a void lattice is shown in figure 15. This was found by Evans [94] in high purity molybdenum after irradiation with 2MeV N^+ ions at a temperature of 870°C. Its particular relevance to this review stems from the dislocation in the lattice indicated by the arrow! Similarly, the collective response of dislocation networks to irradiation is also only poorly understood. Radiation will often stimulate recovery and recrystallization processes with premature formation of domain structures in stressed materials, and only recently have we begun to study the question of inherent stability of such dislocation distributions to irradiation. The indications are that irradiation can indeed have a significant effect on such phenomena as high temperature thermal creep[53,83]; a notion that raises obvious interpretive problems.

(vi) The rate theory currently developed describes only the growth or development of existing microstructures. It is not designed to deal with the important question of nucleation of the various sink-types. Although some useful studies have been made on various aspects of the nucleation problem, a comprehensive treatment that includes all the contributory influences is not yet available. In this connection, although there

is considerable understanding of the factors that influence the nucleation of interstitial loops, there is little or no real understanding as to why vacancy loops can form so relative easily and apparently athermally within the denuded zones of displacement cascades.

ACKNOWLEDGMENTS

The author is most grateful to Drs C. A. English, J. H. Evans and D. J. Mazey for providing advice and several beautiful micrographs.

REFERENCES

1. Eyre, B.L. (1973) J.Phys.F., 3, 422.

2. Eyre, B.L., Loretto, M.H. and Smallman, R.E. (1977) Vacancies '76: The Metals Society, London.

3. Wilkens, M. (1970) Modern Diffraction and Imaging Techniques: North-Holland, Amsterdam. 4. Wilkens, M. (1977) Vacancies '76: The Metals Society, London.

4. Wilkens, M. ('70) Modern Diffraction and Imaging Techniques: North-Holland, Amsterdam.

5. Eyre, B.L. (1984) Proc. of the Eshelby Memorial Symposium on 'Fundamentals of Deformation and Fracture": Sheffield University, C.U.P.

6. Frank, F.C. (1949) Proc.Phys.Soc., London, A62, 202.

7. Hussein, M.A. and Dodd, R.A. (1971) Phil.Mag. 24, 1441.

8. Eyre, B.L. and Bullough, R. (1965) Phil.Mag. 12, 31.

9. Balluffi, R.W. (1976) Proc. of Int.Conf. on 'Properties of Atomic Defects in Metals': Argonne, Illinois, North-Holland.

10. Schilling, W. (1976) Ibid.

11. Holder, J. Granato, A.V. and Rahn, L.E. (1974) Phys.Rev. B10, 363.

12. Dederichs, P.H. (1977) Vacancies '76: The Metals Society, London.

13. Volterra, V. (1907) Ann.Ecole Normale Supér. 24, 401.

14. Mura, T. (1963) Phil.Mag. 3, 625.

15. Bacon, D.J., Bullough, R. and Willis, J.R. (1970) Phil.Mag. 22, 31.

16. Bullough, R. and Foreman, A.J.E. (1964) Phil.Mag. 9, 351.

17. Meissner, N., Savino, E.J., Willis, J.R. and Bullough, R. (1974) Phys.Stat.Sol. 63, 139.

18. Bullough, R. and Newman, R.C. (1970) Rep.Prog. in Physics 33, 101.

19. Willis, J.R. (1970) Phil.Mag. 21, 931.

20. Barnett, D.M. (1972) Phys.Stat.Sol. 49, 741.

21. Bacon, D.J., Barnett, D.M. and Scattergood, R.O. (1979) Prog. in Materials Science 23, 51.

22. Peach, M. and Koehler, J.S. (1950) Phys.Rev. 80, 436.

23. Kroupa, F. (1961) Czech.J.Phys. B11, 847.

24. Bullough, R. and Newman, R.C. (1960) Phil.Mag. 5, 921.

25. Bullough, R., Wells, D.W., Willis, J.R. and Wood, M.H. (1980) Proc.of Int.Conf. on 'Dislocation Modelling of Physical Systems': Gainesville, Florida, Perg.Press.

26. Bacon, D.J. (1965) Ph.D Thesis, Battersea College of Technology, London.

27. Bullough, R. and Willis, J.R. (1975) Phil.Mag. 31, 855.

28. Eyre, B.L. (1975) Proc.of Int.Conf. on 'Fundamental Aspects of Radiation Damage in Metals', Gatlinburg, Tenn. USA.

29. Mazey, D.J. (1972) M.Sc.Thesis, University of Salford.

30. Bullough, R. and Perrin, R.C. (1968) Proc.Roy.Soc. A305, 541.

31. Ingle, K.W., Perrin, R.C. and Schober, H.R. (1981) J.Phys.F. 11, 1161.

32. Little, E.A., Bullough, R. and Wood, M.H. (1980) Proc.Roy.Soc. A372, 565.

33. Kiritani, M. (1975) Proc.of Int.Conf. on 'Fundamental Aspects of Radiation Damage in Metals', Gatlinburg, Tenn. USA.

34. Hayns, M.R. (1980) Harwell Res. Reports AERE-R.9708 and R.9818.

35. English, C.A. (1982) Jnl.Nucl.Mater. 108 and 109, 104.
36. Riley, B. (1983) Ph.D. Thesis, University of Birmingham.

37. Eyre, B.L., Maher, D.M. and Bartlett, A.F. (1971) Phil.Mag. 23, 439.

38. Eyre, B.L. and Maher, D.M. (1971) Phil.Mag. 24, 767.

39. Brailsford, A.D. and Bullough, R. (1973) Phil.Mag. 27, 49.

40. Brailsford, A.D. and Bullough, R. (1972) Proc. of Conf. on 'Irradiation Embrittlement and Creep in Fuel Cladding and Core Components', BNES London.

41. Lewthwaite, G. (1973) J.Nucl.Mater. 46, 324.

42. Bacon, D. J. and Bullough, R. (1968) Phil.Mag. 18, 561.

43. English, C.A. and Jenkins, M.L. Unpublished work.

44. Bullough, R. and Eyre, B.L. Unpublished work.

45. Black, T.J. (1984) D.Phil.Thesis, Oxford University.

46. Northwood, D.O. (1977) At.Energy Rev. 15, 548.

47. Bullough, R., Hayns, M. R. and Woo, C. H. (1979) J.Nucl.Mater. 84, 93.

48. Brailsford, A.D. and Bullough, R. (1972) J.Nucl.Mater. 44, 121.

49. Silcox, J. and Whelan, M. J. (1960) Phil.Mag. 5, 1.

50. Cottrell, A. H. and Bilby, B. A. (1949) Proc.Phys.Soc. London 62, 49.

51. Eshelby, J.D. (1957) Proc.Roy.Soc. A241, 376.

52. Bullough, R. and Willis, J.R. (1984) Proc. of the Eshelby Memorial Symposium on 'Fundamentals of Deformation and Fracture: Sheffield University, C.U.P.

53. Nabarro, F.R.N., Bullough, R. and Matthews, J.R. (1982) Acta.Metall. 30, 1761.

54. Heald, P.T. and Speight, M.V. (1974) Phil.Mag. 29, 1075.

55. Bullough, R. and Heald, P.T. (1977) Vacancies '76: The Metals Society, London.

56. Balluffi, R.W. and Grenato, A.V. (1979) 'Dislocations in Solids' (Chap. 13), vol4, (Edited by F.R.N. Nabarro) North-Holland.

57. Bullough, R. and Quigley, T.M. (1981) Proc.Yamada Conf. on 'Point Defects and Defect Interactions in Metals', Kyoto, Japan, Tokyo press.

58. Bullough, R. and Perrin, R.C. (1968) Dislocation Dynamics, McGraw-Hill, New York.

59. Miller, K.M. (1981) J.Phys.F. 11, 1175.

60. Brailsford, A.D. and Bullough, R. (1977) Vacancies '76: The Metals Society, London.

61. Brailsford, A.D., Bullough, R. and Hayns, M.R. (1976) J.Nucl.Mater. 60, 246.

62. Bullough, R. and Hayns, M.R. (1977) 'Continuum Models of Discrete Systems', University of Waterloo Press.

63. Brailsford, A.D. and Bullough, R. (1981) Phil.Trans.Roy.Soc. 302, 87.

64. Maxwell, J.C. (1892) 'A Treatise on Electricity and Magnetism' Clarendon Press, Oxford.

65. Harkness, S.D. and Li, C.Y. (1971) Metall.Trans. 2, 1457.

66. Windsor, M., Bullough, R. and Wood, M.H. (1979) Harwell Res.Rep. AERE-R.9595; (1981) Harwell Res.Rep. AERE-R.10251; (1982) Harwell Res.Rep. AERE-R.10683.

67. Bullough, R., Eyre, B.L. and Krishan, K. (1975) Proc.Roy.Soc. A346, 81.

68. Bullough, R. and Quigley, T.M. (1983) J.Nucl.Mater. 113, 179.

69. Bullough, R. and Quigley, T.M. (1981) J.Nucl.Mater. 103 and 104, 1397.

70. Mansur, L.K. (1978) Nucl. Technology. 40, 5; (1979) Phil.Mag. A39, 497; (1981) Phil.Mag. A44, 867.

72. Brailsford, A.D. and Bullough, R. (1973) Proc.of Conf. 'Physical Metallurgy of Reactor Fuel Elements', Berkeley, U.K., Metals Society.

73. Brailsford, A.D. and Bullough, R. (1976) J.Nucl.Mater. 69 and 70, 434.

74. Bullough, R., Wood, M.H. and Pierce, S.M. (1981) Met.Science 15, 342.

75. Bullough, R., Hayns, M.R. and Wood, M.H. (1980) J.Nucl.Mater. 90, 44.

76. Rauh, H. and Bullough, R. (1984) To be published.

77. Bullough, R. and Ghoniem, N.M. (1984) J.Nucl.Mater. (in press).

78. Makin, M. J., Walters, G. P. and Foreman, A.J.E. (1980) J.Nucl.Mater. 95, 155.

79. Hudson, J.A. (1976) J.Nucl.Mater. 60, 80.

80. Kenfield, T.A., Appleby, W.K., Busboom, H.J. and Bell, W.L. (1978) J.Nucl.Mater. 75, 85.

81. Hesketh, R.V. (1962) Phil.Mag. 7, 1417.

82. Wolfer, W.G. and Ashkin, M. (1976) J.Appl.Phys. 47, 791.

83. Bullough, R., Finnis, M.W. and Wood, M.H. (1982) J.Nucl.Mater. 103 and 104, 1263.

84. Mosedale, D., Lewthwaite, G. and Ramsay, I. (1972) Proc. of Conf. on 'Irradiation Embrittlement and Creep in Fuel Cladding and Core Components', BNES, London.

85. Bullough, R. and Hayns, M.R. (1975) J.Nucl.Mater. 57, 348.

86. Bullough, R. and Ball, R.D. Unpublished work. 87. Jostons, A., Kelly, P.M. and Blake, R.G. (1977) J.Nucl.Mater. 66, 236.

88. Murgatroyd, R.A. and Rogerson, A. (1979) J.Nucl.Mater. 90, 240.

89. Bullough, R. and Wood, M.H. (1979) J.Nucl.Mater. 90, 1.

90. Buckley, S.N., Bullough, R. and Hayns, M.R. (1979) J.Nucl.Mater. 89, 283.

91 Hood, G.M., Schultz, R.J. and Jackman, J.A. (1984) J.Nucl.Mater. (in press).

92 Finnis, M.W. and Sinclair, J. (1984) Phil.Mag. 50, 45.

93. Rauh, H., Bullough, R. and Wood, M.H. (1983) Proc.Roy.Soc. A388, 311.

94. Evans, J.H. (1971) Nature 229, 403.

CAPTIONS

1. Distribution of faulted, perfect and double interstitial loops in proton irradiated copper at a range of temperatures [29].

2. Dark-field micrograph of neutron irradiated molybdenum [35] at 600°C. In (a) $\underline{g} = [211]$, (b) $\underline{g} = [\bar{2}11]$. The loops in the groups arrowed have all got the same Burger's vector.

3. (a) Micrograph of neutron irradiated molybdenum[36] at 600°C showing enhanced loop density adjacent to an edge dislocation.
   (b) Schematic diagram indicating the wedge shaped volume on the dilatation side of the dislocation in which the loops were found.

4. Micrographs of neutron irradiated ordered Cu_3Au foils. (a) Dark-field showing disordered zones by structure factor contrast. (b) Bright-field showing zones with loops (arrowed) and zones where collapse has not occurred (circled). Further details of this work by English and Jenkins [45] are given in the text.

5. The circular dislocation loop and its effective sphere.

6. Vacancy activation energy surfaces adjacent to the loop core.

7. Schematic illustration of the shrinkage rates of (a) an interstitial loop and (b) a vacancy loop when subject to annealing conditions.

8. The three orthogonal orientations of externally applied tensile stress τ, in relation to a straight edge dislocation lying along the x_3-axis with $\underline{b} = (b,0,0)$.

9. The microstructure in a PE16 alloy after irradiation by 46 MeV Ni^{4+} ions at 525°C for a total dose of 60 dpa. (D. Mazey, Harwell).

10. A long straight edge dislocation embedded in the lossy continuum.

11. The temperature dependence of the swelling in M316 steel irradiated with Ni^{6+} ions. The x and o indicate experimental swelling values[79] at 16 and 40 dpa respectively. The theoretical curves [68] at 40 dpa have been obtained by predicting the swelling development from the 16 dpa state. The dashed curve ($\varepsilon = 0$) indicates the result of neglecting vacancy loop formation.

12. The temperature dependence of the swelling in M316 steel irradiated with fast neutrons [80]. The x and o indicate experimental swelling values at 39 and 62.5 dpa respectively. The theoretical curves [68] at 62.5 dpa have been obtained by predicting the swelling development from the 39 dpa state. The dashed curve (ε = 0) indicates the result of neglecting vacancy loop formation, whereas the solid curve has been obtained with the same vacancy loop parameter as used for the corresponding curve in figure 11.

13. The theoretical irradiation creep strain [85], ε, versus dose and the relevant experimental data on solution treated and cold worked M316 steels.

14. The growth strain versus dose in pure zirconium foils in the HVEM [90]. The experimental data points are indicated by • and the continuous curve is the result of a rate theory analysis.

15 A void lattice containing a dislocation [94] in high purity molybdenum after irradiation with 2 MeV N^+ ions at 870°C.

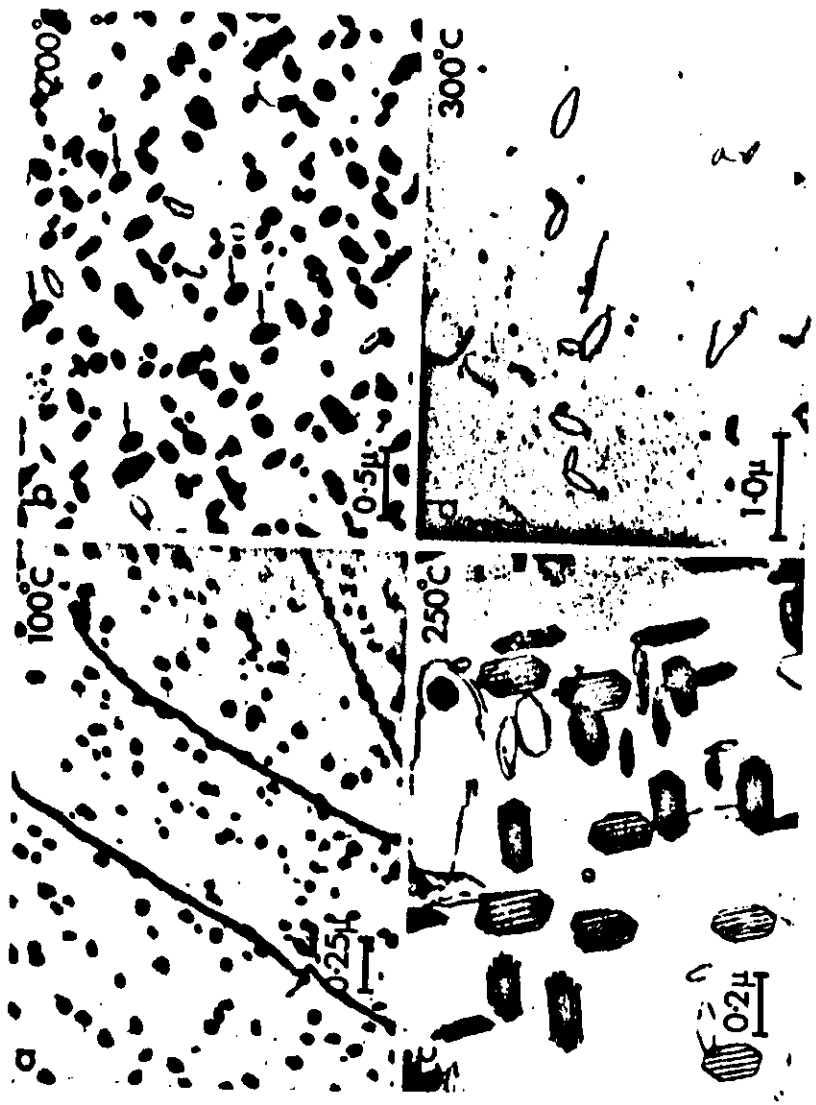

Fig. 1

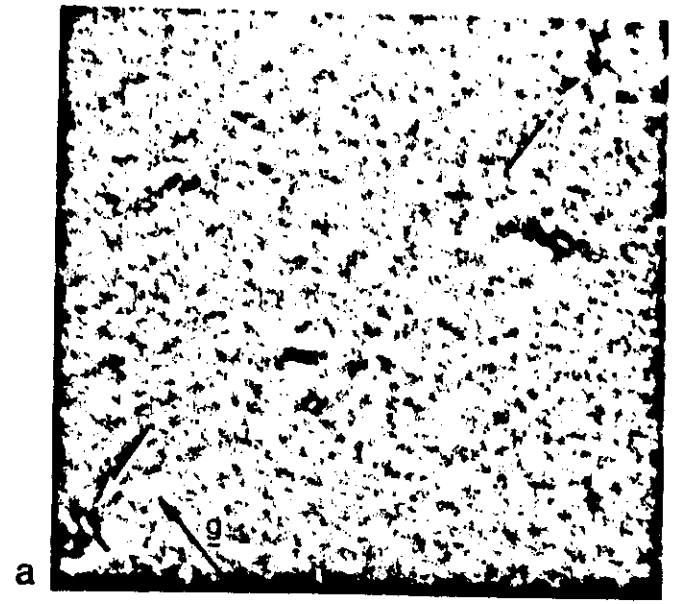
a
g
b
g
30 nm

Fig. 2

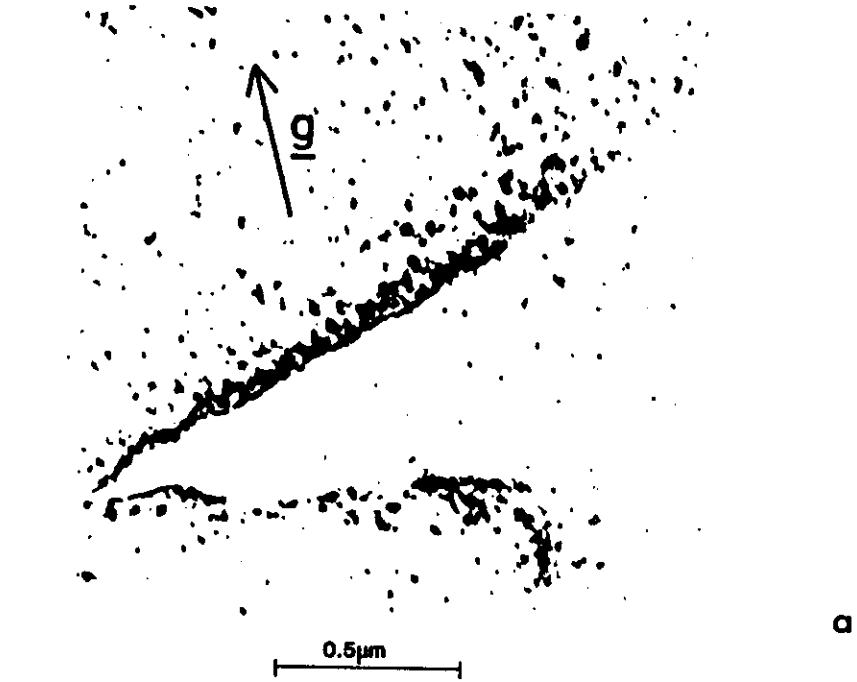
g
0.5μm
a
wedge
edge
dislocation
denuded
zone
extra half plane
~0.5 μm
b

Fig. 3

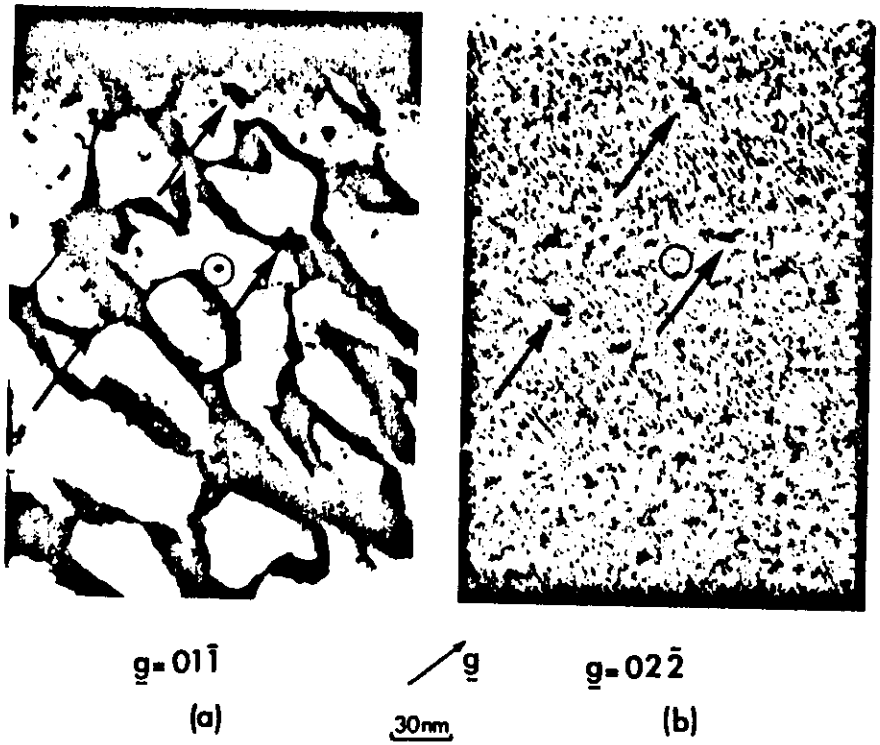

Fig. 4

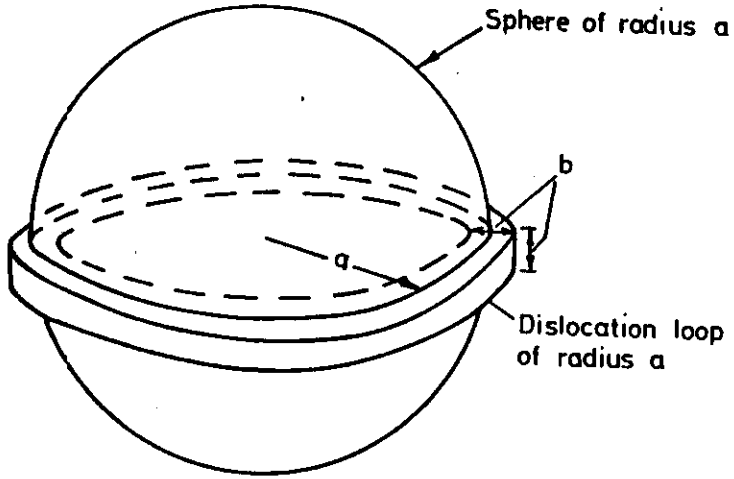

Fig. 5

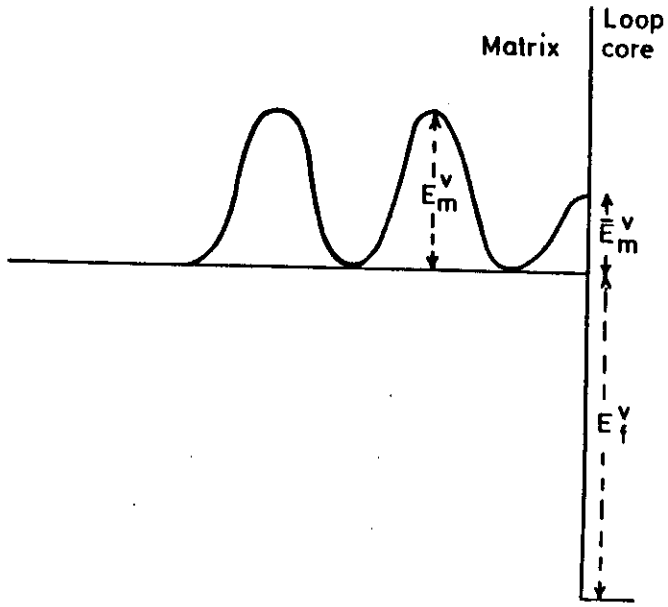

Fig. 6

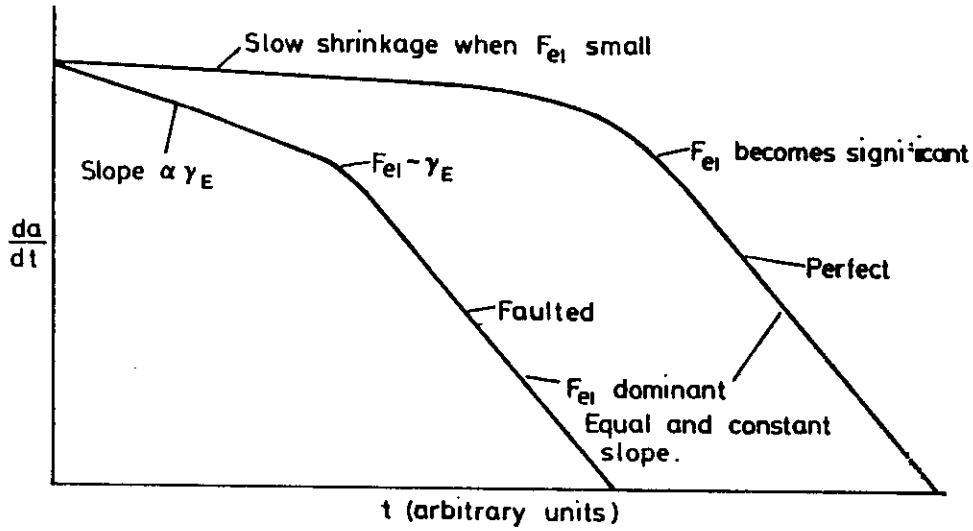

(a)

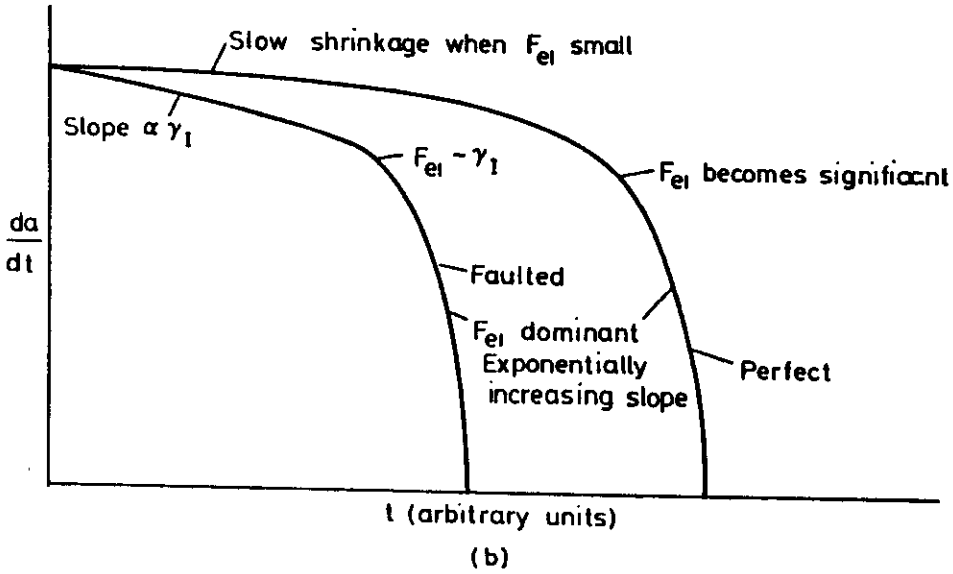

(b)

Fig. 7

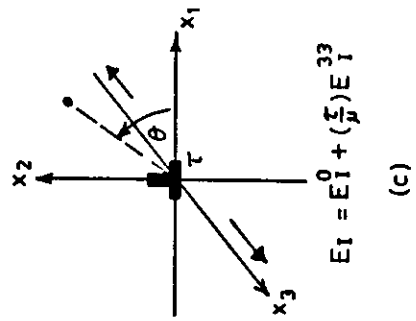

(c)

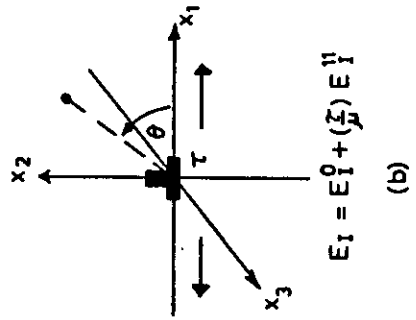

(b)

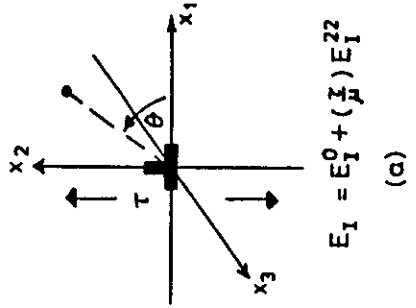

(a)

Fig. 8

Fig. 9

EFFECTIVE MEDIUM
(Lossy continuum)

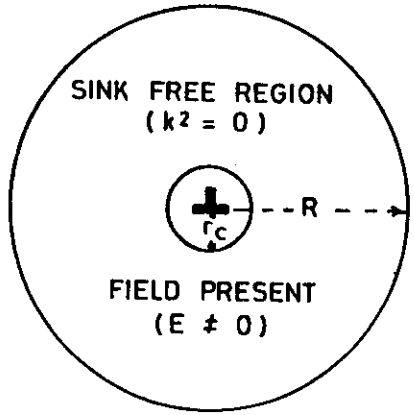

SINKS PRESENT
$(k^2 \neq 0)$

ZERO FIELD
$(E = 0)$

Fig. 10

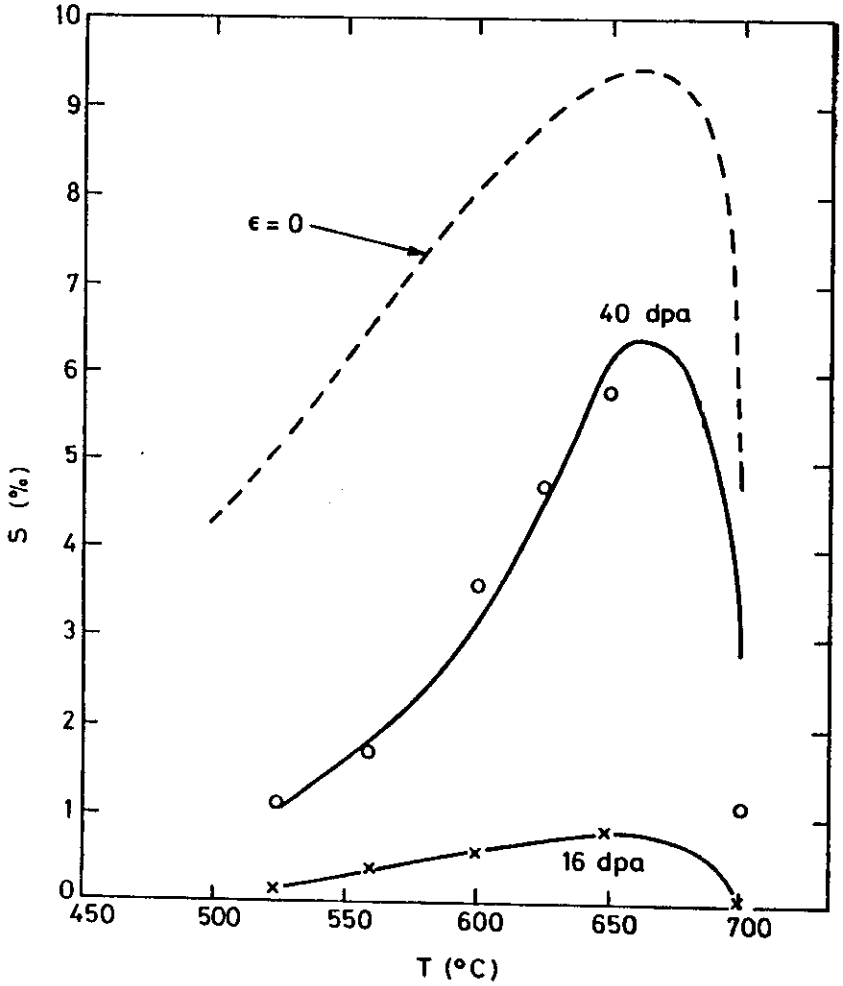
10
9
8
7
6
5
4
3
2
1
0
S (%)
ε = 0
40 dpa
16 dpa
450
500
550
600
650
700
T (°C)

Fig. 11

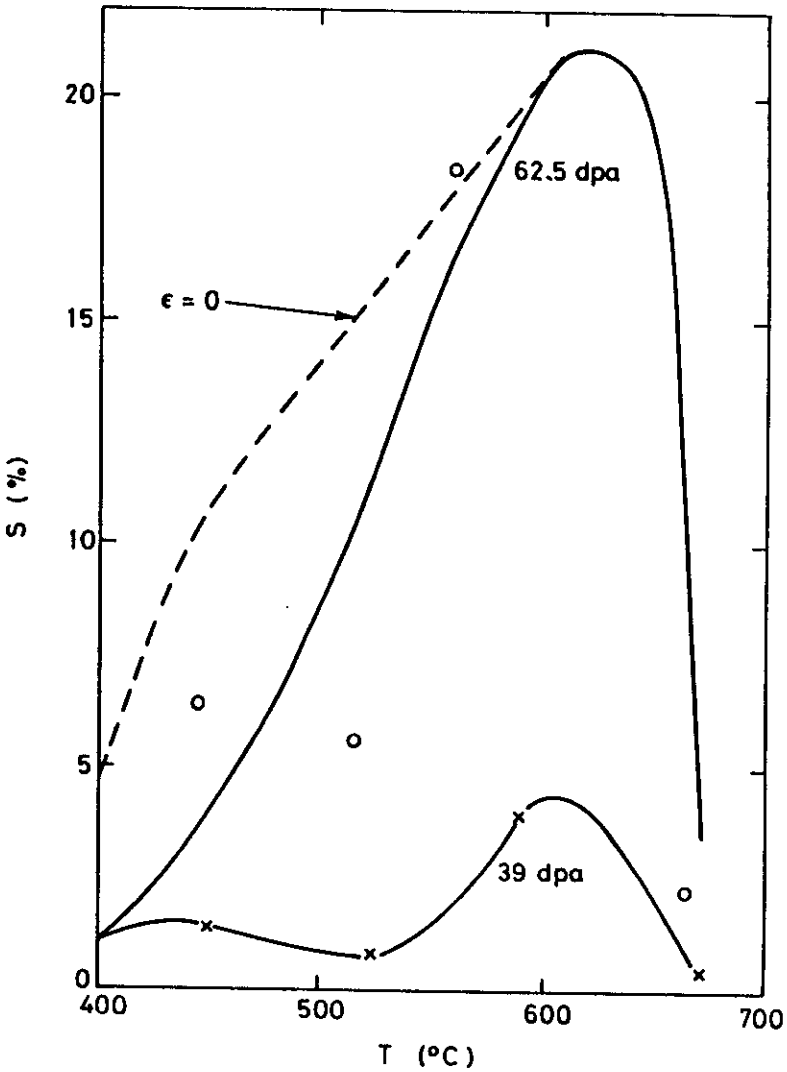
20
15
10
5
0
S (%)
62.5 dpa
ε = 0
39 dpa
400
500
600
700
T (°C)

Fig. 12

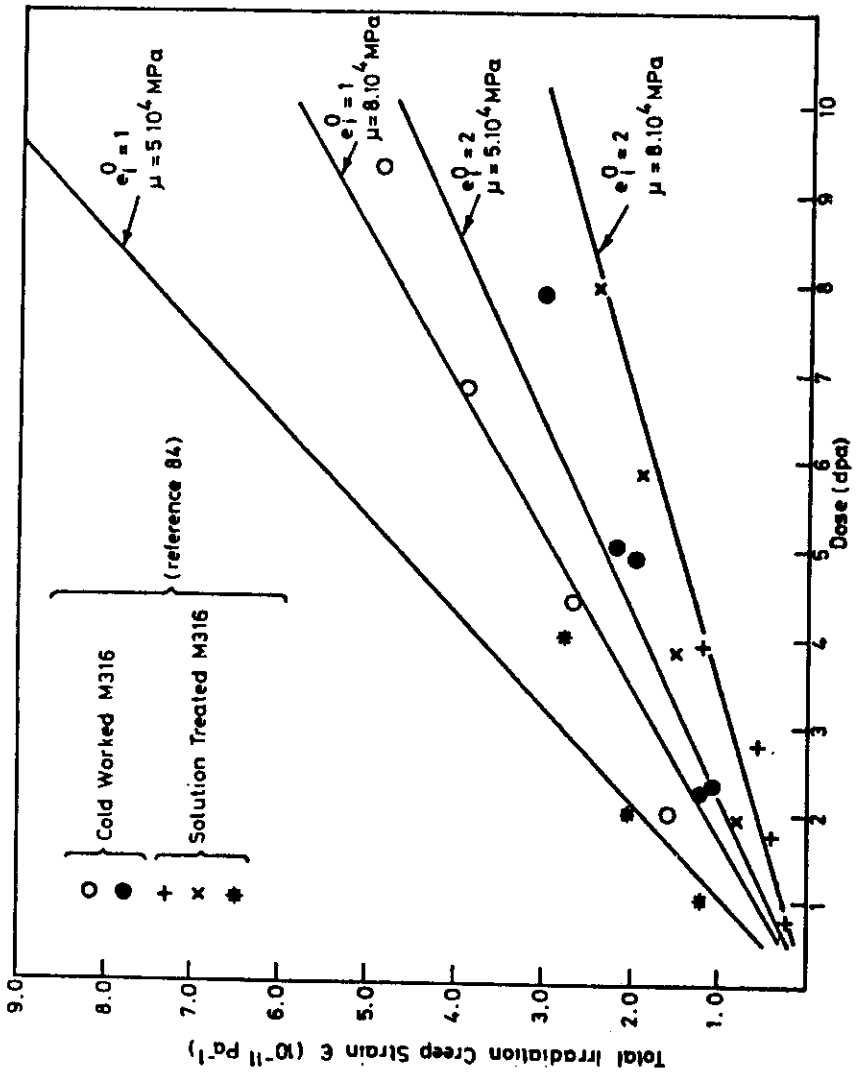
Total Irradiation Creep Strain ε (10⁻¹¹ Pa⁻¹)
Dose (dpa)
$e_i^0 = 1$ $\mu = 5.10^4$ MPa
$e_i^0 = 1$ $\mu = 8.10^4$ MPa
$e_i^0 = 2$ $\mu = 5.10^4$ MPa
$e_i^0 = 2$ $\mu = 8.10^4$ MPa
(reference 84)
Cold Worked M316
Solution Treated M316

Fig. 13

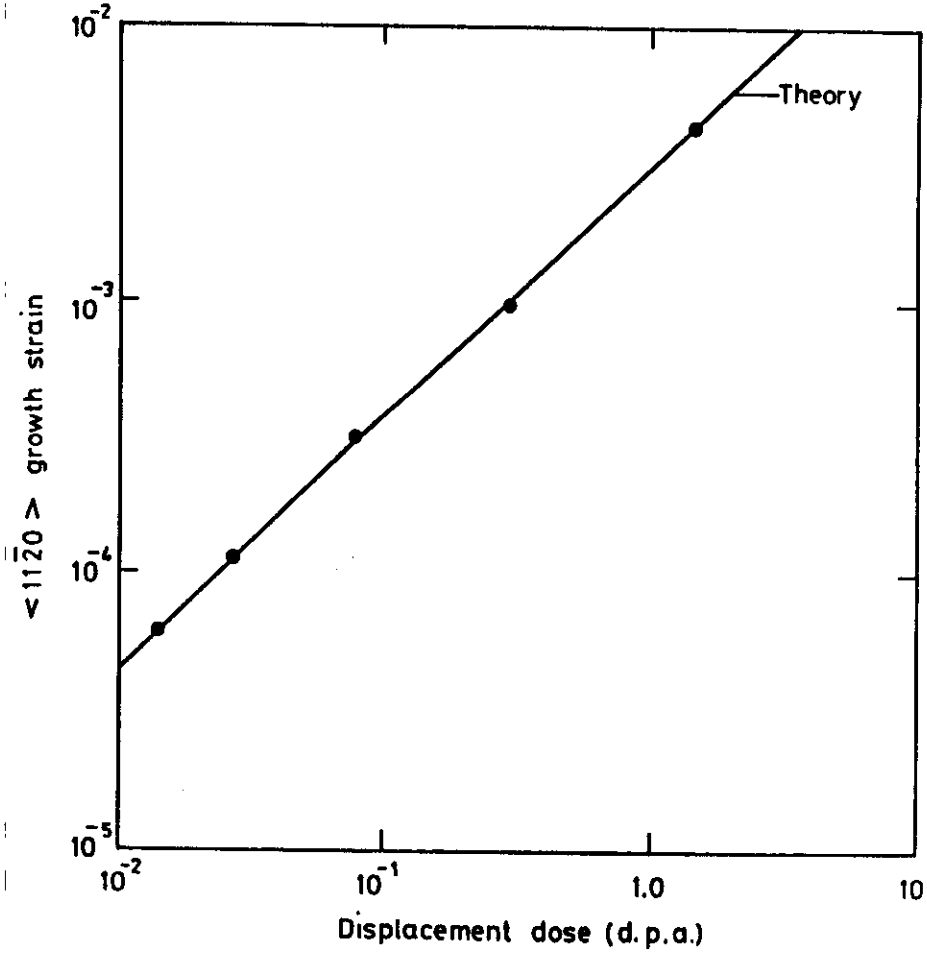
$<11\bar{2}0>$ growth strain
Displacement dose (d.p.a.)
Theory

Fig. 14

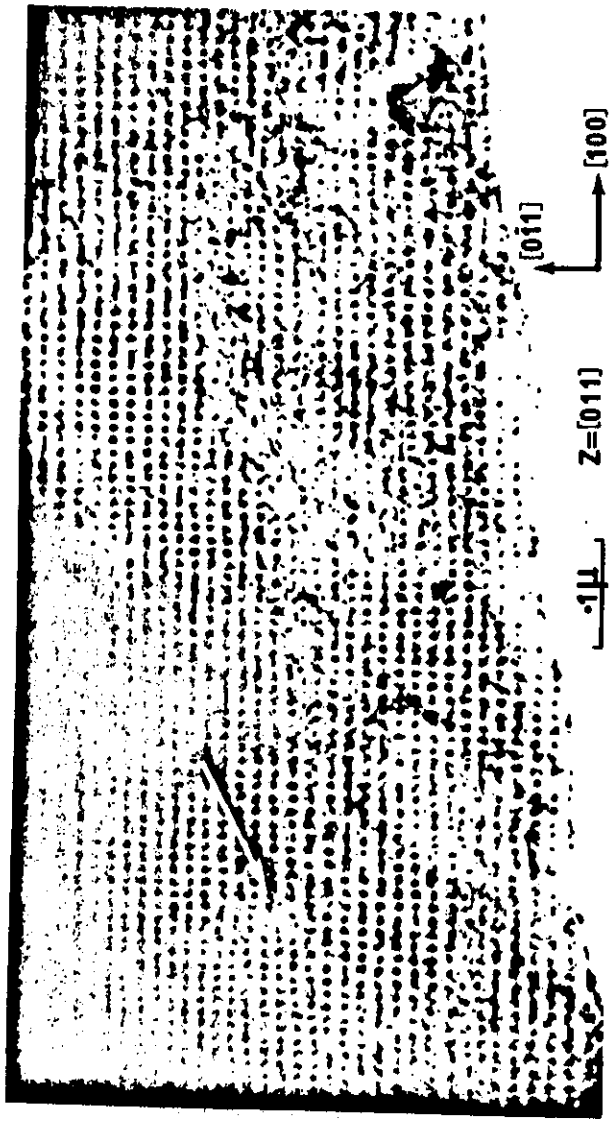

Fig. 15

Theory of Microstructural Evolution

R. BULLOUGH [1] and M.H. WOOD [2]

Theoretical Physics Division,
AERE Harwell,
Oxon OX11 ORA, UK

[1] Now: Materials Development Division, AERE Harwell, Oxon OX11 ORA, UK
[2] Now: Safety and Engineering Science Division, AEE Winfrith, Dorset DT28DH, UK

Physics of Radiation Effects
in Crystals
Edited by
R.A. Johnson and A.N. Orlov

8 9

Contents

1. Introduction

In this chapter the theory of microstructural evolution in pure metals and alloys during irradiation is reviewed. It is the microstructural development which must be understood before adequate modelling of void swelling and irradiation creep can be undertaken. Microchemical effects are also included in the review.

Some important fundamental notions are introduced in section 2, and this is followed by a presentation of the mathematical rate theory representation of radiation damage in section 3. Theoretical problems inherent in the use of simulation for neutron damage predictions are discussed in section 4 together with an example of a recent successful prediction. In the final section our conclusions regarding the present and future role and status of theory are presented.

2. Fundamental considerations

The topics covered in this section are: (a) a discussion of the microstructural state prior to irradiation, including definitions of sinks, defects, dislocations, etc; (b) the displacement defects, where some important properties of the point defects are reviewed and the cascade collapse process to vacancy loops is alluded to; (c) interactions between the displacement defects and the microstructure, which are fundamental to the macroscopic phenomena of void swelling and irradiation creep; (d) extended defect nucleation, where attention is focussed on the problem of the nucleation of voids; and, (e) microchemical concepts, upon which much attention has been focussed recently.

2.1. The pre-irradiation microstructural state

The overall microstructutal state of a metal prior to irradiation naturally influences its response to subsequent irradiation. It is conveniently defined by

identifying the various defect types that together constitute the initial microstructure. These defect types can act as sinks for any migrating point defect. However, in this section, the sink aspects of the microstructure are only briefly alluded to and then considerably amplified in the subsequent discussion of the evolution of the microstructure during irradiation.

A bulk specimen is normally polycrystalline and the *grain boundaries* constitute an important "surface" defect that can act as a sink for migrating point defects. In this review the term "point" defect is used to describe all such defects including *self-interstitials, vacancies and solute atoms* either occupying interstitial or substitutional sites; "*displacement*" defects refer only to *self-interstitials* or *vacancies* and if these require distinction they are referred to simply as either interstitials or vacancies. The grain boundaries are usually non-saturable sinks for the displacement defects but very often, in practical materials, the grain size is sufficiently large that their boundaries are not an important sink during irradiation. The external surface of the specimen may also be regarded as a similar sink type to the grain boundaries but again, in practice, the point defect losses to the surface are not usually important. Of course, an important exception to this is when the specimen is a thin foil as required for studies of high energy electron irradiation effects in the High Voltage Electron Microscope (HVEM). In this case the foil surfaces can be significant sinks for migrating point defects and should be considered as a component of the overall microstructural state.

A more important pre-irradiation defect than the grain boundaries is the *dislocation network* present within each grain. A dislocation is a "line" defect that may be defined, in general, as the line that divides areas of slip planes where glide has occurred from those where no glide has occurred. In solution annealed material the initial, pre-irradiation, dislocation density is low, 10^{12} to $10^{13}\,m^{-2}$ in 316 steel, whereas in cold-worked material the initial density is high, 10^{15} to $10^{16}\,m^{-2}$ in 316 steel. When dislocation networks are generated by deformation processes they consist of roughly equal proportions of edge and screw types. Both these kinds of dislocations can act as sinks for migrating point defects but, as we shall see below, the edge dislocations play a predominant role in the irradiated materials. In fact, it is clear that their presence is essential to the macroscopic phenomena known as void swelling and irradiation creep.

In general, a metal contains at least one impurity species prior to irradiation; such impurities may be either atomically dispersed or be precipitated into a second phase. The atomically dispersed solute may trap displacement defects, either interstitials or vacancies depending upon the nature of the solute. These *solute atom traps* are regarded as saturable, in

that they may trap only a single point defect at a time, and are characterised by the energy with which they bind a point defect. *Precipitates* may also be sinks for migrating species; a consideration of their role is deferred to §2.5.

It is possible to define a pre-irradiation thermal equilibrium state which is the state a metal achieves if it is aged for a sufficiently long time, at temperature, prior to irradiation. The equilibrium point defect concentrations (fractional) are given by expressions of the form $c^e = \exp(-E^f/k_B T)$, where c^e is the equilibrium concentration of interstitials, c_i^e, or vacancies, c_v^e; E^f is the interstitial, E_i^f, or vacancy, E_v^f, formation energy, k_B is Boltzmann's constant and T is the absolute temperature. In fact, E_i^f is sufficiently large that, at all temperatures of interest, $c_i^e \sim 0$. In face centred cubic (fcc) transition metals and alloys, such as 316 steel, E_v^f is of the order of an electron volt.

In general co-existing with the thermal equilibrium concentration of vacancies is a network of dislocations; although such dislocations have very high formation energies (~ 7 eV per atom plane) it is difficult to remove them by ordinary annealing procedures and a polygonised network is often the only recovered state that is achievable by a combination of glide and climb processes (Bullough et al. 1981). Thus a metal, after ageing at temperatures sufficiently high for appreciable self-diffusion to occur, that is $\gtrsim 600$°C for 316 steel, retains a density of dislocations of at least $10^{12}\,m^{-2}$. Finally it should be recalled that the equilibrium phase diagrams, for multi-phase alloys, show a marked sensitivity to temperature.

2.2. The displacement defects

A comprehensive review of the displacement damage processes, for neutron and various simulation damage, is presented in chapter 2 in Part I. In this section the discussion is confined to some points relevant to modelling the overall microstructural evolution.

When a metal is bombarded with high energy particles, atoms are displaced from their equilibrium lattice sites; the atoms come to rest some distance away in interstitial, non-lattice-site, positions. The holes left in the lattice are termed vacancies.* From the previous section it is already clear that the interstitials and vacancies thus formed can, at *sufficiently high* temperatures, migrate through the matrix and accumulate at suitable point

*The irradiation is characterised by the rate at which interstitials and vacancies are formed, K. K is expressed in the units of displacements per atom per second ($dpas^{-1}$). The unit of time generally employed in irradiation damage studies is the time for one displacement per atom (dpa), that is K^{-1}. K is often referred to as the *dose rate*, and Kt, with t in seconds, as the *dose*.

defect sinks, such as dislocations. During irradiation at typical reactor operating temperatures vacancies are found to cluster into 3-dimensional cavities known as *voids*; it is the nucleation and growth of these that gives rise directly to the macroscopic phenomenon of void swelling. In material with a fairly low pre-irradiation dislocation density, irradiation-produced interstitials are also observed to aggregate, into planar *dislocation loops*. These rapidly assume the overall appearance of the as fabricated dislocation network as irradiation proceeds.

It has been shown by computational atomic simulation studies of the interstitial defect (Gehlen and Beeler 1972) that the interstitial shares a normal lattice site with another atom by forming a split, or dumb-bell, configuration. This has been found in both fcc and body centred cubic (bcc) materials. In fcc nickel for example, the ⟨100⟩ dumb-bell configuration has been calculated to be the stable configuration for the single interstitial, and in bcc iron the ⟨110⟩ dumb-bell has been shown to be the most stable configuration. This geometrical feature of the interstitial is understood to have important consequences for the plane of nucleation of the interstitial dislocation loops, and is believed to influence the ease of acceptance of interstitials at dislocation sinks, as is discussed in §2.3. Calculations of the mobility of the dumb-bell interstitial have yielded a low migration energy and consequent high mobility at reactor operating temperatures. A typical calculated value of the migration energy is of the order of 0.2 eV for an fcc metal, which is in good agreement with experiment.

Vacancies are considerably less mobile than interstitials, a typical value for the monovacancy migration energy for an fcc metal being of the order of an electron volt (Balluffi 1978). Experiments have shown that vacancies can bind together and that these small vacancy clusters can also migrate through the crystal lattice. Generally, reliable information from such annealing studies is restricted to the divacancy. The limited available information about even divacancies in fcc metals indicates that they possess binding energies around 0.2 eV, and migrate with slightly lower migration energies than the corresponding monovacancies. In calculations of microstructural evolution during irradiation it is generally considered adequate to ascribe an effective migration energy to the monovacancy and to ignore formally possible cluster mobility.

A further basic property of the point defects, important to studies of void swelling and irradiation creep, are their relaxation volumes, ΔV_i and ΔV_v. These volumes, which are rather poorly known, represent the volume changes associated with the introduction of each defect type into the lattice in place of a lattice atom. They are most conveniently expressed in terms of

the average crystal atomic volume, Ω, and reasonable values in fcc metals are believed to be, $\Delta V_i \sim 1.2\Omega$ and $\Delta V_v \sim -0.5\Omega$. A discussion of the role of these relaxation volumes is given in §2.3.

When damage is created by particles carrying high momentum, such as high energy neutrons or charged particles, cascades of displaced lattice atoms are created rather than single atom displacements. Many of the interstitials and vacancies recombine within the cascade region but, because of their very high mobility, the remaining interstitials rapidly migrate from this damage zone. Most of the remaining vacancies created by the damage also escape into the body of the crystal, but experiments show that a significant fraction of the cascades collapse to form dislocation loops, which are platelets of vacancies rather than interstitials as discussed above. To distinguish between the two types of dislocation loops the terms *vacancy loops* and *interstitial loops* are employed. Because of the high, 14 MeV, energy of fusion neutrons compared with the vast majority of those emanating from fission, cascade features are expected to assume greater significance in the fusion environment than in a thermal or fast fission reactor. At present the exact mechanism of cascade collapse to form vacancy loops is not understood, although investigations, including large molecular dynamic simulation studies, are underway. Suffice it to remark that the inner zone (the so-called denuded or Seeger zone) of the cascade often contains a sufficiently high concentration of vacancies for supersaturation conditions appropriate for the nucleation of a vacancy aggregate; the high vacancy concentration also means that many of the as created vacancies are near neighbour to other vacancies and thus the apparent high mobility of the vacancies could well be due to a propensity of di-vacancies. In general, the vacancy aggregates formed by this rapid collapse process are loops and sometimes vacancy tetrahedra but never voids.

During reactor operation the point defects produced migrate through the crystal lattice. Many of these eventually find their way to the various point defect sinks. However, depending upon the density of such sinks and the operating temperature, a significant fraction of opposite types, that is interstitials and vacancies, meet in the matrix and mutually annihilate through spontaneous recombination. This process, which must be considered in numerical studies of microstructural evolution, is termed *bulk recombination*.

Another important defect produced during both fission and fusion reactor operation is the *transmutation gas*. This consists of helium, by (n,α) reactions, and hydrogen, by (n,p) reactions, in various proportions depending on the neutron energy spectrum. This gas, particularly the helium,

plays an important role in the nucleation of voids, as discussed in §2.4, and, also, in grain boundary embrittlement.

2.3. Interactions between displacement defects and the microstructure

The presence in a metal of sinks for migrating point defects is not in itself sufficient to cause void swelling and irradiation creep. An additional requirement is that a bias should exist in the system of sinks such that there is a net flow of vacancies to voids. In fact it has been shown that dislocations (network and both loop types) have a small bias for interstitials which allows the dislocations to *climb* by a net influx of interstitials and, hence, the voids to grow by a net influx of vacancies.

The interaction energy between a dislocation and a nearby point defect can be estimated by representing the point defect as a misfitting inhomogeneity of small volume V with a bulk and shear modulus $\bar{\kappa}$ and $\bar{\mu}$ respectively, that may differ from the corresponding host moduli, κ and μ; the misfit is defined by the uniform misfit strain, which is the strain required to deform the inclusion back to the size and shape of the hole in the host into which it was forced. Since the inclusion is of atomic dimensions the spatial variations of stress and strain within it may be ignored and for this situation the interaction energy between such an inclusion and a general applied strain field $e^{\wedge}_{ij}$ has the form (Bullough and Willis 1975, Nabarro et al. 1982):

$$E = -V\left[\mu A' e^{\wedge\prime}_{ij} e^{\wedge}_{ij} + \frac{\kappa}{2} C(e^{\wedge})^2 + 2\mu B' e^{\wedge\prime}_{ij}\bar{e}_{ij} + \kappa D e^{\wedge}\bar{e}\right], \tag{2.1}$$

where $e = e_{kk}$ and $'e_{ij} = e_{ij} - \frac{1}{3}e\delta_{ij}$ is the deviatoric part of e_{ij}. In equation (2.1) we have:

$$\left.\begin{aligned} A &= (\mu - \bar{\mu})/[\mu - \beta(\mu - \bar{\mu})], \\ B &= \bar{\mu}/[\mu - \beta(\mu - \bar{\mu})], \\ C &= (\kappa - \bar{\kappa})/[\kappa - \alpha(\kappa - \bar{\kappa})], \\ D &= \bar{\kappa}/[\kappa - \alpha(\kappa - \bar{\kappa})], \end{aligned}\right\} \tag{2.2}$$

where,

$$\left.\begin{aligned} \alpha &= (1+\nu)/3(1-\nu), \\ \beta &= 2(4-5\nu)/15(1-\nu), \end{aligned}\right\} \tag{2.3}$$

and ν is Poisson's ratio for the host medium. If the applied strain field $e^{\wedge}_{ij}$ arises from a dislocation strain field e^{D}_{ij} and a strain field e^{E}_{ij} due to an external applied stress, such that

$$e^{\wedge}_{ij} = e^{D}_{ij} + e^{E}_{ij} \tag{2.4}$$

then the interaction energy between a dislocation and the inclusion, in the presence of an external stress follows from equations (2.1) and (2.4):

$$E^{D} = -V\{\mu A['e^{D\prime}_{ij}e^{D}_{ij} + 2'e^{E\prime}_{ij}e^{D}_{ij}] + \frac{\kappa}{2}C[(e^{D})^2 + 2e^{E}e^{D}] + 2\mu B' e^{D\prime}_{ij}\bar{e}_{ij} + \kappa D e^{D}\bar{e}\}. \tag{2.5}$$

This expression may be further simplified by dropping the terms of second order in the dislocation strain field and by assuming the misfit strain is the pure dilatation strain $\bar{e}$, so that

$$'\bar{e}_{ij} = 0, \tag{2.6}$$

whence equation (2.5) becomes (Bullough and Willis 1975):

$$E^{D} = -V\{2\mu A' e^{E\prime}_{ij}e^{D}_{ij} + \kappa C e^{E}e^{D} + \kappa D e^{D}\bar{e}\}. \tag{2.7}$$

If the dislocation lies along the x_3-axis of a Cartesian coordinate system (x_1, x_2, x_3) with Burgers vector $\boldsymbol{b} = (b, 0, 0)$, then its strain field e^{D}_{ij} has the deviatoric components

$$\left.\begin{aligned} 'e^{D}_{11} &= -L\frac{\sin\theta}{r}(1 - 2\nu + 6\cos^2\theta), \\ 'e^{D}_{22} &= -L\frac{\sin\theta}{r}(1 - 2\nu - 6\cos^2\theta), \\ 'e^{D}_{33} &= 2L\frac{\sin\theta}{r}(1 - 2\nu), \\ 'e^{D}_{12} &= 3L\frac{\cos\theta}{r}(2\cos^2\theta - 1), \end{aligned}\right\} \tag{2.8}$$

and dilatation

$$e^{D} = -6L(1 - 2\nu)\frac{\sin\theta}{r}, \tag{2.9}$$

where $L = b/12\pi(1-\nu)$. Similarly if the e^{k}_{ij} strain field is due to the application of a uniaxial tensile stress σ parallel to the Burgers vector of this edge dislocation (i.e. parallel to the x_1-axis) then

$$\left.\begin{aligned} {}^{\sigma}e^{E}_{11} &= \sigma/3\mu, \\ {}^{\sigma}e^{E}_{22} &= {}^{\sigma}e^{E}_{33} = -\sigma/6\mu, \end{aligned}\right\} \tag{2.10}$$

and

$$e^{k} = \sigma(1-2\nu)/2\mu(1+\nu), \tag{2.11}$$

with obvious permutations when the applied tensile stress is rotated parallel to either of the other two axes. When the external stress is removed the interaction energy, equation (2.7), becomes the well know size-effect interaction E^{D}_{S} and for this dislocation has the explicit form (Cottrell and Bilby 1949):

$$E^{D}_{S} = \frac{\alpha b\mu}{\pi}\Delta V\frac{\sin\theta}{r}, \tag{2.12}$$

where ΔV is the *relaxation volume** suffered by the arbitrarily large but *finite* host when the point defect is introduced into it.

*We note that ΔV is related, for this general misfitting inhomogeneity, to the misfit strain $\hat{e}$ of the inclusion by

$$\Delta V = D\,V\,\hat{e},$$

and to the "hole strain" (i.e. the strain defined by the displacement of the surface of the hole into which the inclusion is forced) $\hat{e}_0$ by

$$\Delta V = V\hat{e}_0/\alpha.$$

The "hole strain" $\hat{e}_0$ may be formally identified with the relaxation volume change ΔV_∞ when the point defect is introduced into an *infinite* body:

$$\hat{e}_0 = \Delta V_\infty/V.$$

However ΔV and not ΔV_∞ is the observable quantity usually referred to as the *relaxation volume* of the point defect. Finally, for completeness, the actual strain within the inclusion, when embedded in the host is

$$e_1 = \hat{e} - \hat{e}_0 = \frac{\Delta V\kappa}{V\hat{\kappa}}(1-\alpha).$$

98

It follows, from equation (2.7) and the above explicit formulae, that the long-range interaction between the point defect and the dislocation depends critically on the magnitude of ΔV and will be sensitive to both the magnitude and direction of any external applied stress. For the stress free situation, defined by equation (2.12), it is immediately clear that as the interaction energy for the interstitial, $\Delta V_i \sim 1.2\Omega$, is greater than that for the vacancy, $\Delta V_v \sim -0.5\Omega$, a bias exists for the capture of an interstitial by a dislocation. The same basic conclusion holds equally for edge dislocation loops of vacancy and interstitial type, although the magnitude of the bias in this case depends upon the loop size and has been shown (Bullough et al. 1980) to decrease with decreasing loop radius.

The sensitivity of the interaction energy to the magnitude and direction of the external applied stress has important consequences in theories of irradiation creep (Heald and Speight 1974, Bullough and Willis 1975). It can be shown that the dumb-bell configuration of the interstitial leads to its relative local softness in shear (Dederichs and Lehman 1973, Holder et al. 1974) compared to the vacancy. This behaviour can be represented in the above elastic inclusion model by assuming that the shear modulus $\tilde{\mu}_i$ of the inclusion representing the interstitial is much less than the shear modulus μ of the host. When this assumption is put into the various terms in equation (2.7) it is found that edge dislocations with their Burgers vectors aligned parallel to the stress axis have a preferred bias for interstitials compared to such dislocations in other orientations relative to the stress axis; this causes the body to undergo climb creep. The phenomenon is generally referred to as Stress Induced Preferred Absorption, or *SIPA*, creep.

The dislocation is not the only sink in the microstructure for which a sink–point defect interaction exists. The interaction between the spherical void and a nearby point defect is induced by the distortion field of the point defect and is thus much shorter ranged (Bullough and Willis 1969) than that between the dislocation and a point defect which arises from the direct interaction between the dislocation stress field and the point defect field. The induced interaction energy, E_C, between a spherical void and a centre of dilatation (to represent the point defect), at a radial distance r, has the series form (Bullough and Willis 1969):

$$E_C = -\frac{G}{r_C^3}\sum_{n=2}^{\infty}\frac{n(n-1)(4n^2-1)}{n^2+(1-2\nu)n+(1-\nu)}\left(\frac{r_C}{r}\right)^{2n+2}, \tag{2.13}$$

where,

$$G = \frac{\mu(1+\nu)^2}{36\pi(1-\nu)}(\Delta V)^2. \tag{2.14}$$

99

r_c is the cavity* radius, μ is the shear modulus (as above), ν is Poisson's ratio, and ΔV is the relaxation volume of an interstitial or vacancy (defined as above). Calculations taking account of this interaction (Quigley et al. 1981) show that a lower void swelling results than when the interaction is ignored. However, this effect can be subsumed, to a good approximation, into the dislocation bias and the interaction neglected explicitly, thus simplifying models of void swelling.

The above discussion has indicated that, because of the long-range dislocation–point defect interaction field, a bias exists for the capture of interstitials relative to vacancies at the dislocation sinks. However, an effect which could have similar importance is the efficiency with which point defects are absorbed through the crystal matrix–sink interface. This has been recognized for sometime, and has been considered by Mansur (1978) for the void sink. Recent work (Bullough and Quigley 1981, 1983) has concentrated on the boundary conditions at the dislocation core where it is necessary to consider the formation of jogs, the activation energy required to enter the core, and the fraction of sites adjacent to the core available for entry into the core. Comparison of experimental measurements of void swelling in electron irradiated 316 steel with those from model calculations employing appropriate core boundary conditions and the interaction field effects (Bullough and Quigley 1981, Bullough et al. 1983a), shows that a very good agreement is achieved between the two sets of results if entry into the core is made more difficult for interstitials than for vacancies.

2.4. *Extended defect nucleation*

As discussed in §2.2., during irradiation new types of extended defect can appear. The three most important examples are probably vacancy loops, interstitial loops and voids. Of these, the vacancy loops appear as a direct consequence of the cascade nature of the damage, whereas the interstitial loops and the voids result from the subsequent agglomeration of point defects. It is the nucleation of these latter defects that is the subject of the following discussion.

*The term *cavity* is often employed in the theory of radiation damage. It implies more generality than the term void, and includes gas bubbles. Hence, a void is a cavity in which the internal gas pressure is significantly lower than the surface tension forces, whereas a gas bubble is a cavity in which the gas pressure and surface tension forces are in equilibrium. This distinction between voids and gas bubbles is important in some cases, especially in the theory of void nucleation, discussed in §2.4.

The initial stages of interstitial loop nucleation have been studied by atomic simulation (Ingle et al. 1981). These calculations provide information on the stability of clusters of a few interstitials, and on their morphology. It is not possible to model accurately the formation of sizeable interstitial loops without a sufficient appreciation of the early stages of clustering. In certain cases it is likely that the behaviour of the small interstitial loop embryo is crucial to the overall performance of the material during irradiation; this may be the case for the ferritic steels (Little et al. 1980). To calculate the evolution during irradiation of the interstitial loop number density-size distribution function it has been found necessary to adopt a sophisticated numerical scheme (Hayns 1980a). A comparison of calculated results with those from an experiment at a single temperature has shown encouraging agreement for the loop number density in nickel and for their subsequent growth (Hayns 1980a). One important feature of interstitial loop nucleation to emerge from such calculations is that it is completed in only a very short irradiation time, of the order of 10^{-3} dpa. This suggests strongly that only their growth need be considered in calculations of void swelling and irradiation creep, greatly simplifying such studies.

Following the initial aggregation of interstitials into interstitial loops, and/or flow of interstitials to the pre-existing dislocation network, the (slower) vacancies may also aggregate. In practice, it is believed that a three-dimensional vacancy aggregate (void) can only nucleate in the simultaneous presence of an adequate number of gas atoms, surface active impurities, or at certain other structural defects, such as incoherent precipitates. It has been shown by Bullough and Perrin (1969) that, for a pure metal, if no gas atoms are present in the vacancy aggregate, it should always energetically collapse to form a small vacancy loop; in fact it has been shown that the void-like embryo must contain several thousand vacancies before the three-dimensional morphology is energetically favoured. Furthermore, even if the energy argument is ignored, it is clear that, although such three-dimensional vacancy aggregates could possibly nucleate homogeneously from the background vacancy supersaturation, they would be far too small to grow and would rapidly disappear because of the large surface tension force present in the term defining the probability of vacancy emission from the void. For these reasons, it is generally accepted that the presence of gas atoms is essential to the nucleation of voids homogeneously in pure metals, although it is known that voids often nucleate heterogeneously in complex alloys.

Theories of nucleation have a long history and, recently, the principles of homogeneous nucleation theory relevant to the nucleation of voids in metals

have been reviewed by Clement and Wood (1980). The problem can be presented formally as a system of discrete non-linear coupled rate equations describing the time evolution of the defects in an idealised metal containing only vacancies, interstitials, gas atoms and vacancy–gas atom aggregates of various sizes. However, apart from the fact that certain of the rate constants are not well known, this hierarchy of equations presents a formidable computing problem (Hayns 1980b). The classical nucleation approach has been developed formally for the void nucleation problem without gas, where a single nucleation path over an effective nucleation barrier exists; this gives a simple expression for the steady state nucleation rate. Unfortunately, the approach can only be applied to the void nucleation case proper if some assumption is made about the gas; such as no gas is present, or the voids are assumed to contain a constant amount of gas. Moreover, there appears to be no rigorous nucleation theory which can treat fluctuations in two-dimensional, vacancy and gas atom, space.

The most useful approach to the nucleation of voids with continuous gas generation, as exists in nuclear reactors and in continuous gas injection simulation studies, is probably to consider nucleation as two separate, but linked problems. The first problem concerns the formation of very small clusters consisting of just a few vacancies and gas atoms. It is possible to consider these explicitly within a hierarchical approach. For larger clusters and small voids the deterministic continuity equation may be used to describe the second problem of the transition from essentially gas bubble to void growth kinetics. This approach has been adopted by Hayns (1980b) to produce a tractable computational scheme. In a theory of growth as discussed in section 3, it is possible to adopt a semi-empirical approach and to treat only the second of these nucleation problems explicitly; that is the void concentration is assumed known, from experiment say, and the time-scale for void nucleation is calculated using the deterministic approach. This introduces the important concept of *incubation dose* naturally into the void swelling problem. The incubation dose is the critical dose required for the cavities to make the transition from gas bubble to void growth kinetics. Both the incubation dose and associated critical cavity radius have been calculated, and found, to be extremely temperature dependent. Hence, above a certain temperature void swelling is not observed within the lifetime of reactor components. Analytic expressions have been derived for both the incubation dose and critical cavity radius (Clement and Wood 1980).

The ideas developed for homogeneous void nucleation may be carried over in principle to the problem of heterogeneous void nucleation, that is to nucleation at particular sites within the crystal matrix. Extra features must be

considered in this latter case; for example the number density of such sites and the energies with which they bind the migrating vacancy and gas atom defects. Some progress towards a combined homogeneous–heterogeneous model has been reported (Hayns and Wood 1979).

2.5. Microchemical concepts

As discussed in §2.1., a complex, multi-phase, alloy, such as 316 steel, contains solute dissolved within the crystal matrix and incorporates various precipitates within its basic, unirradiated, structure. During irradiation this phase structure may be unstable, and the partitioning of solutes between precipitates and the matrix be changed (Marwick 1981) as a result of recoil mixing and solute segregation. The relative importance of these effects depends on the irradiation conditions and the nature of the alloy. Such changes in the alloy can modify the material properties, and the void swelling and creep response.

In an irradiated metal local gradients of vacancy or interstitial concentration exist around the various point defect sinks. Such gradients imply a flow of defects, with an accompanying flow of atoms. In an alloy, if solute atoms do not participate in this flow strictly in proportion to their local concentration, a net drift of solute atoms relative to the lattice planes occurs. Now, consider a binary alloy A–B whose components are at fractional concentrations c_A and c_B. In a *dilute alloy*, with A being solute in B, interstitials and/or vacancies can combine with A atoms to form mobile complexes, iA and vA, with binding energies E^B_{iA} and E^B_{vA}, and migration energies E^M_{iA} and E^M_{vA}. The defect–solute complexes can diffuse to sinks and/or dissociate thermally. The total fluxes of vacancies, interstitials, and A-atoms are set equal to the sum of the controlling fluxes of individual mobile species (Lam et al. 1979):

$$\left.\begin{aligned} J_v &= -(1+\sigma_v c_A)D_v\nabla c_v - D_{vA}\nabla c_{vA},\\ J_i &= -(1+\sigma_i c_A)D_i\nabla c_i - D_{iA}\nabla c_{iA},\\ J_A &= -D_{iA}\nabla c_{iA} - D_{vA}\nabla c_{vA} - \sigma_i c_A D_i\nabla c_i + \sigma_v c_A\nabla c_v. \end{aligned}\right\} \qquad (2.15)$$

Here, D_v, D_i, D_{iA} and D_{vA} are the diffusion coefficients of the vacancies, interstitials, interstitial–solute and vacancy–solute complexes respectively, and c_v, c_i c_{iA} and c_{vA} are their corresponding fractional concentrations. The constants σ_v and σ_i are the capture factors for vacancy–solute and interstitia–solute encounters. The total fluxes of defects consist of two

contributions each, that is those of the free defect fluxes and those of the defect–solute complexes. The total solute flux is the sum of the fluxes of complexes and of free solutes driven to sinks by coupling with the free interstitial and vacancy fluxes.

For *concentrated alloys*, the concept of migrating defect–solute complexes becomes ill-defined since most of the time a defect has as nearest neighbours several atoms of the component A which are likely to change their identity as the defect migrates. If diffusive motions of A and B type atoms in a non-dilute A–B alloy are assumed to occur only by vacancy and by interstitial jumps, the fluxes of defects and atoms are related to their concentration gradients by (Lam et al. 1979):

$$\left.\begin{aligned} J_v &= (d_{Av} - d_{Bv})\alpha c_v \nabla c_A - D_v \nabla c_v, \\ J_i &= (d_{Ai} - d_{Bi})\alpha c_i \nabla c_A - D_i \nabla c_i, \\ J_A &= -D_A \alpha \nabla c_A - c_A(d_{Ai}\nabla c_i - d_{Av}\nabla c_v). \end{aligned}\right\} \tag{2.16}$$

In these equations, α is the thermodynamic factor to account for the difference between the concentration and chemical potential gradients; d_{Av}, d_{Bv}, d_{Ai} and d_{Bi} are the diffusion coefficients of the elements A and B via vacancies and interstitials, respectively; and $D_v = d_{Av}c_A + d_{Bv}c_B$, $D_i = d_{Ai}c_A + d_{Bi}c_B$ and $D_A = d_{Av}c_v + d_{Ai}c_i$ are the average local diffusion coefficients of vacancies, interstitials and A-atoms respectively. Equation (2.16) predicts that, in an irradiated solid, the solutes that are slow vacancy diffusers (small d_{Av}) become enriched on point defect sinks, while the faster thermal diffusers are depleted there. Such behaviour is observed experimentally in irradiated steels and Fe–Cr–Ni alloys; for example, nickel (slow diffuser) has been shown (Marwick et al. 1978) to be enriched, relative to iron (fast diffuser), in the neighbourhood of voids in ion-bombarded PE16 steel.*

It is clear from the above discussion that solute can segregate towards, or away from, a point defect sink, such as a void, depending upon the particular alloy and irradiation conditions. This in turn can directly influence the defect loss at the various sinks. If a precipitate is itself a sink then this process of segregation can lead to a re-distribution of solute between the precipitate and the matrix, with important consequences for void swelling and creep. The sink efficiency of precipitates is obviously important in this context. The most

*It should be noted that this data can also be accounted for by the hypothesis that nickel atoms are enriched at the void by preferential enrichment of the interstitial flux.

important factor considered to determine the sink efficiency of a precipitate is whether or not it is coherent with its matrix phase. The surface of an incoherent precipitate, or any disordered interface, is expected to be a sink, because the disorder allows temporary rearrangements necessitated by the absorption of a defect to be readily accommodated. At a coherent interface where the atomic lattice is carried through from one phase to another with minimal disturbance the interface would not be expected to be a sink, but might be a trapping site at which defects could be immobilised. Annihilation of trapped defects by recombination could then lead to loss of defects at the interface.

A second process which can contribute to a re-distribution of solute is termed *irradiation induced re-solution*. This is a process whereby irradiation tends to return precipitating phases to solution in the matrix (Marwick 1981). The simplest possible process that can be envisaged is a direct recoil contribution to the solute outflow from a precipitate (Nelson et al. 1972). An alternative description of the recoil dissolution process is as a manifestation of the athermal (radiation enhanced) diffusion process which accompanies atomic displacements (Marwick 1981). This latter approach is favoured by experimental evidence.

In summary, theory has indicated that point defect gradients existing around sinks during irradiation can results in solute flow towards, or away from the various point defect sinks. The first possible, direct, consequence of such solute segregation is on the defect flow to the sinks. Hence, for example, the bias of a dislocation for an interstitial relative to a vacancy could be negated, at least partially, by a build-up of solute close to the dislocation core. If a precipitate is itself a sink then it is immediately clear that the solute segregation process can lead to a re-distribution of solute between the precipitate and the matrix. The extent to which this is possible depends upon the efficiency of the precipitate as a sink, and it has been indicated that the most important factor determining the sink efficiency is expected to be the degree of coherency the precipitate has with its matrix phase. Another process, irradiation induced re-solution, is also important in re-distributing solute between precipitates and the matrix; this process is one of dissolution by atomic recoil. In a real, multi-phase, alloy a dynamic equilibrium is established during irradiation between the various precipitate phases and the solute in the matrix. All of the processes discussed in this section can have important consequences for the microstructural evolution and, hence, void swelling and creep during irradiation.

3. Mathematical rate theory

The approach most widely adopted to describe mathematically the microstructural evolution in a metal during irradiation is that of *chemical rate theory*. This basic approach is used in many branches of the physical and natural sciences to model time dependent processes. Although the formalism is sufficiently powerful to handle both nucleation and growth processes during irradiation damage, it has been applied most successfully to growth studies. This is because of both the general difficulty of defining rate constants, which is especially marked in the nucleation regime, and the computational effort required to describe adequately the two phenomena simultaneously. However, as discussed in §2.4. above, some preliminary numerical studies of interstitial loop and void nucleation have been undertaken. Moreover, in that section it has been noted that in the rate theory approach to void growth, void nucleation is handled in a semi-empirical manner. Also neglected in the general rate theory of microstructural evolution, at least until very recently, is any treatment of microchemical effects, such as solute segregation and the evolution of the phase structure, as discussed in §2.5. This area is especially difficult to treat, although some preliminary studies are underway.

The following topics are discussed in this section: (a) the lossy continuum, which includes a short discussion of the basic philosophy of the rate theory approach as applied to microstructural evolution; (b) the general rate equations, where the mathematical structure of the rate theory equations is elucidated briefly; (c) the sink strengths, where the approach to the derivation of the rate constants appearing in the rate equations is outlined; (d) recoil effects, where those modifications to the general rate equations, as given in §3.2., required to treat the cascade nature of the damage are presented; and, (e) other topics, which includes brief discussions on void nucleation, microchemical, stress and gas effects.

3.1. The lossy continuum

The most detailed and successful model for representing a complex irradiation situation, which incorporates the sensitivity of the void growth to the presence of the other sinks in the microstructure and the various physical parameters, is based on a chemical rate theory description of the intrinsic point defect population (Brailsford and Bullough 1972). The basic rate theory approach can be adopted for both a regular array (lattice), and random distribution, of point defect sinks.

106

For the most important case of a random distribution of sinks, the point defect diffusion in the real material with discrete sinks is described in some average sense by diffusion in a *lossy continuum* containing a *homogeneous distribution* of these same sinks, with strengths determined from separate detailed treatments of defect transport to one sink of each type.

The fundamental idea of this *effective medium* approach for two phase systems which are *random on a macroscopic scale* appears to have been visualized first by Maxwell (1892) in a theory of the electrical resistivity of a composite comprised of spheres of one material embedded in a continuous second phase of a different resistivity. On a microscopic scale an equivalent concept finds application in several branches of modern physics (Elliott et al. 1974). The central theme of Maxwell's approach is as follows. For one type of inhomogeneity only, for example spherical inclusions of radius r_0, distributed randomly, an equivalent homogeneous resistive medium is assumed to exist. This must be such that if a spherical volume of radius R is excavated from it, and replaced by an equal volume comprised of a spherical shell of the real continuous phase surrounding just one inclusion, then the macroscopic properties of the composite thus formed must be the same as those of the medium itself, provided the radius R is chosen to give the correct volume fraction, S, of the discrete phase: $R^3 = r_0^3/S$. This furnishes a self-consistent scheme for finding the properties of the medium.

3.2. The rate equations

The theoretical description of irradiation damage by chemical rate theory has about a 10 year history (Harkness and Li 1971, Brailsford and Bullough 1972) and has reached the stage where general purpose codes for calculating void swelling and irradiation creep are being made available to an audience wider than just those workers involved deeply in the theoretical development (Windsor et al. 1979, 1981, 1982).

In the following, the rate equations are presented for a system under irradiation and containing voids, interstitial loops, dislocation network and grain boundaries as sinks (Bullough and Hayns 1978, Windsor et al. 1979). The equations are:

$$\frac{dc_v}{dt} = K_v - k_v^2 D_v c_v - \alpha c_i c_v, \tag{3.1}$$

$$\frac{dc_i}{dt} = K_i - k_i^2 D_i c_i - \alpha c_i c_v, \tag{3.2}$$

107

$$\frac{dq_{vC}}{dt} = k^2_{vC} D_v c_v - k^2_{iC} D_i c_i - K^e_{vC}, \tag{3.3}$$

$$\frac{dq_{iN}}{dt} = k^2_{iN} D_i c_i - K^2_{vN} D_v c_v + K^e_{vN}, \tag{3.4}$$

$$\frac{dq_{iIL}}{dt} = k^2_{iIL} D_i c_i - k^2_{vIL} D_v c_v + K^e_{vIL}, \tag{3.5}$$

$$\frac{dq_{vGB}}{dt} = k^2_{vGB} D_v c_v - k^2_{iGB} D_i c_i - K^e_{vGB}. \tag{3.6}$$

Here, α is the rate constant for the bulk recombination of interstitials and vacancies, c_v and c_i are the fractional concentrations of vacancies and interstitials in the medium respectively; q_{vC}, q_{iN}, q_{iIL} and q_{vGB} are the fractional number of vacancies in cavities, interstitials in network and interstitial loops, and vacancies in grain boundaries respectively; D_v and D_i are the vacancy and interstitial diffusion coefficients (as above); and K_v and K_i their production rates, both through the irradiation and by thermal emission from the sinks. Hence, if K is the defect production rate through irradiation:

$$K_i = K, \tag{3.7}$$

and

$$K_v = K + K^e_{vC} + K^e_{vN} + K^e_{vIL} + K^e_{vGB}, \tag{3.8}$$

where K^e_{vC}, K^e_{vN}, K^e_{vIL} and K^e_{vGB} are the vacancy emission rates from cavities, network, interstitial loops and grain boundaries respectively; the exact form of these is not presented herein, but can be obtained from Windsor et al. (1979). The terms such as $k^2_{vC} D_v c_v$ describe the loss rates of point defects to the various point defect sinks, in this case vacancies to cavities. The quantities such as k^2_{vC} are called *sink strengths*, in this case the sink strength of cavities for diffusing vacancies. The total sink strengths for vacancies, k^2_v, and interstitials, k^2_i, are written;

$$k^2_v = k^2_{vC} + k^2_{vN} + k^2_{vIL} + k^2_{vGB}, \tag{3.9}$$

and

$$k^2_i = k^2_{iC} + k^2_{iN} + k^2_{iIL} + k^2_{iGB}, \tag{3.10}$$

and the quantities $(k_i)^{-1}$ and $(k_v)^{-1}$ are the mean distances a free interstitial

or vacancy moves in the medium before becoming trapped. The central problem in the rate theory of microstructural evolution is the determination of the various sink strengths for migrating point defects.

3.3. The sink strengths

Two approaches have been proven for deriving sink strengths for use in the rate theory of microstructural evolution. One of these is concerned with spatially periodic sink arrays, and the other with completely random sink distributions. The fundamental validity of these two approaches has been discussed at length recently by Brailsford and Bullough (1981). In the present short summary, only the effective medium model for a random distribution of sinks is discussed, since long-range order is only rarely observed. Nevertheless, it is noted that Ham's eigen-function method (Ham 1958) for a void lattice is useful in answering several questions of principle; for example, to what extent can sink strengths derived from steady state be generally applicable (Brailsford and Bullough 1981).

The case of the void sink is chosen to illustrate the effective medium method for obtaining sink strengths. As is usual, an initial simplification is invoked; namely, the concept of so-called steady state growth, which enables time to be removed explicitly from the point defect continuity equations. The only alternative to this would be to confront partial differential equations with moving boundary conditions in a finite domain. A second approximation is to neglect bulk recombination in the sink strength derivation. This is also generally adopted although in some cases, including that of the void sink (Rauh et al. 1981), sink strengths including recombination are available. Nevertheless, the approximation is a good one (Rauh et al. 1981).

Following the philosophy outlined in §3.1., the void should be surrounded by a sink free region before being placed in the effective medium containing all the sink types in the microstructure, and extending to infinity. For simplicity, and because it has been shown that the void sink strength is only slightly sensitive to the thickness of the matrix shell that is considered to surround each void, such a sink free region is omitted entirely. The void, of radius r_C, is thus imagined to be embedded directly in the effective medium. The problem then is to find the defect flux to the central cavity embedded in the medium. The defect concentration, now written simply* as c, is the

*The subscripts i and v have been dropped since the equations for interstitials and vacancies are of identical form and uncoupled when bulk recombination is ignored.

solution of,

$$\frac{D}{r^2}\frac{\mathrm{d}}{\mathrm{d}r}r^2\frac{\mathrm{d}c}{\mathrm{d}r} - Dk^2c + K + K^e = 0, \tag{3.11}$$

where k^2 and K^e include the contributions from the void sinks. The defect flow boundary condition at the medium–sink interface is,

$$D\left.\frac{\mathrm{d}c}{\mathrm{d}r}\right|_{r=r_c} = v[c(r_c) - \bar{c}_c], \tag{3.12}$$

where v is the transfer velocity from the matrix to the sink and $v\bar{c}_c$ the thermal emission rate from the cavity. The solution of this problem is,

$$c = c^{\infty} - \frac{(c^{\infty} - \bar{c}_c)vr_c/D}{1 + kr_c + vr_c/D}\frac{r_c}{r}e^{-k(r-r_c)}, \tag{3.13}$$

where $c^{\infty} = (K + K^e)/Dk^2$. Hence, the surface integral of the flux into the cavity, J, is given by

$$J_c = \frac{4\pi(c^{\infty} - \bar{c}_c)vr_c^2(1 + kr_c)}{1 + kr_c + vr_c/D}. \tag{3.14}$$

It is evident that this must equal the net flux to a cavity in the medium; that is,

$$J_c = (Dk_c^2c^{\infty} - K_c^e)/C_c, \tag{3.15}$$

where C_c is the volume concentration of cavities. Hence, the cavity sink strength, k_c^2 is given by,

$$k_c^2 = \frac{1}{c^{\infty}}\left[C_c\frac{4\pi(c^{\infty} - \bar{c}_c)(1 + kr_c)vr_c^2/D}{1 + kr_c + vr_c/D} + \frac{K_c^e}{D}\right]. \tag{3.16}$$

Applying the low temperature limit when, by definition, K_c^e/D vanishes, and $\bar{c}_c$ tends to zero, equation (3.16) yields;

$$k_c^2 = 4\pi r_c C_c(1 + kr_c)\frac{vr_c/D}{1 + kr_c + vr_c/D}. \tag{3.17}$$

Furthermore, since equation (3.16) must hold at all temperatures, it follows

that,

$$K_c^e = Dk_c^2\bar{c}_c, \tag{3.18}$$

with k_c^2 given by equation (3.17). These are the general results of this model for the most general form of boundary condition. For the case of diffusion-controlled transfer through the matrix–sink interface, v is of the order of D/lattice spacing. So, for voids of any significant size, $vr_c/D \gg 1$, and equation (3.17) becomes

$$k_c^2 = 4\pi r_c C_c(1 + kr_c). \tag{3.19}$$

Thus, it is seen that the void sink strength, k_c^2, depends upon all the sinks in the medium, through the term kr_c.

The above discussion has demonstrated the power of the effective medium approach for determining sink strengths, at least for neutral sinks of simple geometry. For the dislocation sinks, the geometry is complex and the dislocation–point defect interaction must be included (Brailsford and Bullough 1981). Much attention has been paid to this topic and, recently (Bullough and Quigley 1981), a new sink strength has been derived rigorously for a long straight dislocation, and applied successfully to the electron, heavy ion and neutron irradiation of 316 steel (Bullough and Quigley 1983). Sink strengths have been derived also for saturable solute atom traps (Brailford and Bullough 1976, Bullough and Hayns 1978), as discussed in §2.1. For such a trap which binds only vacancies, the probability of trapping a vacancy is proportional to the number of unoccupied sites at the trap, that is to the probability that the trap is not fully occupied. On the other hand, such a trap can only trap an interstitial if it already has trapped a vacancy with which the interstitial can recombine; the probability of trapping an interstitial is thus proportional to the occupation probability of the trap. The sink strengths of a vacancy trap for migrating interstitials and vacancies thus depend on the occupation probability of the trap; this is given by ensuring that it remains stationery at the trap. It is found that these sinks, at which only enhanced recombination occurs, have sink strengths that are sensitive to the slightest presence of bulk recombination elsewhere in the system. As a result of this sensitivity, some theoretical problems remain in this area.

A study, following a procedure suggested by Brailsford and Bullough (1981), has also been made of the theory of dynamic sink strengths for both pulsing and arbitrary damage rate conditions. Such pulsing conditions might

be expected to prevail, for example, in certain proposed fusion reactors. This recent work (Rauh et al. 1982, 1983) has shown that for pulsing conditions it is not necessary under most conditions to use complex dynamic sink strengths and the corresponding steady-state forms can continue (Ghoniem and Kulcinski 1978) to be used. However, dynamic sink strengths are necessary if the sink densities are very high (Rauh et al. 1982, 1983).

3.4. Recoil effects

The rate theory equations reviewed in §3.2. do not deal with the effects of the damage cascade collapse to form vacancy loops. Here, those modifications required to treat this phenomenon are outlined (Bullough et al. 1975). Two additional rate equations describe the number of vacancy loops per unit volume, N_{vL}, and the fractional number of vacancies in vacancy loops, q_{vVL}. Thus:

$$\frac{dN_{VL}}{dt} = \frac{n_{VL}}{\Omega} - \frac{N_{VL}}{\tau}, \tag{3.20}$$

and

$$\frac{dq_{vVL}}{dt} = \varepsilon K - k^2_{iVL} D_i c_i + k^2_{vVL} D_v c_v - K^e_{vVL}. \tag{3.21}$$

In these equations, n_{VL} is the fractional concentration of vacancy loops created per second:

$$n_{VL} = \frac{\varepsilon K b^2}{\pi r^2_{VL}(0)}, \tag{3.22}$$

where b is the magnitude of the Burgers vector (as above) and Ω, the atomic volume, has been set equal to b^3, εK is the fractional rate at which vacancies are removed from solution to form vacancy loops, and $r_{VL}(0)$ is the initial radius of newly formed vacancy loops. τ is the lifetime of the vacancy loops and is given, from a Taylor series expansion of $r_{VL}(t)$, by,

$$\tau = -\frac{r_{VL}(0)}{(dr_{VL}/dt)_{r_{VL}(0)}} \tag{3.23}$$

The loop shrinkage rate, dr_{VL}/dt, can be expressed in terms of the vacancy

loop sink strengths for interstitials, k^2_{iVL}, and vacancies, k^2_{vVL}, and the vacancy emission rate from vacancy loops, K^e_{vVL}. To complete the modifications, equations (3.8) to (3.10) of §3.2. become, respectively:

$$K_v = (1-\varepsilon)K + K^e_{vC} + K^e_{vN} + K^e_{viL} + K^e_{vGB} + K^e_{vVL}, \tag{3.24}$$

$$k^2_v = k^2_{vC} + k^2_{vN} + k^2_{viL} + k^2_{vGB} + k^2_{vVL}, \tag{3.25}$$

and

$$k^2_i = k^2_{iC} + k^2_{iN} + k^2_{iiL} + k^2_{iGB} + k^2_{iVL}. \tag{3.26}$$

This formalism to include the formation of vacancy loops from displacement cascades therefore introduces two new parameters into the rate theory model: (i) $r_{VL}(0)$, the radius of the vacancy loops immediately following their "athermal" formation, which can be estimated directly from experiment; and (ii) ε, where εK is the fractional rate at which vacancies are removed from solution to form vacancy loops. In practice ε is the adjustable parameter which distinguishes between electron ($\varepsilon = 0$) and cascade damage ($0 < \varepsilon < 1$), and may be derived in the manner outlined by Bullough and Quigley (1983) and Bullough et al. (1975). Alternatively, it may be possible to gain more direct information on ε from detailed experimental observations of displacement cascades. It is the values of $r_{VL}(0)$ and ε in the theory which chiefly serve to distinguish fusion and fast fission neutron damage.

3.5. Other topics

In this section, certain other topics are discussed briefly in terms of their treatment within the rate theory representation of microstructural evolution effects.

As intimated in §2.4., void nucleation is treated in a semi-empirical manner in the rate theory of void swelling and irradiation creep. The calculations are started with an assumed concentration of small, ~1 nm, equilibrium gas bubbles, the concentration being taken from experimental observations of void densities. Hence, the initial nucleation phase is not treated explicitly. As the calculation proceeds, gas is fed into the cavities according to the chosen gas generation rate; for numerical simulation of a particular experiment this rate would be that pertaining during the experiment. In virtually all the calculations performed to date the total quantity of generated gas has been allocated to the cavities. The increasing cavity gas pressure tends to reduce

strongly the vacancy thermal emission from the cavities, which grow by the irradiation-induced net flux of vacancies to them. When the cavities reach a certain critical size they are able to grow without the further addition of gas; that is they can grow as voids rather than as gas bubbles (Clement and Wood 1980). This treatment allows the incubation dose before the onset of substantial void swelling, as observed in experimental void swelling studies, to be modelled physically. The incubation dose is found to be particularly sensitive to the irradiation temperature and the gas generation rate, and as such is important in fusion material studies. Recent investigations of void swelling in 316 steel (Bullough et al. 1983a,b) have indicated that it is more appropriate to partition the gas between all the sink types in the microstructure (Yoo and Mansur 1979), rather than simply allocate it all to the cavities; further work is required in this area.

The problem of introducing microchemical concepts into the general rate theory of swelling is indeed a difficult one. To model rigorously the redistribution of solute between the matrix and the various precipitates together with any associated phase changes during irradiation, would require sink strength derivations for the intimately coupled system of point defects and various solute atoms migrating to a general precipitate sink. So far this has not been attempted. However, it is possible to make some progress in modelling the consequences of the microchemistry. Sink strengths have been derived, as discussed in the previous section, for solute atoms acting as saturable traps for migrating point defects. Also, the effect of restricted point defect access to their various sinks, such as voids and dislocations, through solute build-up close to them, can be modelled through a judicious choice of the matrix–sink transfer velocities (Mansur 1978). Recently, a mechanism of precipitate-enhanced cavity swelling during irradiation has been investigated by Mansur (1981). It is often observed experimentally in complex alloys that the largest cavities produced during irradiation are attached to second phase precipitate particles. One hypothesis that such observations suggest is that the precipitate–matrix interface may assist in the collection of point defects, which are channelled to the attached cavities. Mansur's analysis suggests that those cavities attached to precipitates may grow several times larger than cavities isolated in the matrix. This effect is relatively easily incorporated into the rate theory through the introduction of an extra rate equation describing the net flow of vacancies to a second population of voids with an increased "capture radius". It is likely that the acquisition of gas is also enhanced by the nearby presence of a precipitate sink; hence, the void incubation dose should be lowered significantly for such cavities.

If a metal sample is irradiated whilst being subjected to a uniaxial tensile

stress, its dimensions can change without a change in its volume. Of course, in the void swelling regime it is necessary to substract out the void swelling contribution to get the volume conserving dimensional changes. This phenomenon is known as creep and, in general, is made up of two, not necessarily additive, components; these are termed thermal creep, which is a high-temperature phenomenon, and irradiation creep, which is found at temperatures below those at which thermal creep is possible.

Several mechanisms have been proposed for irradiation creep, based on climb, glide or combined climb–glide processes (Mansur 1979, Bullough and Wood 1980, Nabarro et al. 1982). However, the SIPA climb creep mechanism, the basis of which has been discussed in §2.3., is the most well developed and widely applied model. Its incorporation into the rate theory framework is well documented, and it is the mechanism included in a recent computer program to model simultaneously void swelling and irradiation creep (Windsor et al. 1981). Because of the concern that the existing rate theory does not embody any representation of the dynamics of the dislocation evolution a climb creep model is currently being developed (Bullough et al. 1981). The model simultaneously describes void swelling, SIPA creep, and thermal creep of the type discussed by Nabarro (1964). The processes turn out to be inextricably coupled via the evolving dislocation distribution, for which rate equations have been derived from simple microscopic models of dislocation generation and annihilation. It is believed that these developments will greatly extend the range of applicability of the rate theory of microstructural evolution. For power law creep at high temperatures further development is surely required.

4. *Simulation of neutron damage*

In developing materials for future application in fusion reactor devices, it is necessary to make recourse to simulation of the actual fusion environment owing to the lack of a prototype 14 MeV neutron source. Those 14 MeV neutron sources which do exist are limited by low neutron fluxes and small sample volumes. The simulation tools which might be employed are: the HVEM, heavy ion damage sources, proton accelerators and both thermal and fast fission neutron sources. In this section the discussion is centred around those issues seen as particularly important to the use of simulation. The topics considered are: (a) the philosophy of simulation, (b) the temperature shift, (c) gas effects and (d) microchemical and recoil effects. Finally, in §4.5. we illustrate the present state of the art by outlining a recent

successful prediction of the swelling in neutron irradiated 316 steel based on a correlation with simulation data.

4.1. The philosophy of simulation

Already, a great deal of research has gone into investigating the damage behaviour of a wide range of pure metals and alloys. Parallel efforts have been made to develop methods for analyzing and extrapolating the data, particularly to higher doses. These data analyses have proceeded along two main lines. The more widely accepted approach, which is being used to develop rules for predicting high-dose reactor void swelling and creep behaviour, is to subject the existing data to statistical analysis and thus obtain comparatively simple empirical relationships. Such an approach requires the input of only the void swelling (for example) as a function of dose, dose rate, stress and temperature, and does not require any detailed knowledge or understanding of the damage structure. The second approach has been to construct the theoretical rate theory model based on physical understanding which provides a framework for describing the evolution of the damage structure as a whole. Whilst this model has been successful in identifying the important physical processes involved it is not, as can be judged from the discussion of the previous sections, an ab initio theoretical model and, hence, requires quantitative calibration using input based on accurate experimental observations of the damage structure, particularly at low doses. Unfortunately, much of the experimental work on reactor materials has involved obtaining void swelling data without detailed structural observations. Thus, it has not been possible to develop the physical models to the stage where they could be used to predict quantitatively the swelling behaviour of reactor components.

It is clear that the second of the two approaches outlined above, that is the use of the physically based rate theory model, is very preferable to the statistical approach, particularly when extrapolating well outside of the available data base, which is inevitable if simulation is employed to construct that data base. Hence, in the case of reactor material development, an important aspect of the overall programme should be the further development of the theoretical model together with a programme of data collection relevant to the model requirements. Overall, a systematic approach is recommended (Bullough et al. 1977).

4.2. The temperature shift

Many techniques for the simulation of fusion reactor materials, such as the HVEM and the Variable Energy Cyclotron (VEC), were originally adopted for simulating the damage in fast breeder reactors. The aim there was primarily to shorten the timescale of the damage, that is to reach high displacement damage doses in short times. This is not the sole aim in the simulation of fusion damage where, because of the lack of any prototypic irradiation facility, it is desirable to simulate as closely as possible the characteristics, for example the nature of the cascades, of the 14 MeV neutron damage. Nevertheless, techniques giving a high displacement damage dose rate, often about three orders of magnitude higher than in the reactor situation, are found useful in fusion reactor materials development, even though the damage characteristics are not as desirable as they might be.

A major problem in the use of high-dose rate simulation of neutron damage, which requires substantial theoretical interpretation, is the resultant shift in void swelling to higher temperatures (Brailsford and Bullough 1972). This phenomenon is explained as follows: a typical void swelling versus temperature profile shows a maximum at some temperature. The reduction in swelling at low temperatures is due to the presence of bulk recombination of the point defects, whereas the reduction in swelling at high temperatures is caused by the eventual dominance of the self-diffusion term $D_v c_v^e$. At higher dose rates the steady-state concentrations of vacancies and interstitials at a particular temperature rise, with a consequent increase in the proportionate loss of defects by recombination. This shifts the low-temperature "cut-off" to higher temperatures at higher dose rates. The high-temperature "cut-off" is similarly shifted because the eventual dominance of the self-diffusion term is moved to higher temperatures. Temperature shifts of over a 100 °C are commonly found. Such temperature shifts are particularly difficult to interpret when two swelling peaks are observed under neutron irradiation, for example in solution annealed 316 steel. In these circumstances, the simulation might show only a single peak, with perhaps a shoulder. Then it is necessary to relate the single simulation peak to one of the two neutron peaks.

To further confound the situation it must also be recognized that the sink densities vary with temperature and dose rate; thus the reduction of swelling at low temperatures is also dependent on the recombination losses *at the sinks* as well as in the bulk and therefore changes in this loss will also affect the precise shift; clearly a physically based theory is indispensible for such correlations since all such contributions are simultaneously included.

4.3. Gas effects

In neutron-irradiation environments helium and hydrogen are produced in structural metals through (n, α) and (n, p) reactions respectively. The exact quantities produced depends upon the composition of the material and the neutron energy spectrum. In the fusion environment, the high gas production rates in steel are sure to influence the microstructural response of the material, particularly at higher temperatures. The importance of helium as a nucleating agent for cavities has been discussed in earlier sections; the role, if any, of hydrogen (a fast diffuser) is not unambiguously determined.

In high-energy proton simulation of neutron damage gas is generated in situ, but for other simulation techniques, such as the HVEM and VEC, gas is not generated by the source of damage. Several approaches have been adopted to circumvent this problem. The earliest of these was the development of the technique of pre-implanting materials with helium prior to the damage simulation. This procedure does not, however, reproduce the conditions pertaining under neutron irradiation of a continuous injection of gas into the material. Hence, more recently, experimental facilities have been developed to allow the simultaneous injection of helium, from an α-particle beam, and displacement damage, by heavy ions. Measured void swelling shows a marked sensitivity to the method of gas implantation (Packan and Farrell 1979), as would be expected from the theory of void nucleation. An adequate theoretical understanding of gas behaviour is, therefore, considered essential to the success of these simulation techniques.

Even if, as in the case of proton simulation, gas is generated in situ during irradiation, variations in the ratio of the gas production rate to dose rate can lead to misleading conclusions. This is especially true of information collected at low doses, where the measured swelling at high temperatures is particularly sensitive to the void incubation dose. A general theoretical analysis of the expected sensitivity of the high-temperature swelling to variations in dose rate and gas generation has been published (Hayns et al. 1978).

4.4. Microchemistry and recoil effects

It is now well established that during the simulation of neutron damage at high dose rates, the microchemistry is altered relative to that found during actual neutron irradiation. New phases are often observed and phases found under neutron irradiation disappear at higher damage rates. At present there is no real understanding of this behaviour and, therefore, theoretical effort is required in this area.

As discussed earlier, one of the major differences found between the 14 MeV fusion neutron damage and other neutron and simulation damage is in the displacement cascade structure. An interplay is required here between the theory, where cascade effects are modelled through the $r_{VL}(0)$ and ε parameters, and detailed experimental observations, such as those of English and Jenkins (1981). Molecular dynamics studies should also be helpful in explaining the relationships between the different sources of damage.

4.5. The correlation for 316 steel

In this section we outline a recent attempt to predict the swelling behaviour of 316 steel under heavy ion and neutron irradiation (Bullough and Quigley 1983). In that study the microstructure was assumed to consist primarily of network dislocations and voids and the various physical parameters required to define the sink strengths of these two sink types were determined by fitting the theoretically predicted swelling under electron irradiation to relevant HVEM data (Makin et al. 1980). This calibrated rate theory was then used, without further modification, to predict the swelling behaviour of the steel under 46.5 MeV Ni^{6+} and fast neutron irradiation; the only further "parameter" required is the cascade collapse efficiency ε (described in §3.4.) to account for the very different recoil spectra of heavy ions and fast neutrons compared with the electrons.

Two theoretical curves for the Ni^{6+} irradiation are shown in figure 1 together with the experimental results of Hudson (1976) at 40 dpa. The calculations were started with the experimental swellings at 16 dpa, so that only the transition from the swelling at 16 dpa to the swelling at 40 dpa was predicted. The dashed curve in fig. 1 was obtained without vacancy loops ($\varepsilon = 0$) and the very good correlation at 40 dpa (the solid curve) was obtained with $\varepsilon = 1.2\%$. The results clearly demonstrate the importance of cascade collapse processes for the heavy ion irradiation of this steel.

With no further adjustement of *any* parameters, including ε, the dose rate was reduced to that appropriate for the fast reactor and the predictions given in fig. 2 for the swelling transition from 39 dpa to 62.5 dpa were obtained. The relevant data (Kenfield et al. 1978) at these two doses is also shown in the figure. We now see a much reduced sensitivity to ε and a prediction of the swelling at 62.5 dpa (the solid line) that is quite close to the observed values over the entire temperature range. The lack of sensitivity to the recoil spectrum under fast neutron irradiation occurs in this steel because the total sink densities are rather high at the lower temperatures and thus the presence of vacancy loop sinks do not make a significant increase to the total

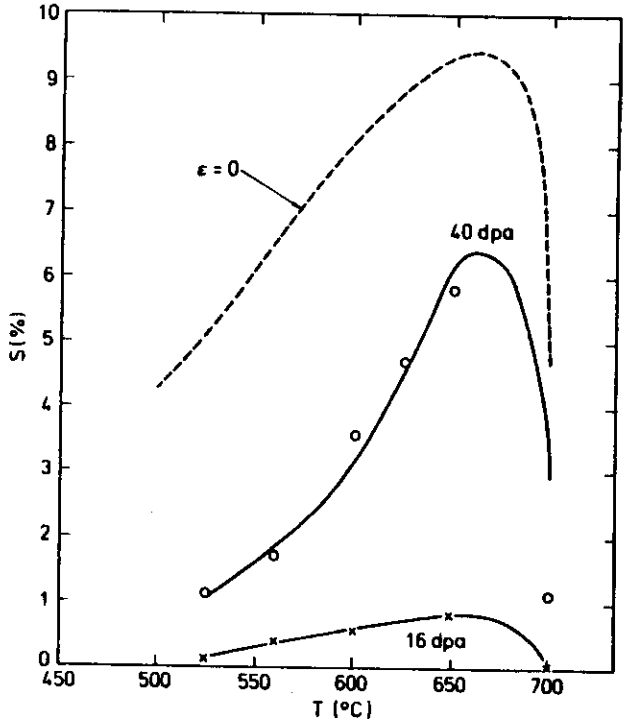

Fig. 1. The temperature dependence of the swelling in 316 steel irradiated with Ni^{++} ions. (x) and (o): experimental swelling values (Hudson 1976) at 16 and 40 dpa respectively. The theoretical curves at 40 dpa have been obtained by considering the swelling development from the 16 dpa state for the data given by Bullough and Quigley (1983). The dashed curve ($\varepsilon = 0$) indicates the result of neglecting vacancy loop formation, whereas the solid curve has been obtained with the vacancy loop parameter $\varepsilon = 0.012$.

sink strength of the microstructure. It follows that, for this steel, recoil effects are not qualitatively significant and the high energy electron simulation can itself enable a reasonable prediction of the swelling under fast neutron irradiations to be made.

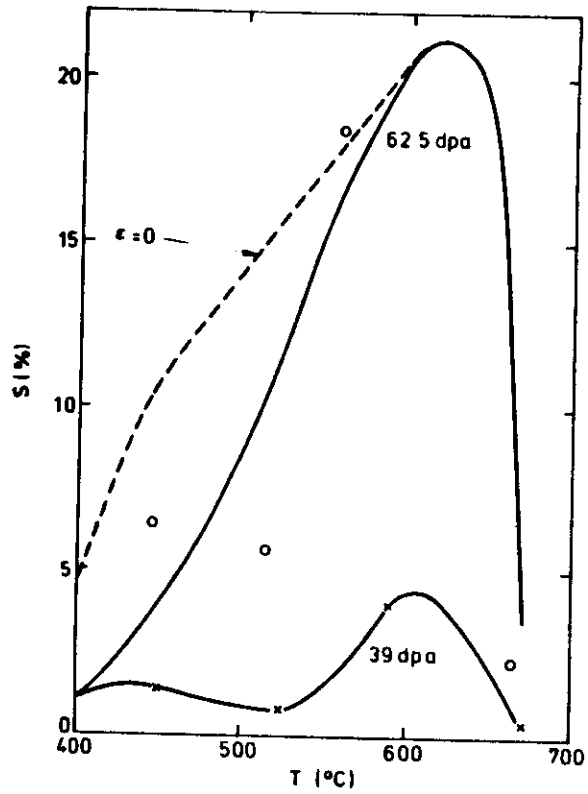

Fig. 2. The temperature dependence of the swelling in 316 steel irradiated with fast neutrons. (x) and (o): experimental swelling values (Kenfield et al. 1978) at 39 and 62.5 dpa respectively. The theoretical curves at 62.5 dpa have been obtained by considering the swelling development from the 39 dpa state for the data given by Bullough and Quigley (1983). The dashed curve ($\varepsilon = 0$) indicates the result of neglecting vacancy loop formation, whereas the solid curve has been obtained with the same vacancy loop parameter as used for the corresponding curve in figure 1.

5. Conclusions

In this chapter the present and future role and status of the theory of microstructural evolution during irradiation damage has been reviewed. Here the conclusions of the review are drawn together.

The role of theory is basically fourfold:

(1) To increase our fundamental understanding of the important processes governing void swelling and irradiation creep in metals and alloys.

(2) To build computational models of the microstructural evolution so that reliable predictions of void swelling and irradiation creep can be made under a wide range of irradiation conditions.

(3) To enable the link between reactor and simulation conditions to be made convincingly.

(4) To help in the design and analysis of reactor and simulation experiments.

All of these roles are applicable at present and will remain so in the future.

The present status of the theory shows some areas to be well developed, and other much less so. Overall, a good fundamental understanding of the microstructural evolution during irradiation exists. However, a notable exception to this encouraging picture is that the microchemical effects are not worked out in detail; for example, the effect, if any, of solute segregation on the dislocation bias has not been investigated. Also our knowledge of the cascade collapse process is inadequate. The mathematical rate theory representation of the damage processes is widely accepted, and the central problem of the determination of the sink strengths within the effective medium approximation is well understood in principle, and essentially solved for many of the sinks in the microstructure. Some examples of outstanding problems here are: (i) a minimal representation of microchemical effects, (ii) a less than adequate treatment of void nucleation, (iii) the lack of a fully consistent treatment of dislocation generation and recovery, and (iv) only a preliminary treatment of pulsed irradiation. All of these particular inadequacies are currently being investigated. The theoretical understanding of the complex relationships between reactor and various simulation techniques is generally well advanced but, of course, it can only be as complete as is our overall appreciation of the damage processes. For the future, five pressing areas are identified:

(1) The fundamental understanding of the nature of the cascade damage and the cascade collapse to form vacancy loops should be improved.

(2) The rate theory treatment of void nucleation and gas effects in general should be developed further.

(3) The theoretical nature of the evolution of the dislocation structure during irradiation should be investigated further, and fully consistent rate equations formulated.

(4) The current rate theory treatment of pulsed irradiation should be further developed.

(5) Microchemical effects should be investigated further from the fundamental standpoint, and a rate theory treatment should be developed.

References

Balluffi, R.W., 1978, J. Nucl. Mater. 69–70, 240.

Brailsford, A.D., and R. Bullough, 1972, J. Nucl. Mater. 44, 121.

Brailsford, A.D., and R. Bullough, 1976, J. Nucl. Mater. 69–70, 434.

Brailsford, A.D., and R. Bullough, 1981, Phil. Trans. R. Soc. (London) A302, 87.

Bullough, R., and M.R. Hayns, 1978, SM Archives 3, 73.

Bullough, R., and R.C. Perrin, 1969, in: Proc. Symp. Radiation Damage in Reactor Materials, Vienna Vol. 2 (IAEA, Vienna) p. 233.

Bullough, R., and T.M. Quigley, 1981, in: Proc. Yamada Conf. on Point Defects and Defect Interactions in Metals, Kyoto, Japan, eds. J.I. Takamura, M. Doyama and M. Kiritani (University of Tokyo Press, Tokyo) p. 839.

Bullough, R., and T.M. Quigley, 1983, J. Nucl. Mater. 113, 179.

Bullough, R., and J.R. Willis, 1969, J. Nucl. Mater. 32, 76.

Bullough, R., and J.R. Willis, 1975, Philos. Mag. 31, 855.

Bullough, R., and M.H. Wood, 1980, J. Nucl. Mater. 90, 1.

Bullough, R., B.L. Eyre and K. Krishan, 1975, Proc. R. Soc. (London) A346, 81.

Bullough, R., B.L. Eyre and G.L. Kulcinski, 1977, J. Nucl. Mater. 68, 168.

Bullough, R., D.W. Wells, J.R. Willis, and M.H. Wood, 1980 in: Proc. Conf. on the Role of Dislocation Theory in Modelling Physical Systems, Florida, eds. M.F. Ashby, R. Bullough, C.S. Hartley and J.P. Hirth (Pergamon Press, London) p. 116.

Bullough, R., M.W. Finnis and M.H. Wood, 1981, J. Nucl. Mater. 103–104, 1263.

Bullough, R., S.M. Murphy, T.M. Quigley and M.H. Wood, 1983a, Symp. on Radiation Damage Analysis for Fusion Reactors, St. Louis, Oct. 1982, J. Nucl. Mater. 117, 78.

Bullough, R., S.M. Murphy and M.H. Wood, 1983b, in: Proc. of Int. Conf. on Dimensional Stability and Mechanical Behaviour of Irradiated Metals and Alloys, Brighton (B.N.E.S., London) p. 43.

Clement, C.F., and M.H. Wood, 1980, J. Nucl. Mater. 89, 1.

Cottrell, A.H., and B.A. Bilby, 1949, Proc. Phys. Soc. (London) 62, 49.

Dederichs, P.H., and C. Lehmann, 1973, Phys. Rev. Lett. 31, 1130.

Elliott, R.J., J.A. Krumhansl and P.L. Leath, 1974, Rev. Mod. Phys. 46, 465.

English, C.A., and M.L. Jenkins, 1981, J. Nucl. Mater. 96, 341.

Gehlen, P.C., J.R. Beeler and R.I. Jaffee, eds., 1972, Interatomic Potentials and Simulation of Lattice Defects, Battelle Institute Materials Science Colloquia, Seattle, WA, USA, and Harrison Hot Springs, BC, Canada, June 1971 (Plenum Press, New York).

Ghoniem, N.M., and G.L. Kulcinski, 1978, Radiat. Eff. 39, 47.

Ham, F.S., 1958, J. Phys. Chem. Solids 6, 335.

Harkness, S.D., and C.Y. Li, 1971, Metall. Trans. 2, 1457.

Hayns, M.R., 1980a, Harwell Res. Rep. AERE-R. 9708 (AERE, Harwell, UK).

Hayns, M.R., 1980b, Harwell Res. Rep. AERE-R. 9818 (AERE, Harwell, UK).

Hayns, M.R., and M.H. Wood, 1979, Proc. R. Soc. (London) A368, 331.

Hayns, M.R., M.H. Wood and R. Bullough, 1978, J. Nucl. Mater. 75, 241.

Heald, P.T., and M.V. Speight, 1974, Philos. Mag. 29, 1075.

Holder, J., A.V. Granato and L.E. Rehn, 1974, Phys. Rev. B10, 363.
Hudson, J.A., 1976, J. Nucl. Mater. 60, 80.
Ingle, K.W., R.C. Perrin and H.R. Schober, 1981, J. Phys. F11, 1161.
Kenfield, T.A., W.K. Appleby, H.J. Busbaom and W.L. Bell, 1978, J. Nucl. Mater. 75, 85.
Lam, N.Q., H. Wiedersich and P.R. Okamoto, 1979, in: Proc. Conf. on Irradiation Behaviour of Metallic Materials for Fast Reactor Core Components, Corsica, eds. J. Poirier and J.M. Dupouy (C.E.A.-D.M.E.C.N., 91190 Gis-sur-Yvette, France) p. 45.
Little, E.A., R. Bullough and M.H. Wood, 1980, Proc. R. Soc. (London) A372, 565.
Makin, M.J., G.P. Walters and A.J.E. Foreman, 1980, J. Nucl. Mater. 95, 155.
Mansur, L.K., 1978, Nucl. Technol. 40, 5.
Mansur, L.K., 1979, Philos. Mag. A39, 497.
Mansur, L.K., 1981, Philos. Mag. A44, 867.
Marwick, A.D., 1981, Nucl. Instr. and Methods 182–183, 827.
Marwick, A.D., W.A.D. Kennedy, D.J. Mazey and J.A. Hudson, 1978, Scr. Metall. 19, 1015.
Maxwell, J.C., 1892, A Treatise on Electricity and Magnetism, 3rd Ed., Vol. 1 (Clarendon Press, Oxford) p. 440.
Nabarro, F.R.N., 1964, Philos. Mag. 16, 231.
Nabarro, F.R.N., R. Bullough and J.R. Matthews, 1982, Acta. Metall. 30, 1761.
Nelson, R.S., J.A. Hudson and D.J. Mazey, 1972, J. Nucl. Mater. 44, 318.
Packan, N.H., and K. Farrell, 1979, J. Nucl. Mater. 85–86, 677.
Quigley, T.M., S.M. Murphy, R. Bullough and M.H. Wood, 1981, Harwell Res. Rep. TP.916 (AERE, Harwell, UK).
Rauh, H., M.H. Wood and R. Bullough, 1981, Philos. Mag. A44, 1255.
Rauh, H., R. Bullough and M.H. Wood, 1982, Harwell Res. Rep. TP.957 (AERE, Harwell, UK).
Rauh, H., R. Bullough and M.H. Wood, 1983, J. Nucl. Mater. 114, 334.
Windsor, M., R. Bullough and M.H. Wood, 1979, Harwell Res. Rep. AERE-R.9595 (AERE, Harwell, UK).
Windsor, M., R. Bullough and M.H. Wood, 1981, Harwell Res. Rep. AERE-R.10251 (AERE, Harwell, UK).
Windsor, M.E., R. Bullough and M.H. Wood, 1982, Harwell Res. Rep. AERE-R.10683 (AERE, Harwell, UK).
Yoo, M.H., and L.K. Mansur, 1979, J. Nucl. Mater. 85–86, 571.